Metodologías para la evaluación de la susceptibilidad a los deslizamientos basadas en el análisis SIG. Aplicación en el NW de Nicaragua

Marta Guinau Sellés

ANEXO

ÍNDICE DE CONTENIDOS DEL ANEXO

I- RESUMEN DE LAS PUBLICACIONES

A. Resumen de la publicación:

A pragmatic approach to debris flow hazard mapping in areas affected by Hurricane Mitch: Example from NW Nicaragua.
(Propuesta para la cartografía de la peligrosidad a los flujos de detritos en áreas afectadas por el huracán Mitch: ejemplo en el NW de Nicaragua)

Raimon Pallàs[1], Joan Manuel Vilaplana[1], Marta Guinau[1], Ester Falgàs[1], Xavier Alemany[1], Angélica Muñoz[2]

1. RISKNAT Research Group, Dpt. Geodinàmica i Geofísica, Universitat de Barcelona, Facultat de Geologia, 08028 Barcelona (Spain)
2. Centro de Investigaciones Geocientíficas, CIGEO, Universidad Nacional Autónoma de Nicaragua, Managua (Nicaragua)

Publicado en; Engineering Geology, vol. 72 Nos. 1-2 (2004) pp. 57-72. ISSN 0013-7952

1. Introducción

Los países en vías de desarrollo a menudo se ven afectados por desastres naturales, debido a su localización en zonas expuestas a peligros geológicos y climáticos y a la alta vulnerabilidad socioeconómica que presentan ante estos fenómenos (Alcántara-Ayala, 2002). Las pérdidas económicas generadas por los desastres naturales en estos países, generalmente son inferiores a las que se producen en países desarrollados (Alexander, 1995, McGuire et al., 2002). No obstante, los periodos de recuperación son tan largos que dificultan el desarrollo socioeconómico. A pesar de esto, en los países en vías de desarrollo frecuentemente faltan normativas para la prevención y la mitigación de los desastres naturales.

Los movimientos de masa causan devastación y pérdidas humanas bajo los efectos de lluvias intensas y movimientos sísmicos, condiciones que se dan en muchos países en vías de desarrollo. Esta situación evidencia la necesidad de metodologías para el análisis de la peligrosidad a los movimientos de ladera adaptadas a los escasos recursos que se encuentran en estas regiones.

El objetivo de este trabajo es proponer una aproximación sencilla a la cartografía de la peligrosidad a los movimientos de ladera, centrada en un área piloto en el Departamento de Chinandega, NW de Nicaragua.

Este estudio piloto se centra en los municipios de Cinco Pinos y San Francisco del Norte (Departamento de Chinandega) (Fig. i). Zona severamente afectada por el huracán Mitch a finales de octubre de 1998. En este evento se registraron lluvias excepcionales que ocasionaron graves inundaciones y miles de deslizamientos generando gran cantidad de muertos y damnificados.

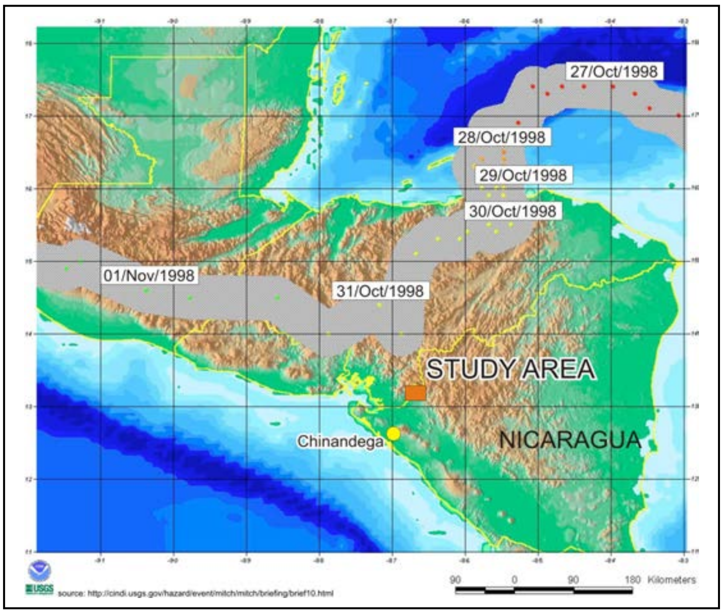

Fig. i; Localización del área de estudio y de la capital departamental, Chinandega. La franja gris indica la trayectoria del huracán Mitch, basada en datos del USGS (1999).
Fuente: http://cindi.usgs.gov/hazard/event/mitch/mitch/briefing/brief10.html

2. Análisis de los datos

A partir de la interpretación de dos series de fotos aéreas (serie Pre-Mitch – 1996 y serie Post-Mitch – 1998) se identificaron las zonas afectadas por deslizamientos durante el huracán Mitch y las zonas afectadas con anterioridad.

Con el fin de realizar un exhaustivo trabajo de campo se seleccionaron tres zonas de estudio. Sobre el terreno se identificaron los deslizamientos generados durante el huracán y se recogieron indicios de posibles movimientos más antiguos. En los puntos afectados se anotaron diversas observaciones como las dimensiones de la zona de rotura de los materiales, el tipo de material afectado, las dimensiones y morfologías de la zona de trayecto y acumulación de los materiales movilizados, la tipología del movimiento y toda la información testimonial que los habitantes de la zona pudiesen aportar sobre los deslizamientos. Con esta información finalmente se obtiene una cartografía de movimientos de masa en la cual se indica la tipología, la extensión y la temporalidad de los movimientos.

Con las observaciones de campo se determinó que las litologías que forman el área de estudio son materiales volcánicos y plutónicos Terciarios, generalmente recubiertos por un manto de alteración de grosor variable, que en algunas localidades está cubierto por una capa de material coluvial posiblemente resultado de antiguos movimientos de ladera. Los materiales de alteración de las diferentes litologías volcánicas presentan características homogéneas de manera que su comportamiento en cuanto a los movimientos de ladera es similar. Por este motivo en este estudio únicamente se diferenciaron dos tipos genéricos de litologías; rocas volcánicas y rocas plutónicas.

El 98% de los movimientos generados por las lluvias del huracán Mitch fueron flujos de detritos o corrientes de derrubios (debris flow) y el resto, flujos o coladas de tierra (earth flow) y desprendimientos de rocas (rock fall). La mayoría de los flujos de detritos tienen trayectorias largas que generalmente confluyen con la red de drenaje.

3. Aproximación al análisis de la peligrosidad (*sensu lato*)

La peligrosidad natural entendida como la probabilidad de ocurrencia de un fenómeno potencialmente dañino en un lugar y en un momento determinado, implica los conceptos de localización geográfica, magnitud y frecuencia del fenómeno (Varnes et al., 1984). En el área de estudio, la escasez de datos cuantitativos (volúmenes implicados y series temporales) hace imposible la determinación de la magnitud y la frecuencia de los deslizamientos. En este estudio se propone una aproximación a la peligrosidad utilizando conceptos que, si bien no forman parte estrictamente de la definición de peligrosidad, si que están relacionados con ella. Por este motivo se utiliza el término peligrosidad (sensu lato) para determinar aquellas zonas expuestas a fenómenos potencialmente peligrosos, donde es necesario aplicar actuaciones preventivas.

- La magnitud

En el caso de la magnitud (energía cinética de los movimientos) se considera que, dada la fragilidad de las infraestructuras del área, por baja que sea la magnitud del fenómeno, su capacidad destructiva es muy alta. Por este motivo en este estudio se considera que la magnitud no es un concepto que permita determinar diferentes grados de peligrosidad.

- La frecuencia

La disponibilidad de dos series de fotos aéreas (una pre-Mitch y otra post-Mitch) en el área de estudio, permite hacer una aproximación a la frecuencia en función de la funcionalidad de los movimientos en relación al huracán Mitch. Así, el terreno se puede clasificar según el siguiente orden descendiente de peligrosidad; 1) dos eventos registrados (p.e. Pre-Mitch + Mitch), 2) un evento registrado (p.e. Pre-Mitch o Mitch) y 3) ningún evento registrado.

- La predictabilidad

Observando las tipologías de movimientos de ladera del área de estudio, se pudo determinar que hay movimientos que se activan de forma súbita y otros que se activan lentamente dando lugar a indicios que permiten detectar el movimiento a tiempo para activar una alerta (p.e. apertura de grietas en el terreno y en infraestructuras, pequeños movimientos precursores, indicios de deformación en árboles y postes, cambios apreciables en la hidrología, etc.). Esto permite establecer dos grados diferentes de peligrosidad en función de la predictabilidad de los movimientos; 1) no predictibles (flujos de detritos y desprendimientos de roca) y 2) predictibles (flujos de tierra).

- La susceptibilidad

Con los conceptos anteriormente introducidos se puede hacer una aproximación a la peligrosidad en aquellas zonas donde se ha registrado algún movimiento de ladera. No obstante, aquellas zonas donde no hay indicios de haberse producido ningún deslizamiento pueden ser potencialmente inestables y por ende hay que introducirlas en el estudio. Para esto se introduce el concepto de susceptibilidad, definido como la probabilidad espacial de que se produzca un fenómeno. Dado que la escasez de datos en el área de estudio impide hacer un análisis cuantitativo de la susceptibilidad, se propone una aproximación cualitativa.

Teniendo en cuenta que los deslizamientos en el área de estudio se dan en un rango de pendientes determinado, y que el gradiente topográfico es un dato fácil de obtener en campo y a partir de del mapa topográfico, se ha utilizado este parámetro para determinar aquellas zonas que sin estar afectadas por deslizamientos tienen un gradiente topográfico similar al de las zonas afectadas. En el área de estudio se determinó que las zonas con pendiente ≥20º son zonas susceptibles a la rotura de los materiales y por ende son zonas potenciales al inicio de deslizamientos.

Con la digitalización del mapa topográfico 1:50.000 se obtuvo una topografía digital a partir de la cual se generó un mapa de pendientes. Sobre este mapa se determinaron las áreas con pendiente ≥20º, consideradas zonas susceptibles a la rotura de los materiales. Esta zonificación de la susceptibilidad únicamente tiene en cuenta la rotura de los materiales y no las posibles zonas de alcance de estos. Dado que en condiciones de lluvias intensas los materiales circulan largas distancias siguiendo la máxima pendiente hasta alcanzar la red de drenaje, se propone una aproximación a la susceptibilidad al alcance. A partir de la topografía digital y mediante el módulo Geopack de MicroStation®, se generan automáticamente líneas de flujo des de las zonas susceptibles a la rotura siguiendo trayectorias de máxima pendiente. Las zonas de concentración de estas líneas de flujo son consideradas zonas susceptibles al alcance máximo del material movilizado. Aceptando que todos los flujos llegan a los torrentes. La unión de las zonas de pendiente ≥20º y las zonas de concentración de líneas de flujo permiten la zonificación de las áreas susceptibles a los flujos de detritos (Fig. ii).

La comparación entre la zonificación de la susceptibilidad a la rotura y los escarpes de rotura cartografiados en el mapa de fenómenos, evidencia que la topografía digital no tiene suficiente resolución para obtener un mapa de pendientes detallado. Para minimizar los efectos de la baja resolución de la topografía digital se generaron líneas de flujo des de las zonas de escarpe que quedaban fuera de las zonas con pendiente ≥ 20º y se incorporaron a la susceptibilidad.

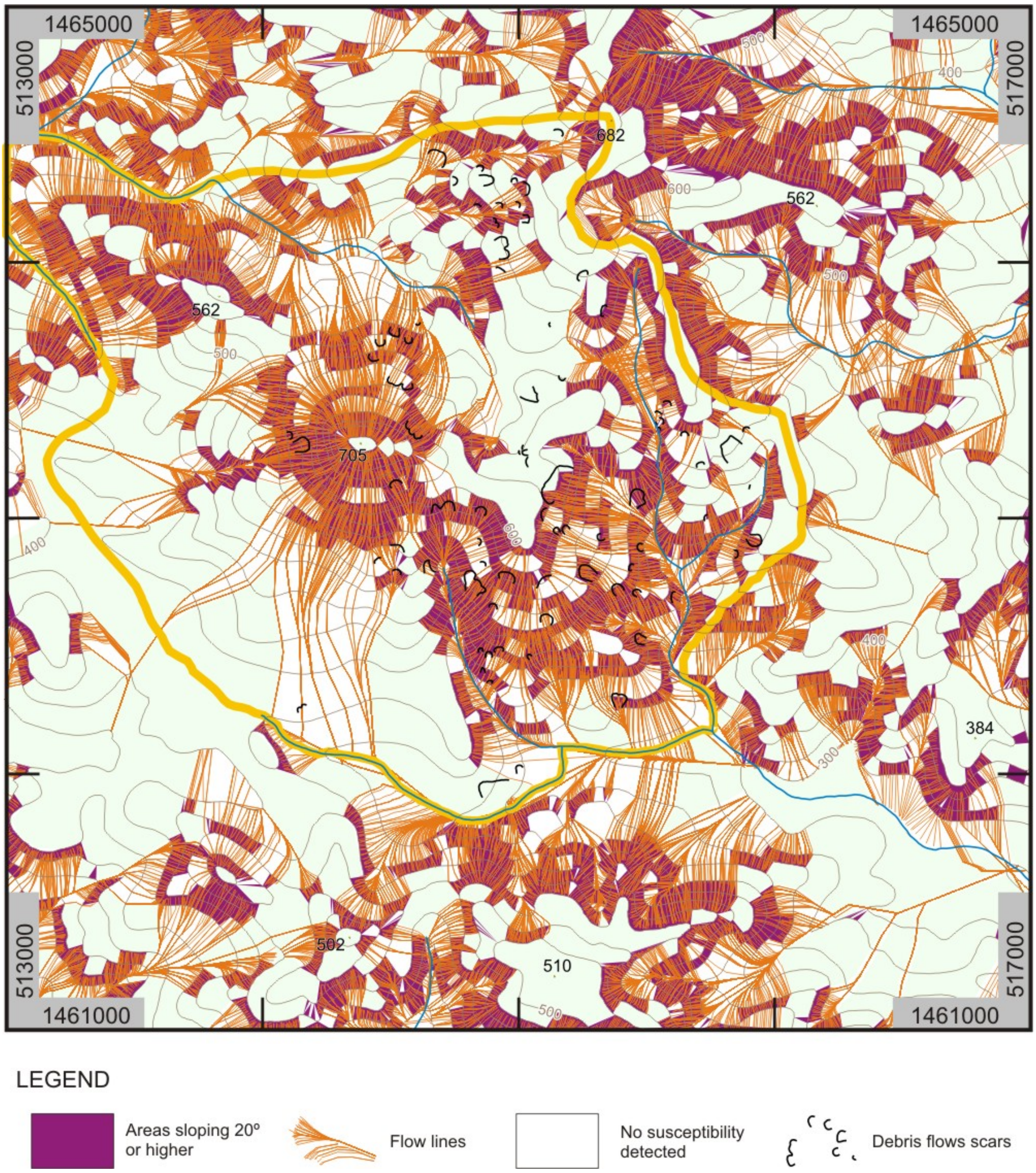

Fig. ii; Ejemplo del Mapa de Susceptibilidad correspondiente al área de Cinco Pinos. Las áreas en violeta corresponden a áreas con pendientes ≥ 20º, las cuales son consideradas susceptibles a la rotura. Las líneas de flujo corresponden a posibles trayectorias de flujos de detritos considerando las áreas marcadas en violeta y los escarpes como posibles zonas de salida.

La combinación de los tres conceptos definidos anteriormente; número de fenómenos registrados, predictabilidad y susceptibilidad, permite definir una escala de 7 grados de peligrosidad (Fig. iii) que se representa en un mapa de peligrosidad a los movimientos de masa (Fig. iv).

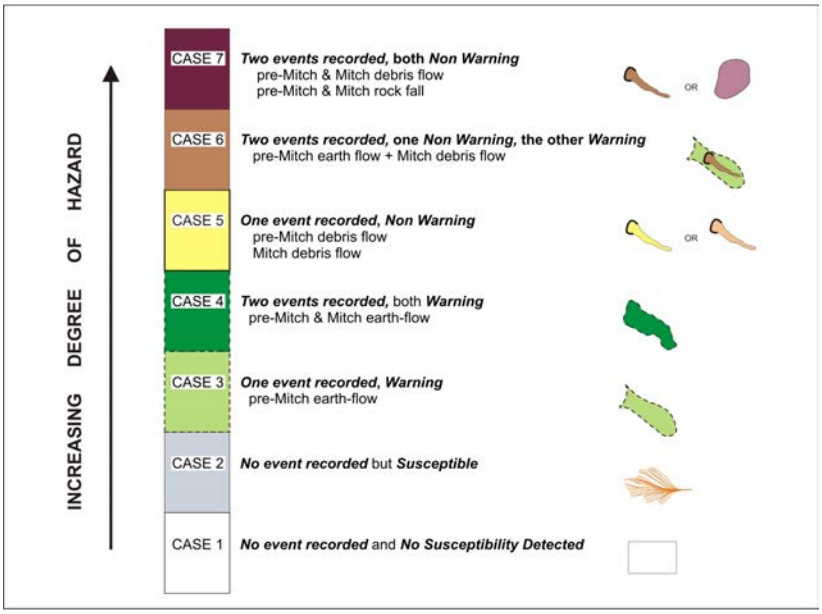

Fig. iii: Relación de posibles casos definiendo grados de peligrosidad. Los diferentes casos del 1 al 7 corresponden a los diferentes grados de peligrosidad representados en el Mapa de Peligrosidad (Fig. iv).

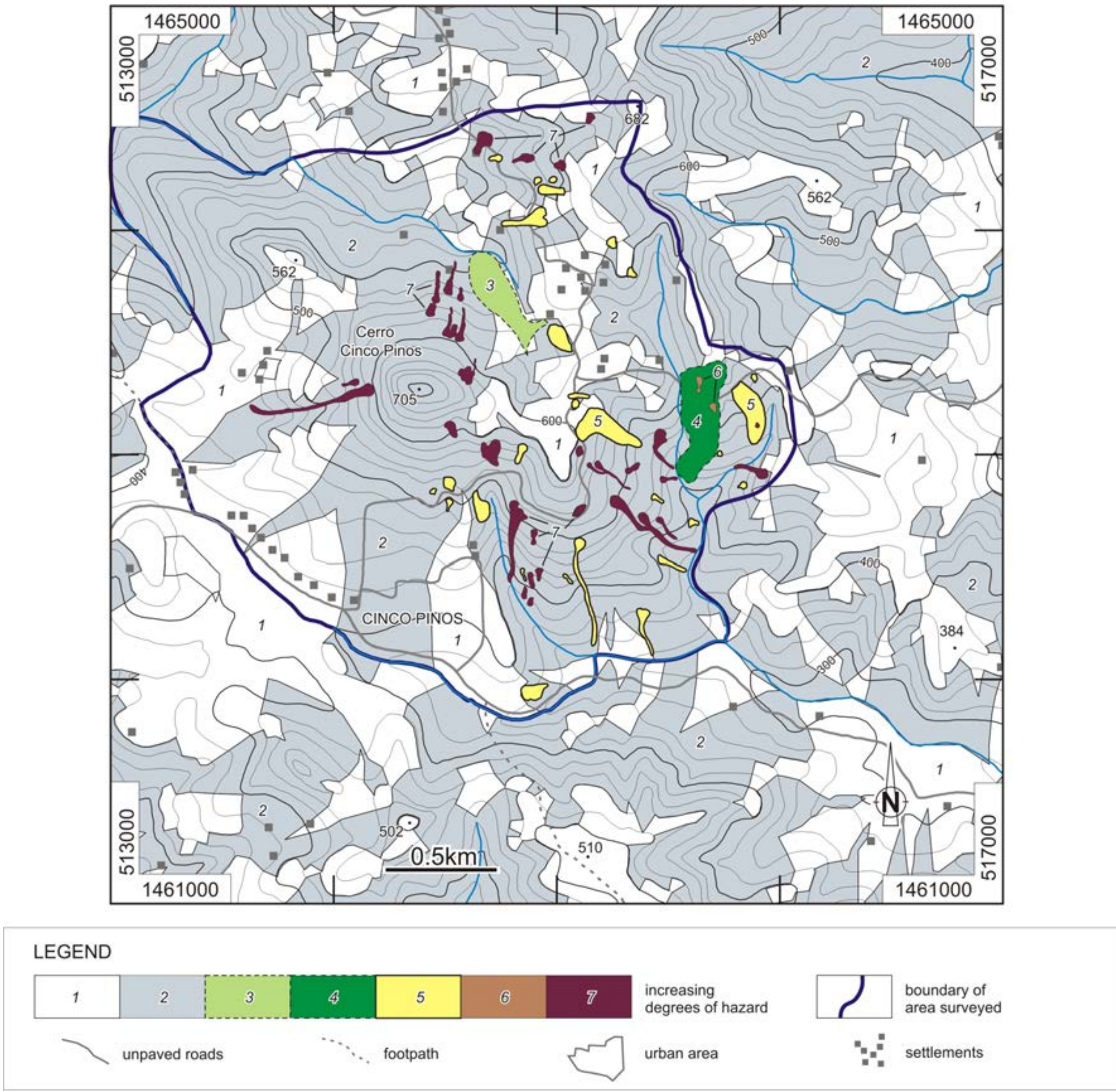

Fig. iv: Ejemplo del Mapa de Peligrosidad a los movimientos de masa correspondiente al área de Cinco Pinos

4. Discusión y conclusiones

La mayor limitación de esta metodología es la baja resolución de la topografía digital. Esta, se debe a la baja resolución del mapa topográfico 1:50.000 y a posibles errores cometidos durante el proceso de digitalización. Esta baja resolución repercute en una baja resolución del mapa de susceptibilidad obtenido y por ende, los límites entre zonas susceptibles y zonas no susceptibles se deben interpretar como una aproximación. Con la existencia de un Modelo Digital del Terreno de mayor resolución que la topografía digital obtenida, se podrían introducir en el análisis otros factores morfológicos que mejorarían sustancialmente los resultados.

Dado que los flujos de detritos son la tipología de movimientos mayoritaria, afectan un porcentaje importante del área de estudio y son muy difíciles de predecir, el análisis de peligrosidad se basa principalmente en la ocurrencia y la susceptibilidad de este tipo de movimientos.

Dado que para este análisis se han utilizado los deslizamientos generados por el huracán Mitch, el mapa de peligrosidad obtenido refleja la peligrosidad asociada a movimientos de masa desencadenados por lluvias intensas y no por movimientos sísmicos. Aunque el hecho de que este sea un evento extremo puede llevar a resultados conservadores, el análisis de los deslizamientos poco tiempo después del huracán aporta datos de alta calidad y confiere un factor de seguridad a los resultados.

Este estudio demuestra que una aproximación cualitativa a la peligrosidad es posible aun cuando el tipo y la calidad de los datos sean limitados. A pesar de la baja resolución del mapa de peligrosidad obtenido, la metodología es sencilla y de bajo coste y permite diferenciar entre zonas seguras y zonas no seguras. Esto proporciona información útil a las autoridades locales para el ordenamiento territorial y el diseño de planes de emergencia con el fin de reducir i mitigar la exposición al riesgo por movimientos de ladera.

B. Resumen de la publicación:

A feasible methodology for landslide susceptibility assessment in developing countries: a case-study of NW Nicaragua after Hurricane Mitch
(Metodología para el análisis de la susceptibilidad a los deslizamientos en países en vías de desarrollo: un caso de estudio en el NW de Nicaragua después del huracán Mitch)

Marta Guinau, Raimon Pallàs and Joan Manuel Vilaplana

RISKNAT Research Group
Departament de Geodinàmica i Geofísica, Facultat de Geologia, Universitat de Barcelona, Zona Universitària de Pedralbes, 08028, Barcelona, Spain

Publicado en; Engineering Geology, vol. 80 Nos. 3-4 (2005) pp. 316-327. ISSN 0013-7952

1. Introducción

Las consecuencias de los desastres naturales dependen de la magnitud del fenómeno y de la vulnerabilidad de los elementos expuestos (Alcántara-Ayala, 2002). Las condiciones en las que se encuentran los países en vías de desarrollo hacen que estos sean más vulnerables ante los desastres naturales que los países desarrollados. Por ende los efectos de los fenómenos naturales son más devastadores en estas zonas.

En las últimas décadas se han desarrollado gran cantidad de metodologías para el análisis de la peligrosidad natural para la prevención y mitigación de los desastres naturales (Brabb, 1984; Carrara et al., 1995; Soeters and van Westen, 1996). Teniendo en cuenta los recursos en países en vías de desarrollo la mayoría de estas metodologías involucran procesos estadísticos demasiado complejos que dificultan su aplicación y la interpretación de los resultados (Clerici, et al. 2002). Esto desvela la necesidad de probar metodologías sencillas y de bajo coste que puedan dar resultados fiables.

En 1998 el huracán Mitch afectó gran parte de Centro América generando deslizamientos (mayoritariamente flujos de detritos o corrientes de derrubios) e inundaciones. Estos fenómenos causaron considerables pérdidas humanas y materiales. Después de este evento se desarrollaron gran cantidad de proyectos para la recuperación y el desarrollo de las zonas más afatadas en los cuales se recogieron y generaron datos que, si bien no se obtenían con el fin de analizar la peligrosidad por movimientos de masa, podían ser útiles para ello.

Los objetivos de este trabajo son; 1) explorar la potencialidad de combinar datos específicos con datos preexistentes no específicos, para el análisis de la susceptibilidad a los movimientos de masa, y 2) mostrar una metodología sencilla y de bajo coste adaptada a las limitaciones de los países en vías de desarrollo, que sea útil para implementar estrategias no estructurales de mitigación del riesgo por movimientos de masa.

El área de estudio, con una extensión de 473Km2, comprende los municipios de San Pedro del Norte, Cinco Pinos, San Francisco del Norte, Santo Tomás del Norte y parte del municipio de Somotillo. Todos ellos en el Departamento de Chinandega, NW de Nicaragua (Fig. v). La zona está formada por rocas volcánicas e intrusiones plutónicas Terciarias. La mayoría de estas litologías están cubiertas por un manto de alteración hidrotermal. Las lluvias torrenciales del huracán Mitch en esta zona afectaron el 32% de la población generando considerables pérdidas humanas y materiales (Solidaridad Internacional, 2001).

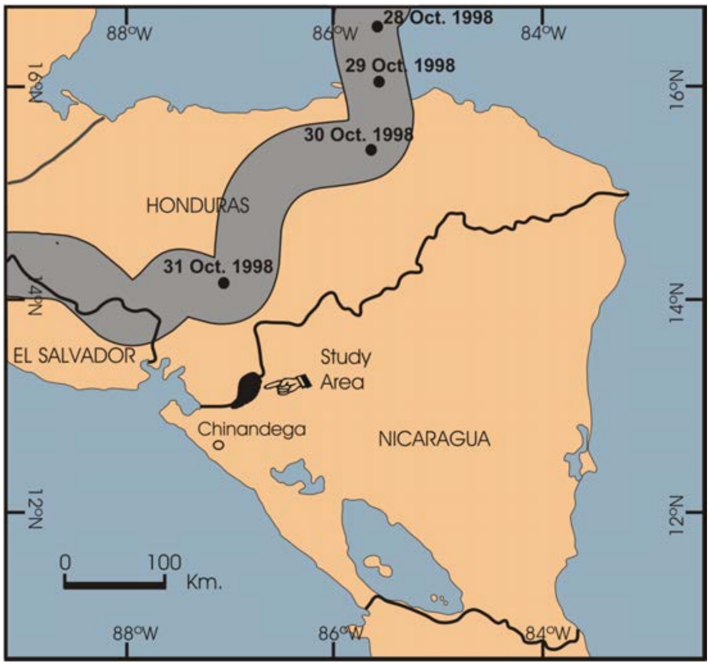

Fig. v: Localización del área de estudio (en negro) y la capital departamental, Chinandega. La franja gris muestra la trayectoria del huracán Mitch, basada en datos del USGS (1999).

2. Datos disponibles

En el área de estudio se dispone de dos tipos de datos para desarrollar una metodología de análisis y cartografía de la susceptibilidad a los movimientos de masa. 1) un inventario de movimientos de masa elaborado por un equipo en el que participó uno de los autores de este artículo, y 2) un mapa de unidades de terreno obtenido en un proyecto de desarrollo rural realizado por la ONG Solidaridad Internacional (Solidaridad Internacional, 2001).

A partir de la interpretación de fotos aéreas y de trabajo de campo se obtuvo un mapa-inventario de movimientos de masa a escala 1:10.000 en el cual se diferenciaron las zonas afectadas por rotura de los materiales, donde se inician los movimientos, de las zonas afectadas por la trayectoria y el depósito de los materiales movilizados.

El mapa de unidades de terreno también se obtuvo por fotointerpretación y trabajo de campo a escala 1:10.000. Cada unidad de terreno está formada por la combinación de 14 características del terreno. A partir de este mapa se pueden obtener diferentes mapas temáticos, cada uno de los cuales mostrando un factor del terreno determinado.

3. Metodología

El análisis de las características del terreno en zonas afectadas por inestabilidad, permite determinar zonas con características similares, las cuales serán propicias para el desarrollo de deslizamientos en el futuro. Estas zonas son zonas susceptibles a los movimientos de masa.

Entre los factores que condicionan los movimientos de masa hay que diferenciar entre los que condicionan la rotura de los materiales y los que condicionan el alcance de estos. Dado que en este estudio únicamente se han considerado las zonas de rotura o de inicio de los movimientos de masa, el mapa de susceptibilidad resultante indicará aquellas zonas susceptibles a la rotura de los materiales.

Para poder validar la capacidad predictiva del mapa de susceptibilidad obtenido es necesario disponer de dos eventos temporalmente diferentes. No obstante, la escasez de datos históricos obliga a escoger otro método para probar la validez del mapa resultante. En este estudio se optó por dividir el área de estudio en dos mitades, una para desarrollar la metodología y otra para probarla.

Teniendo en cuenta las observaciones realizadas en campo y los 14 factores del terreno representados en el mapa de unidades de terreno, se seleccionaron los siguientes factores condicionantes de la inestabilidad del terreno en el área de estudio; la pendiente, la litología, el grosor y la textura del suelo y el uso del suelo.

Mediante el Sistema de Información Geográfica (SIG) ArcView® se combinó el mapa de roturas con cada uno de los mapas temáticos correspondientes a cada uno de los factores condicionantes. Dado que cada factor está definido por un cierto número de clases, se calculó el porcentaje de área afectada por roturas en cada una de las clases. Posteriormente, para cada unidad de terreno se calculó la suma del porcentaje obtenido para cada clase de los diferentes factores condicionantes. El valor obtenido representa la propensión relativa de cada unidad de terreno a la rotura de los materiales. La clasificación de estos valores en intervalos permite definir clases de susceptibilidad, las cuales mediante el SIG, se representan en un mapa de susceptibilidad a la rotura (Fig. vi).

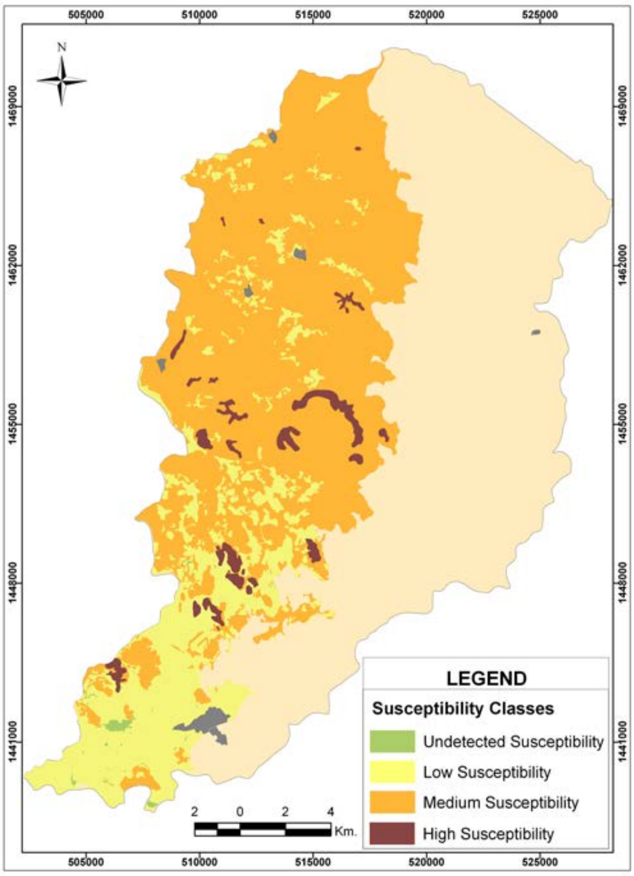

Fig. vi: Mapa de Susceptibilidad a la rotura de los materiales obtenido en el área de desarrollo.

Dado que las características del área de validación son similares a las del área de desarrollo de la metodología, los valores de porcentaje obtenidos en esta zona para cada clase de los diferentes factores condicionantes, se integraron en el área de validación para obtener el mapa de susceptibilidad en esta zona (Fig. viiA). Mediante el SIG, este mapa se comparó con las zonas de rotura en esta área y se calculó el porcentaje de área afectada por rotura en cada clase de susceptibilidad, respecto al porcentaje total de área afectada en toda el área de validación. Estos valores muestran una mayor concentración de zonas de rotura en áreas de susceptibilidad más alta, y van disminuyendo a medida que disminuye el grado de susceptibilidad. Esto permite corroborar que la metodología propuesta es adecuada para obtener mapas de susceptibilidad a los movimientos de masa en el área de estudio (Fig. viiB).

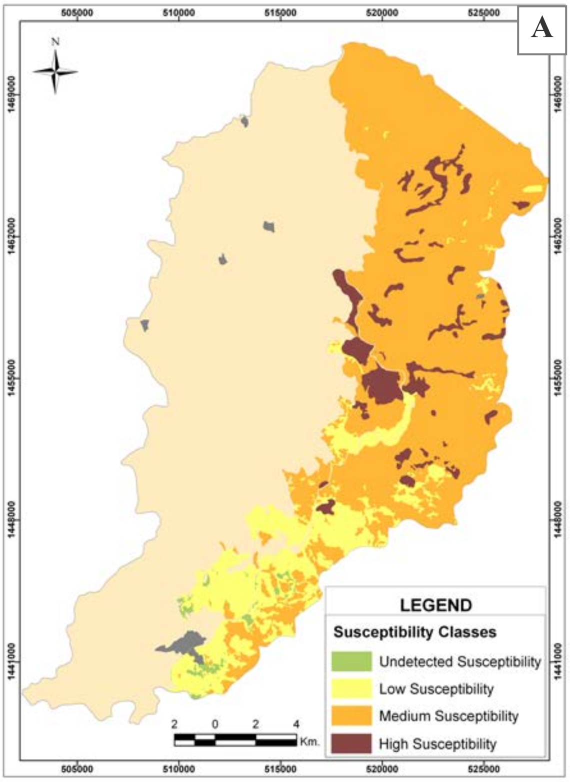

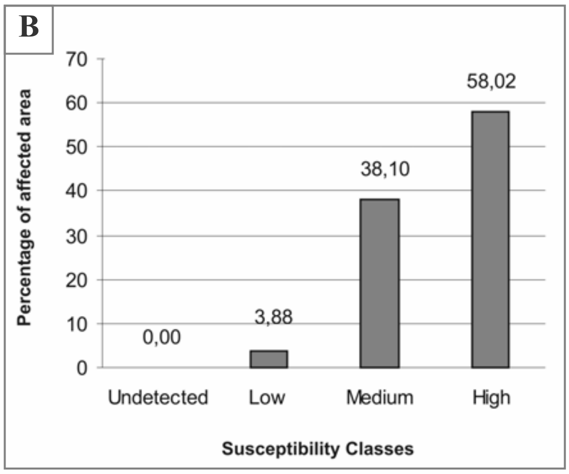

Fig. vii: A: Mapa de Susceptibilidad a la rotura de los materiales obtenido en el área de validación. B: Gráfico del porcentaje de área afectada por roturas en cada clase de susceptibilidad.

4. Discusión y conclusiones

Dado que para este estudio se han utilizado las zonas de inicio de flujos de detritos generados por el huracán Mitch, la metodología propuesta permite detectar zonas potenciales al inicio de flujos de detritos bajo los efectos de lluvias intensas. Esta metodología, complementada con un método basado en establecer trayectorias preferenciales de flujo, como el propuesto por Pallàs et al. (2004), puede aportar un documento útil para la mitigación del riesgo por flujos de detritos mediante la implementación de medidas no estructurales.

Una limitación del análisis de susceptibilidad propuesto es que considera los factores condicionantes independientes, mientras que en realidad estos factores interactúan entre ellos. Esta consideración puede producir una sobreestimación de la susceptibilidad i por ende los valores de susceptibilidad se deben entender como valores relativos y deben ser utilizados como índices cualitativos.

La principal dificultad para el análisis de la peligrosidad por movimientos de masa es la escasez de datos históricos, de campo e instrumentales, situación que se da especialmente en países en vías de desarrollo. Este estudio basado en la combinación de datos de campo de alta calidad y resolución y de datos no específicos a partir de los cuales se pueden extraer algunos de los factores que condicionan la inestabilidad del terreno, permite desarrollar un análisis consistente de la susceptibilidad. Aunque los resultados obtenidos son menos precisos que los obtenidos mediante procesos estadísticos complejos, la metodología propuesta es viable ante la escasez de datos disponibles y es fácil de aprender, comprender y aplicar por técnicos con conocimientos sobre análisis de deslizamientos pero sin un alto nivel de especialización en estadística. El mapa resultante permite separar áreas con diferente grado de susceptibilidad, lo cual se puede interpretar como una buena aproximación a la peligrosidad aplicable en regiones con limitaciones como las encontradas en muchos países en vías de desarrollo.

Cualquier estudio de susceptibilidad requiere algún tipo de validación. Cuando la división del área de estudio en dos zonas homogéneas es posible, la validación mediante un área de test diferenciada del área de desarrollo parece una buena opción cuando no se dispone de datos históricos. Este proceso de validación, a pesar de que no permite conocer la capacidad predictiva del mapa de susceptibilidad, permite comprobar el ajuste de los resultados con la distribución de zonas afectadas.

C. Resumen de la publicación:

GIS-based debris flow source and runout susceptibility assessment from DEM data. A case study in NW Nicaragua.

(Análisis SIG de la susceptibilidad al inicio y al alcance de flujos de detritos a partir de un MDT. Estudio de caso en el NW de Nicaragua)

M. Guinau (1), I. Vilajosana (1) and J.M. Vilaplana (1)

(1) RISKNAT Research Group, Departament de Geodinàmica i Geofísica, Facultat de Geologia, Universitat de Barcelona, Zona Universitària de Pedralbes, 08028, Barcelona, Spain.

Enviado a; Natural Hazards and Earth System Sciences. *NHESS* Print: ISSN 1561-8633 Online: ISSN 1684-9981

1. Introducción

La peligrosidad por movimientos de masa generalmente se define como la probabilidad de que se produzca un deslizamiento en un lugar y en un momento determinado. En algunas ocasiones, el análisis de la peligrosidad no es posible debido a les escasez de datos históricos (Remondo et al. 2003; Ayalew et al., 2005). En estos casos se utiliza la susceptibilidad como una aproximación a la peligrosidad. Los análisis de susceptibilidad asumen que los deslizamientos se producirán en condiciones similares a las que se han producido en el pasado (Varnes, 1984; Carrara et al. 1995) y por ende, el análisis de las características del terreno permite determinar zonas potencialmente inestables.

Para realizar un análisis completo de la susceptibilidad a los movimientos de masa se debe analizar por una parte, la susceptibilidad a la rotura de los materiales, la cual indica las zonas potenciales al inicio de los movimientos y por otra, la susceptibilidad al alcance, que indica las zonas potenciales de ser afectadas por el trayecto o la acumulación de los materiales movilizados.

En muchos países y sobretodo en países en vías de desarrollo, la escasez de datos de calidad, de fondos económicos y de personal especializado, dificultan los análisis de susceptibilidad y de peligrosidad. Esta situación requiere el desarrollo de metodologías sencillas y de bajo coste asequibles para estos países. En algunos países en vías de desarrollo se están implementando Sistemas de Información Geográfica (SIG) y se adquieren datos digitales, como los Modelos Digitales del Terreno (MDT), que aportan grandes ventajas en los análisis geoambientales.

Los objetivos de este estudio son; 1) desarrollar una metodología para la zonificación de la susceptibilidad a los movimientos de masa, integrando la susceptibilidad al inicio y la susceptibilidad al alcance, y 2) proporcionar una metodología sencilla y de bajo coste adaptada a las condiciones de muchos países en vías de desarrollo.

El área de estudio, con una extensión de 68Km2, comprende parte de los municipios de San Nicolás y Santa Rosa del Peñón, en los Departamentos de Estelí y León respectivamente, en el NW de Nicaragua (Fig. viii). Esta región está formada por rocas volcánicas e intrusiones plutónicas Terciarias, cubiertas por un manto de alteración de espesor muy variable y en algunas ocasiones por materiales coluviales. La zona, de clima tropical, está periódicamente afectada por tormentas tropicales y huracanes. En 1998 el huracán Mitch afectó gravemente el NW de Nicaragua, generando miles de movimientos de masa y graves inundaciones.

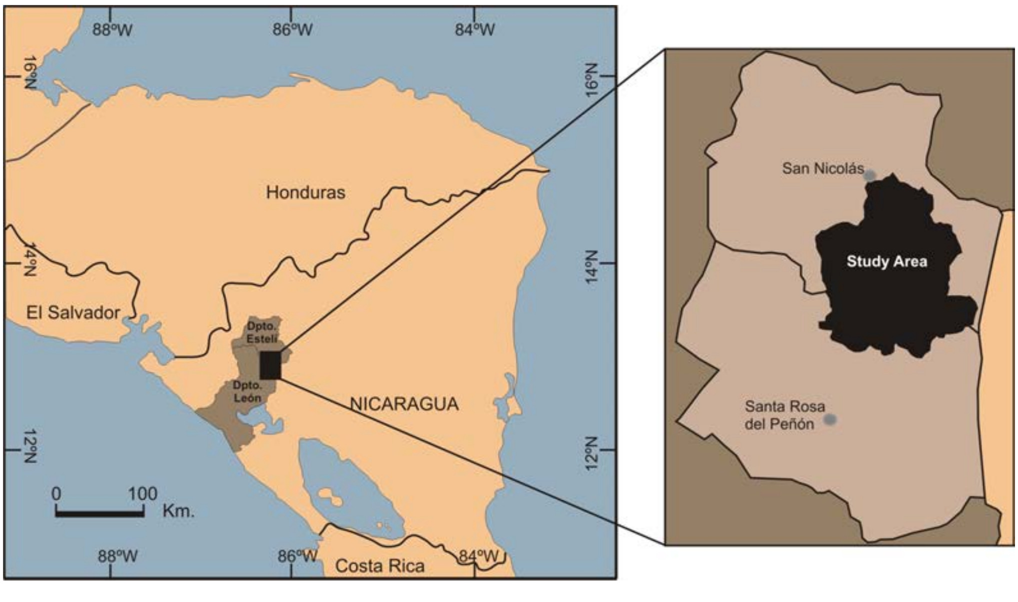

Fig. viii: Localización de los Departamentos de Estelí y León en el NW de Nicaragua. En la ampliación, el área de estudio (en negro) y las localidades citadas en el texto.

En el área de estudio se dispone de dos tipos de datos que permiten el análisis de la susceptibilidad a los movimientos de ladera. Por una parte un MDT y por otra un inventario de deslizamientos elaborado específicamente para este análisis. Este inventarió se representó en un mapa de movimientos de ladera en el cual se diferencian las zonas de rotura de los materiales y las zonas afectadas por el trayecto y la acumulación de los materiales movilizados. A partir de observaciones de campo se terminó la tipologia de los movimientos (mayoritariamente flujos de detritos) y los factores condicionantes de la inestabilidad de los materiales.

2. Análisis de la susceptibilidad a la rotura de los materiales

Dado que en el área de estudio no se dispone de mapas geoambientales, para el análisis de la susceptibilidad a la rotura de los materiales se seleccionaron 4 factores geométricos, que se pueden extraer directamente del MDT y que condicionan la inestabilidad del terreno. Estos factores son; la pendiente, el aspecto (orientación de las laderas), la curvatura planar (curvatura del terreno perpendicular a la dirección de la pendiente) y la curvatura planar (curvatura en la dirección de la pendiente). Para cada uno de estos factores se define un número determinado de clases.

Para poder validar la metodología es necesario disponer de un evento diferente al utilizado para el desarrollo de la metodología. Dado que en el área de estudio no se dispone de datos históricos ni de un evento posterior al huracán Mitch, se dividió el área en una zona de desarrollo y una zona de validación.

En el área de desarrolló, y mediante un SIG, se combinó cada factor condicionante con el mapa de roturas para determinar la influencia de cada clase a la inestabilidad del terreno. Para cuantificar esta influencia se aplicó la siguiente fórmula, desarrollada por Yin and Yan (1988) y utilizada por van Westen (1993) i Saha et al. (2005);

$$Wi = \text{Log}\,[(\text{DensClass}) / (\text{DensTot})]$$

Donde, DensClass es la densidad de roturas en cada clase y DensTot es la densidad de roturas en toda el área de desarrollo.

Una vez calculada la influencia para cada clase se superponen los 4 factores condicionantes y con la suma de los grados de influencia correspondientes en cada píxel se obtuvo el índice de susceptibilidad a la rotura.

Los valores de influencia de cada una de las clases para los 4 factores condicionantes se transfieren al área de validación con el fin de determinar el índice de susceptibilidad para cada píxel de esta zona. El mapa de índices de susceptibilidad obtenido se combinó con el mapa de roturas del área de validación y se calculó el porcentaje de roturas para cada índice de susceptibilidad. Con los valores de porcentaje acumulados se definieron 4 intervalos que definen las 4 clases de susceptibilidad; susceptibilidad muy baja (intervalo con el 0% de roturas), susceptibilidad baja (intervalo con el 10% de roturas), susceptibilidad media (intervalo con el 30% de roturas) y susceptibilidad alta (intervalo con el 60% de roturas). Estas 4 clases de susceptibilidad se utilizaron para zonificar la susceptibilidad a la rotura en toda el área de estudio (Fig. ix).

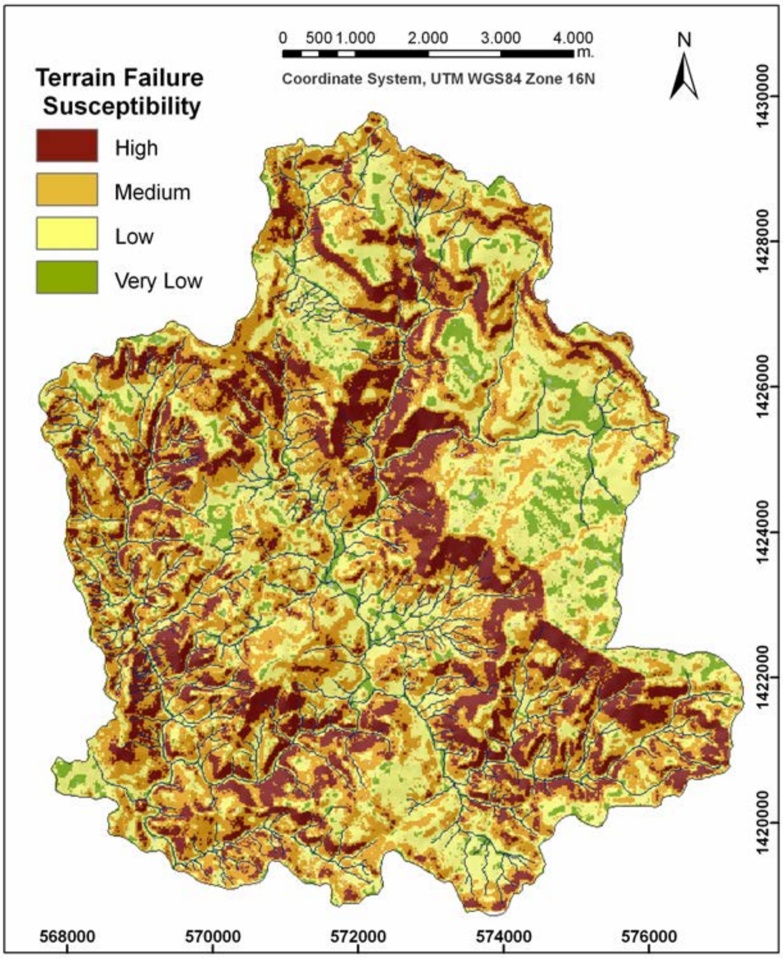

Fig. ix: Mapa de susceptibilidad a la rotura obtenido para toda el área de estudio.

Para validar la metodología se combinó el mapa de susceptibilidad del área de validación con el mapa de roturas de esta zona y se calculó la Densidad Relativa de Roturas (RFD) para cada clase de susceptibilidad;

$$RFD_i = 100 \text{ x } (DensClass_i) / \sum_i^n (DensClass_i)$$

Donde, DensClassi es la densidad de roturas en cada clase de susceptibilidad y n es el número de clases de susceptibilidad.

Los resultados obtenidos muestran un descenso de la densidad de roturas des de las zonas con susceptibilidad alta a las de susceptibilidad muy baja, lo que nos permite interpretar un buen ajuste del modelo a la distribución de roturas de los materiales.

3. Análisis de la susceptibilidad al alcance

Para determinar las zonas potenciales de ser afectadas por el alcance de los materiales movilizados se tiene en cuenta que bajo la influencia de lluvias intensas, los flujos de detritos tienden a circular siguiendo la máxima pendiente des de la zona de salida hasta confluir con la red de drenaje (Montgomery & Dietrich, 1994; Pallàs et al., 2004; Guinau et al., 2005). En este estudio se propone un método basado en el software libre TauDEM desarrollado por Tarboton (1997), disponible en Internet (http://www.engineering.usu.edu/dtarb/taudem). Este software, que se puede ejecutar como una extensión del SIG ArcGIS, dispone de un conjunto de herramientas para el análisis de procesos hidrológicos a partir de un MDT. En este estudio se utilizaron dos de estas herramientas; 1) Flow Direction (D∞), para determinar las direcciones de flujo de cada píxel en función de la pendiente hacia los píxeles de alrededor, y 2) Downslope Influence (DI), para determinar la trayectoria del flujo a partir de una zona de salida determinada, teniendo en cuenta las direcciones de flujo de cada píxel.

Para calibrar el ajuste del modelo con el comportamiento real de los flujos de detritos, se calcularon las trayectorias de flujo a partir de cada uno de los píxeles correspondientes a una rotura producida por el huracán Mitch y que posteriormente hubiera evolucionado a un flujo de detritos. Con las herramientas del TauDEM se obtiene un archivo raster en el cual los píxeles afectados por trayectorias de flujo tienen valores diferentes de 0 y los píxeles externos a las trayectorias tiene valor 0. Comparando las trayectorias obtenidas con el modelo y las trayectorias de los flujos del Mitch se observó que con el modelo se obtiene una sobreestimación de las zonas afectadas por el alcance de los materiales. Para cuantificar esta sobreestimación se calculó la Densidad Relativa de área afectada por flujos de detritos durante el Mitch respecto los diferentes valores de DI obtenidos con el modelo (RRD);

$$RRD_i = 100x(DensDI_i)/\sum(DensDI_i)$$

Con los valores obtenidos se pudo determinar que para valores de DI ≥0.05 la densidad de zona de alcance del huracán Mitch supera el 10%, valor que se tomó como límite para definir las zonas susceptibles al alcance (donde DI ≥0.05) y las zonas no susceptibles (donde DI <0.05). De esta manera se reduce la sobreestimación del modelo.

Una vez calibrado el modelo se analizó la susceptibilidad al alcance a partir de las zonas susceptibles a la rotura. Cada clase de susceptibilidad a la rotura se representa en un archivo raster diferente, en el cual los píxeles susceptibles se identificaron con el valor 1 y los no susceptibles con el valor 0. Para cada uno de estos archivos y mediente la herramienta DI del TauDEM se determinaron las zonas de circulación de flujo, considerando como zonas de salida los píxeles susceptibles a la rotura (identificados con el valor 1). Una vez obtenidos los valores de DI para cada píxel, se clasificaron como zonas susceptibles al alcance de los flujos aquellos píxeles con DI ≥ 0.05. Dado que este proceso se realiza para cada archivo raster correspondiente a cada clase de susceptibilidad a la rotura, y que se trabaja con 4 clases de susceptibilidad, al final de este proceso se obtienen 4 archivos raster en los cuales se identificaron los píxeles no susceptibles con el valor 0 y los susceptibles con un valor diferente en función de si la susceptibilidad al alcance se ha calculado a partir de zonas de susceptibilidad alta (valor 4), media (valor 3), baja (valor 2) o muy baja (valor 1). De esta manera se pudieron combinar los archivos resultantes para obtener el mapa final de susceptibilidad al alcance, en el cual los píxeles se clasificaron en 4 clases de susceptibilidad teniendo en cuenta que en cada píxel dominara el valor más alto asignado entre los 4 archivos (Fig. x).

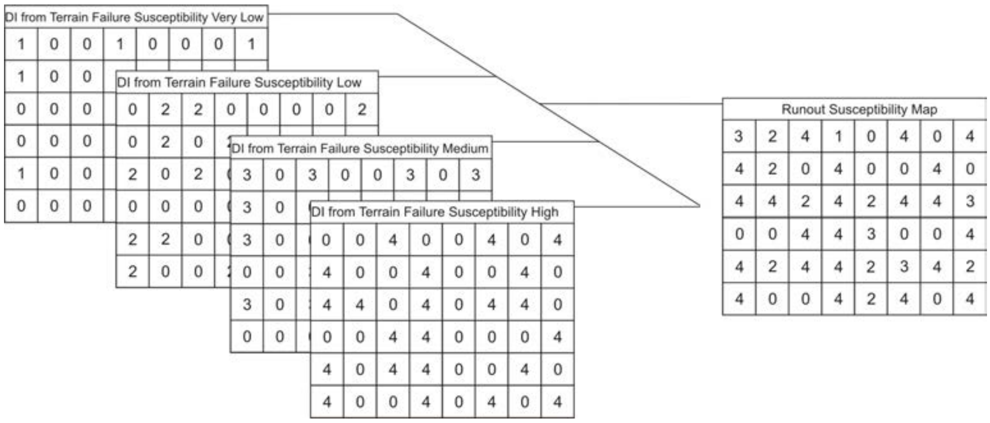

Fig. x: Representación grafica de la combinación de los 4 archivos raster obtenidos después de calcular las trayectorias de flujo a partir de cada clase de susceptibilidad a la rotura. Con la combinación de los 4 archivos raster se obtiene el mapa de susceptibilidad al alcance donde los píxeles se clasifican en 4 clases de susceptibilidad.

Finalmente, con el fin de validar la metodología, el mapa de susceptibilidad al alcance (Fig. xi) se combinó con el mapa de zonas afectadas por trayectorias de flujos de detritos durante el Mitch, para calcular la densidad relativa de zonas afectadas por flujos en el Mitch en cada clase de susceptibilidad al alcance con la siguiente fórmula (RRD);

$$RRD_i = 100 \times (DensClass_i) / \sum_i^n (DensClass_i)$$

Los resultados obtenidos muestran una mayor concentración de zonas afectadas por flujos del Mitch en las áreas con susceptibilidad alta.

4. Integración de la susceptibilidad a la rotura y la susceptibilidad al alcance

Para obtener una zonificación integrada de la susceptibilidad a los flujos de detritos se debe combinar la susceptibilidad a la rotura y la susceptibilidad al alcance. Para combinar las dos susceptibilidades se utilizó una matriz de doble entrada con las 4 clases de susceptibilidad a la rotura en las columnas y las de susceptibilidad al alcance en las filas. Dado que para tener una zona afectada por el alcance de los flujos de detritos es estrictamente necesario tener una rotura previa, se han asignado valores con un orden de magnitud mayor a las clases de susceptibilidad a la rotura (Fig. xii). Para cada píxel del área de estudio se obtuvo el valor de susceptibilidad global sumando los valores correspondientes a cada susceptibilidad. Finalmente se obtiene un mapa de susceptibilidad a los flujos de detritos con 4 clases de susceptibilidad (Fig. xiii).

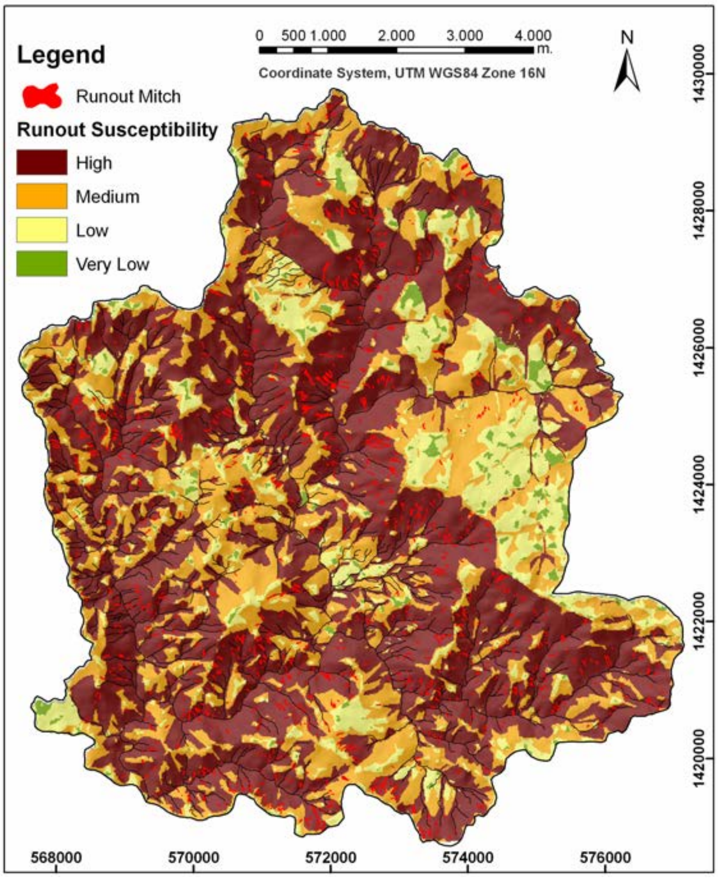

Fig. xi: Mapa de susceptibilidad al alcance obtenido para toda el área de estudio.

El mapa de susceptibilidad obtenido se compara con las zonas afectadas por flujos de detritos durante el huracán Mitch y se observa la distribución de estas áreas en cada clase de susceptibilidad. Esta distribución aporta información útil para determinar el uso del suelo más adecuado para cada clase de susceptibilidad con el fin de mitigar el riesgo causado por los flujos de detritos.

Failure Susceptibility / Runout Susceptibility	High 40	Medium 30	Low 20	Very Low 10
High 4	44	34	24	14
Medium 3	43	33	23	13
Low 2	42	23	22	12
Very Low 1	41	31	21	11

Fig. xii: Matriz de doble entrada para la combinación de la susceptibilidad a la rotura y la susceptibilidad al alcance.

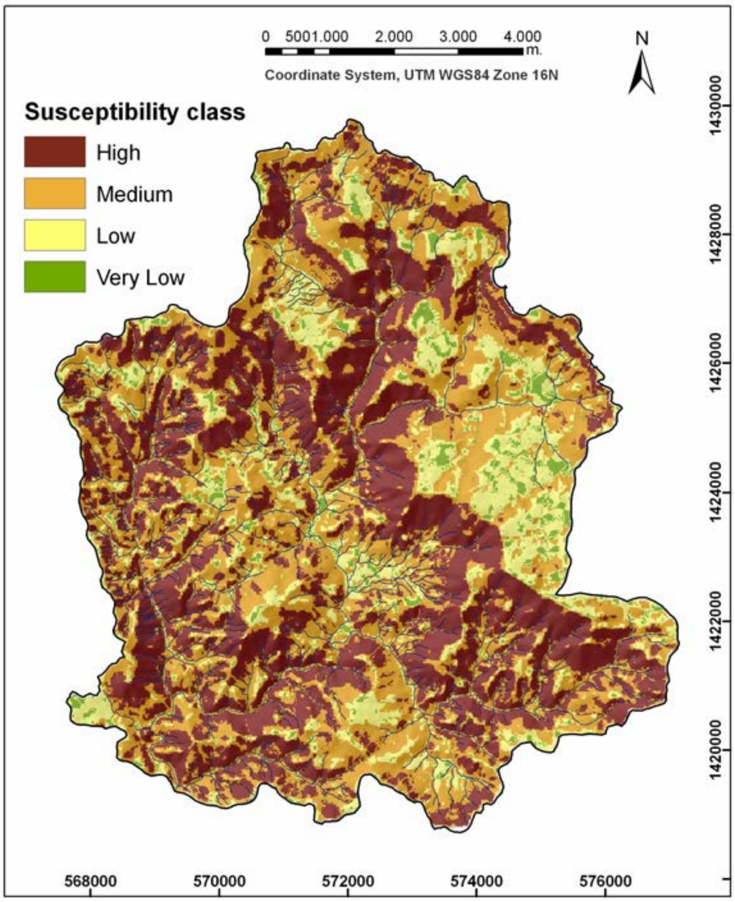

Fig. xiii: Mapa de susceptibilidad a los flujos de detritos obtenido en el área de estudio

5. Discusión y conclusiones

Dado que para este estudio se utilizaron los flujos de detritos causados por el huracán Mitch, los mapas de susceptibilidad resultantes muestran las áreas potenciales a ser afectadas por flujos de detritos bajo la influencia de lluvias intensas. Aunque el Mitch sea un evento extremo en le área de estudio y esto pueda llevar a resultados conservadores se debe considerar el hecho de que confiere un grado de seguridad en los resultados.

A pesar de que los métodos estadísticos multivariantes confieren resultados más precisos que los obtenidos en este estudio, son métodos que utilizan procesos analíticos complejos y largos y requieren conocimientos específicos, características que los hacen inviables teniendo en cuenta los recursos que se encuentran en los países en vías de desarrollo. Por ende, consideramos que el método bivariante, a pesar de sus limitaciones, es el más sencillo y razonable para determinar la susceptibilidad a los deslizamientos como una aproximación a la peligrosidad en regiones con recursos limitados.

La escasez de datos geoambientales es una limitación para el análisis de la susceptibilidad. No obstante, a partir de un MDT se pueden extraer parámetros geométricos como la pendiente, el aspecto, la curvatura del terreno, etc. que condicionan la inestabilidad del terreno y que permiten una zonificación consistente de la susceptibilidad.

El comportamiento de los flujos de detritos depende de muchos factores difíciles de analizar y por ende la determinación de las posibles trayectorias y alcances es muy compleja. La extensión TauDEM permite determinar trayectorias de flujo siguiendo la máxima pendiente des de zonas de salida potenciales hasta la red de drenaje. Teniendo en cuenta que en el área de estudio los flujos de detritos no siempre alcanzan la red de drenaje, el modelo produce una sobreestimación del área de alcance que se debe tener en cuenta a la hora de interpretar los resultados. Con el proceso de calibración del modelo se consigue reducir la sobreestimación producida por el propio modelo y así ajustar un poco los resultados de este al comportamiento real de los flujos de detritos. A pesar de que ni la resolución del modelo ni los datos disponibles son los mejores para obtener una modelización ajustada a la realidad, este modelo parece una buena opción para determinar áreas potenciales al alcance de flujos de detritos y puede ser útil en zonas con escasez de recursos para mitigar el riesgo generado por este fenómeno.

El proceso de validación utilizado para comprobar el modelo de análisis de la susceptibilidad a la rotura, basado en la división del área de estudio, es una buena opción en aquellas áreas donde únicamente se dispone de un evento de referencia. No obstante, este proceso sólo aporta información sobre el ajuste del modelo y no sobre la capacidad predicativa del mapa de susceptibilidad obtenido. Los resultados de este proceso sugieren que una acurada selección de parámetros geométricos a partir de un MDT y la aplicación de funciones sencillas para determinar el grado de influencia de estos factores en la inestabilidad del terreno, permiten detectar zonas potenciales al inicio de flujos de detritos.

En el caso de la susceptibilidad al alcance, los resultados de la validación muestran un buen ajuste del modelo. No obstante, las zonas de susceptibilidad alta y media ocupan una extensión considerable, hecho que puede suponer un inconveniente para la planificación territorial. Este resultado se refleja también en la zonificación de la susceptibilidad final donde se integran la susceptibilidad a la rotura y al alcance. Aunque esta zonificación no parezca demasiado precisa puede ser útil para proponer normas de uso del suelo teniendo en cuenta la estructura socioeconómica de la zona. Así, el uso más adecuado para las zonas de susceptibilidad alta podría ser el uso forestal y el uso agrícola para las zonas con susceptibilidad media. Teniendo en cuenta que los asentamientos son reducidos y dispersos, se podrían reservar para las zonas con susceptibilidad baja y las zonas de susceptibilidad muy baja se podrían destinar para la ubicación de escuelas e iglesias, dado que estos edificios se ocupan como refugio en momentos de emergencia.

II- ORIGINAL DE LAS PUBLICACIONES

Available online at www.sciencedirect.com
SCIENCE DIRECT®
Engineering Geology 72 (2004) 57–72
ENGINEERING GEOLOGY
www.elsevier.com/locate/enggeo

A pragmatic approach to debris flow hazard mapping in areas affected by Hurricane Mitch: example from NW Nicaragua

Raimon Pallàs[a,*], Joan Manuel Vilaplana[a], Marta Guinau[a], Ester Falgàs[a], Xavier Alemany[a], Angélica Muñoz[b]

[a] RISKNAT Research Group, Departament de Geodinàmica i Geofísica, Facultat de Geologia, Universitat de Barcelona, Zona Universitària de Pedralbes, 08028 Barcelona, Spain
[b] Centro de Investigaciones Geocientíficas, CIGEO, Universidad Nacional Autónoma de Nicaragua, Managua, Nicaragua

Received 15 November 2002; accepted 18 June 2003

Abstract

Although developing countries are vulnerable to landslide hazard, they generally lack policies for hazard assessment and mitigation. This may be attributed to the scarcity of good quality data on which to base any sound hazard assessment in addition to insufficient funds and lack of political will. Thus, there is an urgent need for developing feasible methodologies of landslide hazard assessment and mitigation, which can be readily tested and implemented under the conditions found in these countries. To this end, we selected an area of about 20 km^2 badly affected by Hurricane Mitch in October 1998, in the Departamento de Chinandega (NW Nicaragua). Mass movements (mainly debris flows) produced during the Hurricane Mitch rainfall event were investigated using two sets of aerial photographs at 1:60,000 and 1:40,000 scales. Data concerning regolith composition and thickness, landslide dimensions, failure slope angle and land use were obtained for 150 mass movements, and over 450 landslides were mapped at 1:10,000 scale in the field. A pragmatic approach was used to produce a qualitative hazard (sensu lato) assessment, based on the concepts of *number of events recorded*, *predictability* and *susceptibility*. This case study shows that a hazard assessment that is useful for management may be possible even where data are limited. Despite its inherent limitations, similar pragmatic approaches could help the sustainable development of other rural and sparsely populated areas of Central America.

Keywords: Landslide mapping; Landslide hazard mapping; Debris flows; Developing countries; Nicaragua

1. Introduction

Developing countries are prone to natural disasters. Not only are these countries situated in areas exposed to geological and climatic hazards, but they are also, and most importantly, vulnerable to socio-economic factors (Alcántara-Ayala, 2002, in press). These countries pay a high price in human life, loss of fertile soils and pasture land as well as destruction of property and infrastructure. Given that the infrastructure is generally basic and relatively inexpensive, economic loss due to natural hazards in developing countries is smaller than in industrialised ones (Alexander, 1995; McGuire et al., 2002). Nevertheless,

* Corresponding author. Tel.: +34-93-403-59-13; fax: +34-93-402-13-40.
E-mail address: raimonpallas@ub.edu (R. Pallàs).

0013-7952/$ - see front matter
doi:10.1016/j.enggeo.2003.06.002

these comparatively small losses still correspond to a large proportion of their GDP (Alexander, 1995; Alcántara-Ayala, 2002), resulting in long periods of recovery, which severely slow down or prevent growth in the long term. Although natural disasters are clearly a limiting factor for societal and economic growth, developing countries often lack policies for disaster prevention and mitigation.

Landslides cause loss of life and much devastation. They are widespread in areas prone to extreme rainfall and/or areas susceptible to seismic shaking, commonplace conditions in many developing countries. Loss of life attributed to earthquakes is, in many cases, caused by the devastating effect of seismically triggered landslides (Carrara et al. 1999; Guzzetti, 2000; Bommer and Rodríguez, 2002). This implies that mass movements are probably responsible for many more casualties than is generally recognised.

Developing countries are in urgent need of feasible methodologies of landslide hazard assessment and mitigation. *Feasibility* means that the methodologies should be simple and inexpensive, so that they can be learned and readily applied to large territories by governmental or nongovernmental agencies. The aim of the present paper is to provide a feasible approach to hazard mapping centred in a test area in the Departamento de Chinandega, NW Nicaragua.

1.1. Study area

The study area is located in the Interior Highlands of Nicaragua (Fig. 1), an extensive and heavily dissected volcanic plateau (Mc Birney and Williams, 1965; Fenzl, 1988). This region is mainly formed of Tertiary volcanic rocks of the Matagalpa and Coyol groups (Weyl, 1980), and sparse Tertiary plutonic intrusions (unpublished maps). The Oligocene Matagalpa Group is mainly characterised by rhyolitic to dacitic pyroclastic flows and falls, and rare epiclastic deposits, whereas the Miocene–Pliocene Coyol Group is dominated by basaltic to rhyolitic lavas, breccias, lahars and pyroclastic flows (Ehrenborg, 1996). The volcanic succession is cut by extensional faults and basaltic to rhyolitic dikes, and is affected by low-grade burial metamorphism and, locally, by strong hydrothermal alteration (Darce et al., 1989; Ehrenborg 1996). Due to the relatively complex geology, and the fact that bedrock exposures are scarce due to thick regolith and vegetation cover, geological mapping is poor in most areas, including the one under study.

Fig. 1. Location of the study area and localities referred to in the text. The path of Hurricane Mitch is shown in dark grey, based on USGS (1999) data.

Our pilot study is focused on the Cinco Pinos and San Francisco del Norte municipalities (Departamento de Chinandega). The area displays a hilly landscape and is 300 to 700 m in altitude (Fig. 2). It began to be settled approximately one century ago, and since then most of what used to be thickly forested land has been converted into bush land (about 50% of the area), degraded pastures (about 30%), agricultural fields (15%) and open forest (3%) (Consorcio-BIT, 1999b). The economy, which is among the poorest in the country, is based on subsistence corn, bean and cereal agriculture, and, to a lesser extent, on cattle (Consorcio-BIT, 1999b). The two municipalities number over 14,800 inhabitants (Consorcio-BIT, 1999a,b). The environment is being subjected to increasing pressure given the considerable demographic growth of the last decades. Traditionally, settlements were sparse, and construction materials consisted of locally available adobe and wood. Present demographic pressure is

Fig. 2. General aspect of the study area. View looking west from Cerro Chávez (Fig. 4C). Cerro Morroñoso is on the left, and Cerro Nancital on the background. White patches correspond to large debris flows and areas affected by rockfalls, which were triggered by Hurricane Mitch.

producing a rapid shift towards small and denser concentrations of housing promoted by international nongovernmental organisations.

At about 13°N latitude, the region is affected by a savannah climate, with a marked dry season (November to April), which accounts for only about 10% of the annual rainfall (Fenzl, 1988). Like many regions in Nicaragua, Honduras and in El Salvador, the area under study was severely affected by Hurricane Mitch between 28 and 31 October 1998 (USGS, 1999, Fig. 1). In 10 days, 1597 mm were registered in Chinandega, corresponding to 86% of the local mean annual rainfall (INETER, 1998). Based on rainfall data from 1966 to 1998, the return period of the Hurricane Mitch rainfall event was calculated as greater than 100 years for Chinandega (INETER, 1998). The exceptional rainfall event associated with Hurricane Mitch caused extensive damage in the Departamento de Chinandega because of flooding and landsliding. In the Cinco Pinos and San Francisco area, landsliding was the main destructive process experienced, with an estimated 32% of the total population affected by property loss or damage (Solidaridad Internacional, unpublished data).

2. Data and methods

The 1:50,000 topographic base (INETER, 1990) was enlarged by a conventional large-format copier to 1:20,000 scale and was digitised. Printouts of the resulting digital base were plotted at 1:10,000 scale to facilitate mapping tasks in the field. Two black and white aerial photographs sets were available: (1) a 1:40,000 flight from 11 January 1996 (prior to Hurricane Mitch, hereafter referred to as *pre-Mitch*) and (2) a 1:60,000 flight from 4 December 1998 (1 month after Hurricane Mitch, hereafter referred to as *post-Mitch*) (Fig. 3). A detailed study of these two sets of photographs allowed a pre-selection of interesting localities.

Landslide mapping was restricted to three areas (Fig. 4A–C), covering a total area of 19.9 km^2. These target localities were selected on the basis of (1) high landslide density, (2) varied bedrock, (3) presence of vulnerable elements such as settlements and roads, (4) wide range in landslide typology and size, and (5) relatively good accessibility.

Bedrock is generally covered by in situ regolith and/or colluvial soil. Regolith in plutonic areas was sandy, highly porous, commonly including granite corestones, and had a yellowish colour. This was

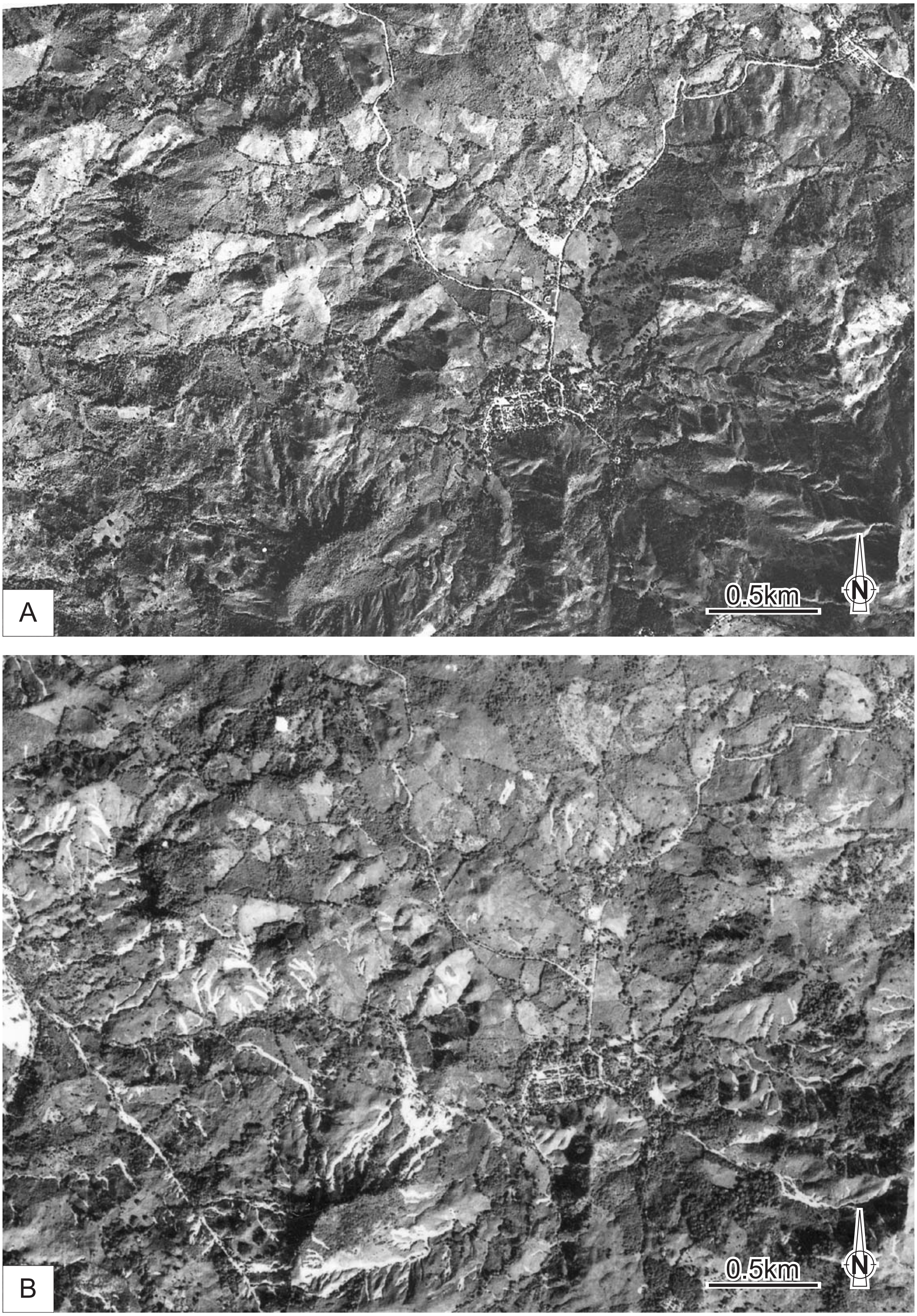
A
0.5km
N
B
0.5km
N

clearly distinguishable from regolith in volcanic areas, which had a finer texture and was dark brown to reddish in colour. Volcanic regolith displayed homogeneous features regardless of specific lithologies. Superimposed on the regolith, most outcrops showed a widespread pervasive colluvium, consisting of massive diamicton, which included angular to subangular rock fragments of local lithologies, ranging up to block size, in a sandy to lutitic matrix.

Two years after Hurricane Mitch, most large to medium mass movement scars were still clearly visible on the landscape and were easily mapped in the field. In contrast, most accumulation areas and small landslides were already overgrown with vegetation, and could only be detected as highly reflective areas in the post-Mitch aerial photographs (Fig. 3B). Moreover, the pre-Mitch aerial photographs, despite the vegetation cover, showed scars, gullies and irregular lobated slopes, revealing extensive slope instability older than 1998. Systematic enquiries to locals about pre-Mitch instability events yielded little information, probably because of the relatively recent settlement in most areas, and because of the overwhelming memory of the Hurricane Mitch event. Qualitative temporal information on landslide activity was reflected in the landslide inventory map (Fig. 4A–C) to show which mass movements corresponded to instability prior to Hurricane Mitch, which ones were associated with Hurricane Mitch, and which were active in both periods (i.e. reactivated).

A range of landslide typologies was observed, including debris flows, earth flows, and rockfalls (classification based on Varnes, 1978). Debris flows were characterised by curved crown scarps (sometimes showing some translational slide blocks at the crown), a large length-to-width ratio, and a lack of clear morphology in the accumulation areas. Earth flows were large mass movements ($>60 \times 10^3$ m^2) with small length-to-width ratios characterised by lobated accumulation areas, and showing, in some cases, a rotational slide component at the head. Areas affected by rockfall were restricted to steep sloping bedrock outcrops, locally involving accumulation of large volumes of fresh angular bedrock fragments. Debris flows were the most abundant type of mass movement, accounting for 98% of the 458 landslides mapped and affecting 1.54×10^6 m^2. Earth flows and areas affected by rockfalls shared the remaining 2% of the total landslides mapped, affecting 0.65×10^6 and 0.73×10^6 m^2, respectively.

Apart from mapping the type, extent and timing of landslides, field work was aimed at obtaining a large number of in situ observations and measurements in the source area. Slope angles at debris flow scars were measured with the aim of establishing the original topographic gradient where failures occurred. Measurements were taken visually by a clinometer along the escarpment flank, as observed from the opposite flank, with an accuracy of $\pm 2°$. Slope angles at 130 debris flow scars were measured, 97 corresponding to areas with volcanic bedrock and 33 corresponding to areas with plutonic bedrock. Debris flow volumes were deduced by estimating scar length, width and depth, and ranged from several tens of cubic metres to 10^5 m^3.

3. Data analysis and interpretation

3.1. Materials affected by instability

The homogeneity of regolith in volcanic areas suggests that the weathering patterns of the volcanic rock types found in this area may yield relatively homogeneous results, probably resulting in similar behaviour with regard to slope instability. This justifies a distinction of bedrock lithologies limited to two generic types: volcanic and plutonic.

The regolith has a maximum measured thickness of 2.5 m, and is commonly covered by a widespread sheet of colluvium, with a measured thickness ranging between 0.1 and 2.5 m. The fact that it supports a well developed organic soil and is often present under thickly forested areas is indicative of former long-term (Pleistocene? or Holocene?) slope activity.

Fig. 3. Cropped and enlarged aerial photographs corresponding to the San Francisco del Norte area (Fig. 4C). Compare photograph (A), taken prior to Hurricane Mitch, from (B) taken after Hurricane Mitch. White patches on (b) correspond to large debris flows and areas affected by rockfalls triggered by Hurricane Mitch. Graphic scale is approximate. The area is illuminated from the south; rotate 180° for easier relief appreciation.

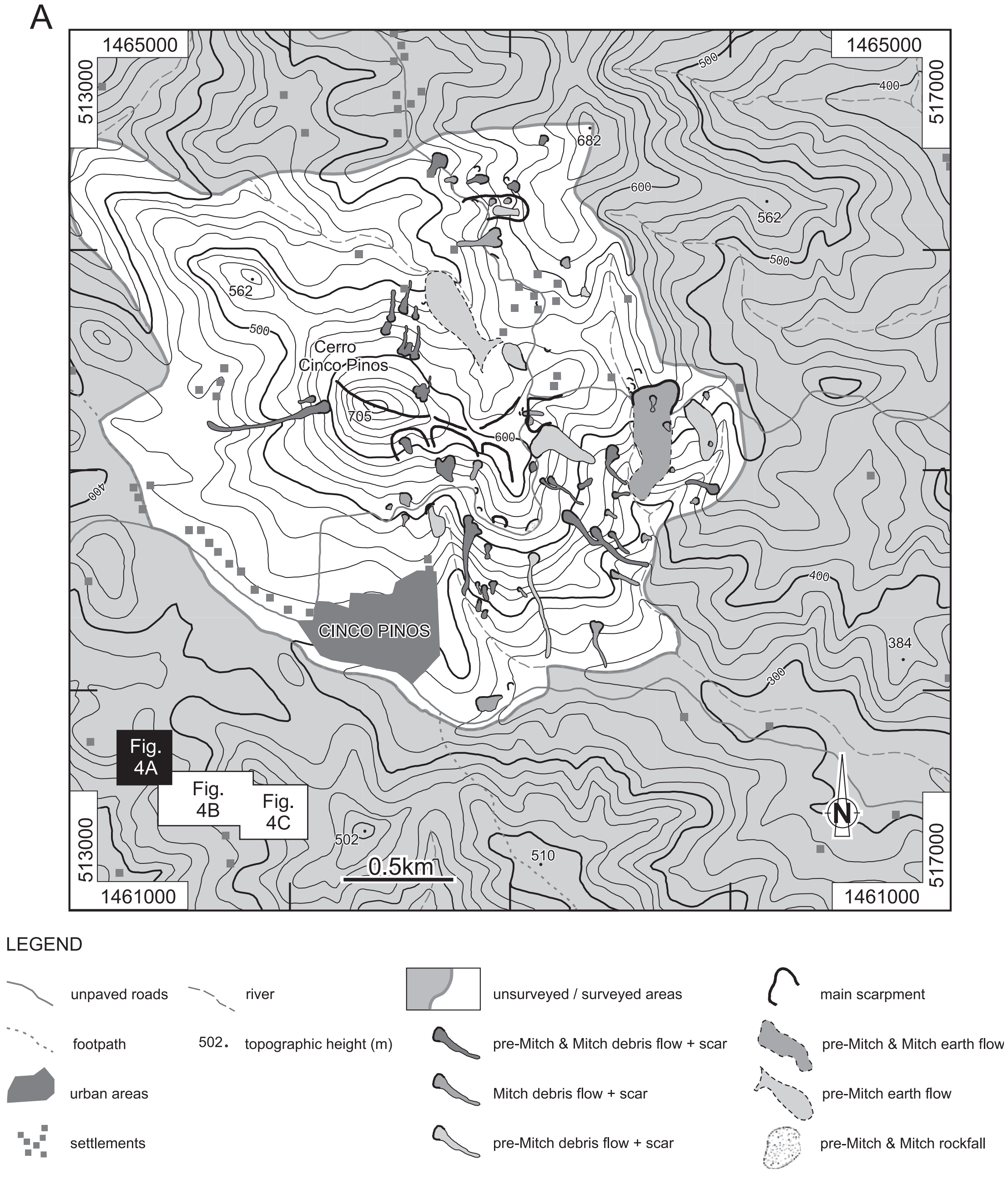

Fig. 4. (A) Landslide inventory map of the Cinco Pinos area. Elevations are in m, and coordinates are Transverse Mercator. (B) Landslide inventory map of the Cerro San Diego and El Nancital areas. Elevations are in m, and coordinates are Transverse Mercator. (C) Landslide inventory map of the San Francisco del Norte area. Elevations are in m, and coordinates are Transverse Mercator.

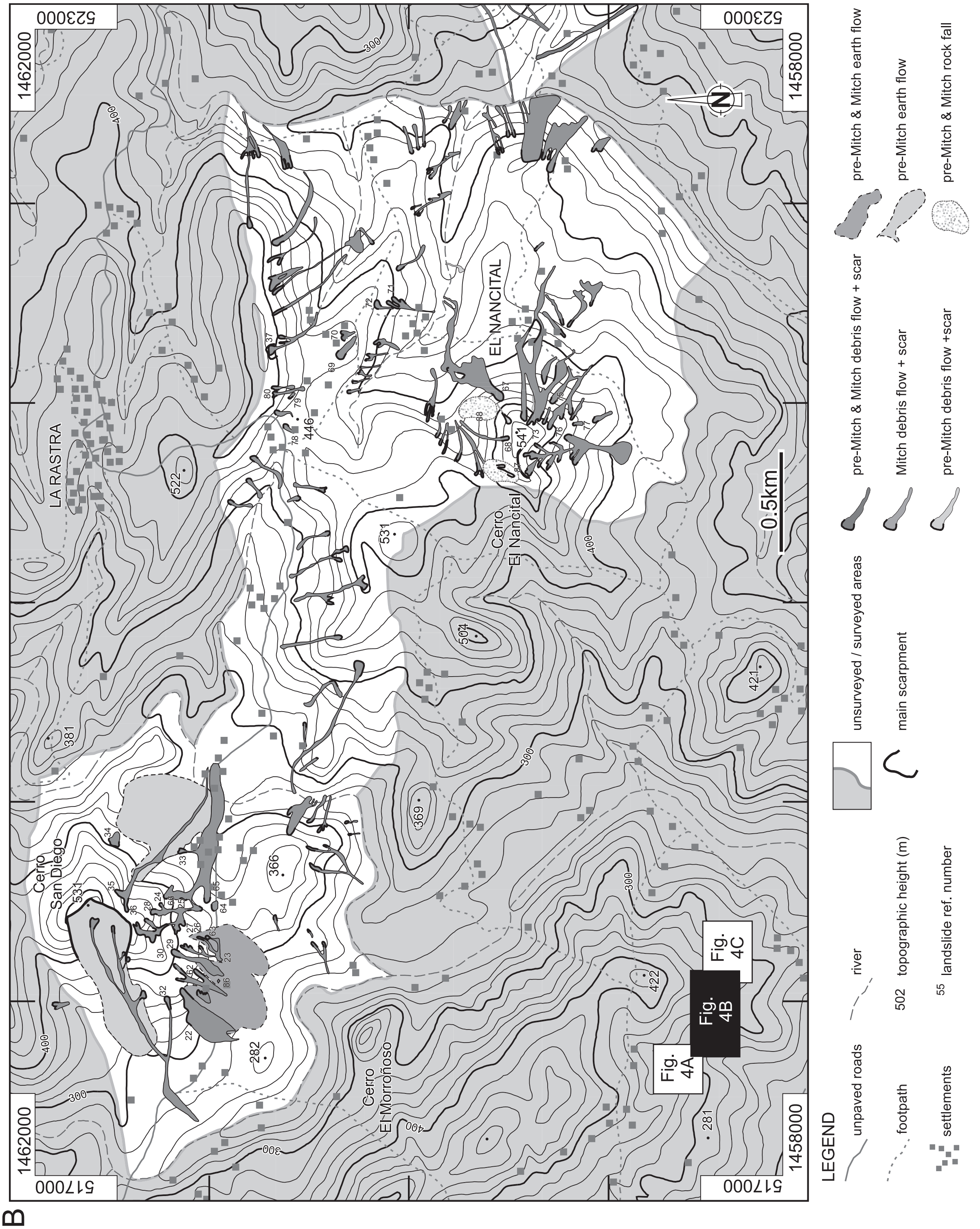

Fig. 4 (*continued*).

Fig. 4 (*continued*).

Landslides in the area generally affect colluvium (where present), and part or all of the regolith. The accumulation areas of large debris flows often show large blocks (up to several metres in diameter) derived from corestones included in the original regolith. Bedrock is rarely entrained, and only in the areas affected by rockfalls.

3.2. Typologies of mass movements: occurrence

Single debris flows were smaller than single earth flows and than the areas affected by rockfalls, but debris flows were the most widespread and most common landslide typology (98% of mapped landslides). The abundance of debris flows observed during Hurricane Mitch is evidence that this must be the favoured rainfall-induced landslide type in this region. According to the post-Mitch aerial photographs and to information obtained through enquiries with locals, most debris flows active during Hurricane Mitch travelled long distances, merging into the drainage network. Thus, there must have been a gradual transition between debris flows, hyperconcentrated flow, and fluvial bedload. Although landslide types other than debris flows are extensive, they are of local occurrence.

3.3. Failure angle of debris flows

When considering both volcanic and plutonic bedrock areas, the sample of 130 measured debris flow failure angles ranged from 20° to 49°. To detect any difference in behaviour between volcanic and plutonic bedrock areas, both subsamples were plotted separately (Fig. 5). To determine the areas with slope angles susceptible to failure, we must focus on the lowest angles of the total range rather than on the central values of the population. The plutonic subsample is close to a normal distribution, with the exception of a sharp drop in frequency at angles lower than 25°, with no angles measured in the 20–24° range. This may be due to undersampling, or to the fact that slopes below 25° may be underrepresented in plutonic areas. This suggests that the lower values of the population may be around 20° not only for volcanic bedrock but also for plutonic bedrock areas. Thus, 20° may be taken as the threshold stability angle of debris flows triggered by the rainfall conditions experienced during the Hurricane Mitch event.

4. Approach to hazard (sensu lato) analysis

The concept of natural hazard, as defined by Varnes (1984), refers to the probability of occurrence of a potentially damaging phenomenon within a given area and within a given period of time. It is generally acknowledged that this definition involves the concepts of *geographical location*, *magnitude* and *frequency* of events (e.g. Guzzetti et al., 1999). In the study area, quantitative information is not available to establish the magnitude or frequency of landslides and, hence,

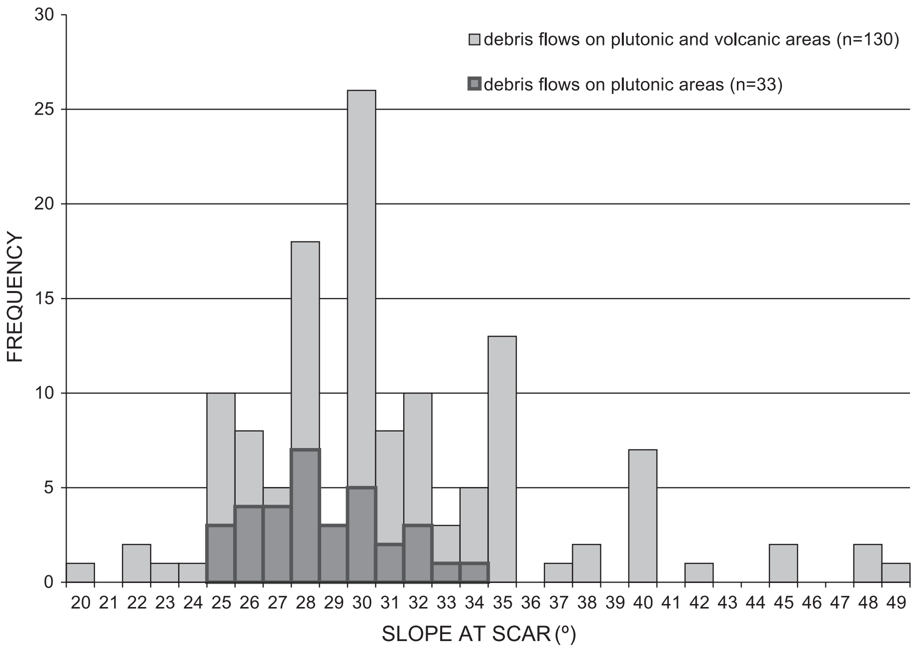

Fig. 5. Frequency distribution of debris flow failure angles measured in the field. The histogram in dark-grey corresponds to angles measured both in volcanic and plutonic areas. The superimposed histogram in white corresponds to angles measured in plutonic bedrock areas.

hazard cannot be quantified. To map areas with different degrees of exposure to potentially hazardous phenomena, we adopt a pragmatic approach based on a combination of concepts which are related to hazard and to some extent to vulnerability. While acknowledging that the concepts included in our analysis do not conform with the strict definition of *hazard*, we use, in the present paper, the term *hazard* (sensu lato) to refer to exposure to potentially damaging mass movements once preventive action (such as regular inspection of unstable areas and implementation of a warning system) has been taken. The term *risk* is not used in the absence of a comprehensive vulnerability assessment. In this section, the main ideas and limitations underlying our hazard (sensu lato) analysis are discussed, including the concepts of magnitude, frequency, number of events recorded, predictability and susceptibility.

4.1. Ruling out the application of magnitude

In principle, large magnitude landslides will be more hazardous than smaller ones. Nevertheless, the extreme fragility of all man-made structures found in the area implies that total destruction can occur whatever the magnitude of a destructive phenomenon; even the smallest magnitude phenomenon observed has the potential for causing extensive damage and loss of life. This means that in this specific case the concept of magnitude is not of practical use for differentiating between degrees of hazard.

4.2. Number of events recorded as an approach to frequency

Quantification of landslide hazard implies determining the *frequency* of instability phenomena. If several sets of aerial photographs are used, the frequency of slope failures can be determined (e.g. Guzzetti et al., 1994; Ibsen and Brunsden, 1996). Given the fact that only two sets of photographs are available in the study area, only a qualitative and imprecise approach to the temporal behaviour of mass movements can be attempted. The concept closest to frequency that can be estimated in this case is the *number of events recorded*; slopes which failed several times in the past may be considered more hazardous than slopes which failed only once. Thus, in descending order of a hazard scale, slopes can be classified as (1) *two events recorded* (i.e. pre-Mitch + Mitch), (2) *one event recorded* (i.e. pre-Mitch or Mitch) and (3) *no event recorded*.

4.3. Predictability

Providing that the areas prone to landsliding are monitored (e.g. inspection by trained locals) and that some kind of warning system is implemented, the most hazardous mass movements are the ones which activate rapidly, without giving any external warning signs. Mass movements which start slowly and provide some warning indicators (e.g. slow movement, tilting of trees or houses, opening of cracks) may be considered less hazardous since they allow sufficient time for evacuation. This concept will be referred to here as *predictability*. In descending order of a hazard scale, slopes can be classified in the study area as follows: (1) *non-warning*, including debris flows and rockfalls; and (2) *warning*, including earth flows.

4.4. Susceptibility

The concepts of *number of recorded events* and *predictability* introduced above may be useful for a qualitative hazard assessment of areas where past mass movements had been detected. Nevertheless, areas where no activity has been previously detected may also be prone to instability and should be considered in the hazard analysis. We include these areas in the analysis using the concept of *susceptibility*, defined as the probability of occurrence of a landslide event (Dai et al., 2002). The susceptibility of a slope to failure will be high if it has the same combination of instability factors as the areas that failed several times in the past. Rainfall-triggered debris flows may be affected by a complex combination of topographic, lithologic, and land use factors (Dai et al., 1999; Zhou et al., 2002; Lorente et al., 2002). Thus, the relationship between these factors would need to be addressed to establish the susceptibility of a slope to debris flows. Such a quantitative susceptibility analysis falls outside the scope of the present study given the lack of data. Nevertheless, a simplified qualitative approach to susceptibility is still possible. Based on the range of slope gradients measured in the field, we can assume that debris flows are more likely to occur on slopes above a certain gradient threshold. This is the case, at least, when an extremely intense trigger (such as Hurricane Mitch) is used as the reference event. Although this might also be true for other factors, such as distance to divide, or contributing area (Baeza and Corominas, 1996), we focused our attention on the topographic gradient because it is simple to measure and readily available in the field and from a DTM. According to the sample of debris flow failure angles, the threshold above which debris flows may occur during extreme rainfall events in the study area can be established at around 20°. Thus, as a first approach, slopes with gradients equal to or greater than 20° can be considered as susceptible to failure, and could act as source areas for debris flows. The areas susceptible to debris flows

Fig. 6. Example of the susceptibility map corresponding to the Cinco Pinos area (locality in Fig. 4A). Areas highlighted in grey correspond to the ones sloping equal to or higher than 20°, and are the ones considered susceptible to failure. Flow lines correspond to possible debris flow paths, taking the areas highlighted in grey and mapped scars as possible source areas. See text for detailed discussion.

include these source areas together with the runout zone. Accordingly, in descending order of the hazard scale, we are able to differentiate between the areas that are (1) *susceptible*, and those that are (2) *non-susceptible* to debris flows.

5. Approach to hazard mapping

5.1. Determining the areas potentially prone to debris flows

A Digital Terrain Model (DTM) was obtained from the digitised 1:50,000 topographic map (contour spacing of 20 m), and a Triangle Irregular Network (TIN) was generated. The TIN model included all the original data points digitised from contour lines, talveg break lines and single elevation points, with no filtering. Based on the TIN model, a slope map was constructed to highlight areas with topographic gradients equal to or higher than 20°. These are the areas considered to be susceptible to debris flow failure. The problem of estimating the runout distance of landslides can be simplified by considering the fact that, in these areas and under intense rainfall events, debris flows tend to travel long distances merging with the drainage network. Debris flows follow the maximum slope and often grade to hyperconcentrated flows and to fluvial bedload while maintaining or increasing most of their destructive power. Flow lines were generated automatically following the maximum slope of the TIN facets, starting from the areas highlighted in the slope map (those considered susceptible to failure, Fig. 6). The starting points were selected by hand to obtain the widest possible assemblage of flow lines for each slope. The resulting flow

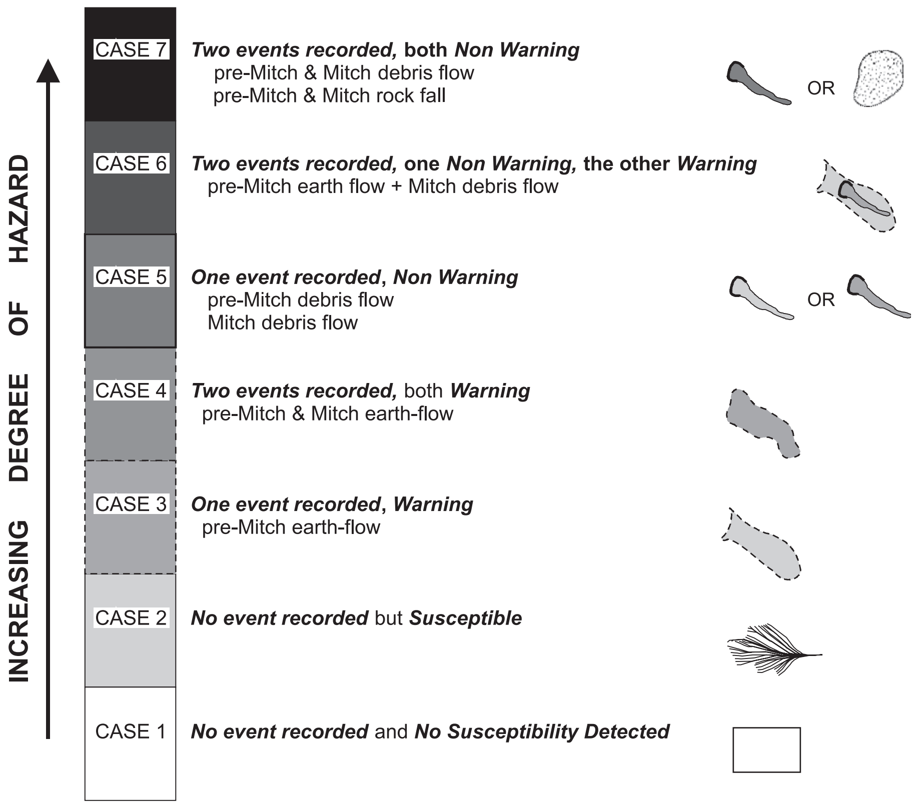

Fig. 7. Range of possible cases from higher to lower hazard. The symbols at the right-hand side are in correspondence with the legend in Fig. 4. Different cases, 1 to 7, correspond to the seven degrees of hazard distinguished in the hazard map (Fig. 8). See detailed discussion in text.

lines merged together along the drainage network and their downslope length was only limited by the extent of the DTM (Fig. 6). The areas potentially affected by debris flows correspond to the union of areas sloping $\geq 20°$ and the areas crossed by the flow lines.

In principle, an accurate DTM should produce a slope map in which the debris flow scars measured in the field should always coincide with the highlighted $\geq 20°$ range. Comparison of the mapped scars and the highlighted areas in the slope map (Fig. 6) reveals that 28% of the scars do not match the slope areas in the model. This indicates that the DTM does not describe all the relevant topographic variations in sufficient detail for an accurate slope map to be constructed. A second set of flow lines were generated using the mapped scars as possible source areas in order to

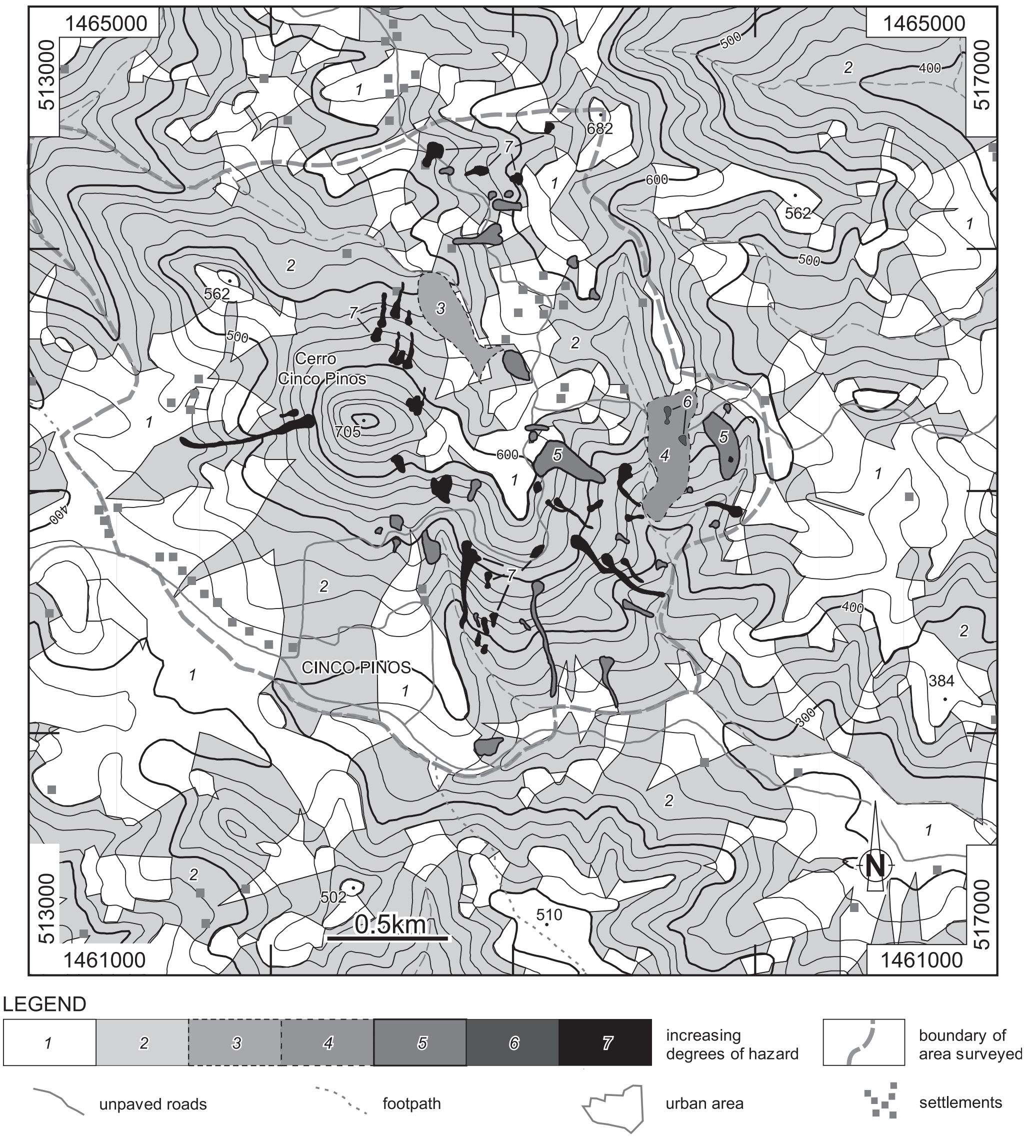

Fig. 8. Example of the landslide hazard map corresponding to the Cinco Pinos area (locality in Fig. 4A). See detailed discussion in text.

minimise the effect of the low resolution of the DTM (Fig. 6).

5.2. Constructing the landslide hazard map

In the study area, there are three concepts which can be used to qualitatively establish different degrees of hazard: *number of events recorded*, *predictability* and *susceptibility*. Each of these concepts allows us to differentiate between a number of situations, and their combination yields seven cases which can be ranked on a hazard scale (summarised in Fig. 7). Cases 1 and 2 correspond to areas with no recorded activity, whereas Cases 3 to 7 correspond to areas where past mass movements had been detected. Note that areas classed as *one event recorded* but showing some *non-warning* phenomena (Case 3) were considered more hazardous than areas classed as *two events recorded* but showing only *warning* landslides (Case 4). The order of the seven cases forms the basis for the construction of the hazard map (Fig. 8).

6. Discussion

Throughout the process of the hazard map generation, there were a number of key steps in which errors were inevitably introduced. Despite the care taken throughout the generation of the DTM, subsequent checking showed maximum horizontal discrepancies of about 15 m between the original and the digitised contours. These inaccuracies, introduced in the copying and digitising stages, may have produced errors as large as $\pm 5°$ for slopes around 20° in the angles calculated from the DTM. Although substantial, these errors occurred only locally. The mismatch between mapped scars and the slope map discussed in Section 5.1 is mainly due to a much more important limitation: the low resolution of the 1:50,000 topographic base. This is the source of the low resolution of the DTM and the source of the low resolution of the susceptibility map (Fig. 6). As a result, the boundaries between *susceptible* and *nonsusceptible* areas in the hazard map can only be seen as approximate.

The final hazard assessment is mainly based on the occurrence of and susceptibility to debris flows. This is in accordance with the (1) much larger proportion of debris flows (98%) triggered by rainfall events, (2) their large extent (affecting the 7.7% of the area surveyed) and (3) their low predictability. Of less relevance are rockfalls, which may be extensive and also difficult to predict, but which are restricted to the few areas where steep bedrock crops out. Earth flows also affect relatively large areas, but their contribution to hazard is relatively small because they occur only locally, and because their reactivation can be predicted if a simple warning system is implemented.

The present study implicitly uses the Hurricane Mitch rainfall event as a reference. Both the landslide map and the susceptibility map (Figs. 4 and 6) are based on data taken from landslides triggered during Hurricane Mitch. For example, all the measurements on slope angles have been taken from debris flows triggered by this extreme rainfall event. Slopes with gradients exceeding 20° could be more than sufficiently stable under most rainfall events and could be triggered only during extreme events such as Hurricane Mitch. Thus, the resulting hazard map (Fig. 8) should be seen as covering worst-scenario cases, involving rainfall intensities similar to the reference event. Obviously, if the recurrence interval of the reference event was very large, the resulting hazard map would be excessively pessimistic, would impose unnecessary constraints on management decisions, and would have the drawback of becoming costly. Nevertheless, the return period of around 100 years estimated for Hurricane Mitch rainfall at meteorological stations in the proximity can be considered suitable for the present assessment. In addition, the worst-scenario approach adopted has the advantage of providing a reassuring safety factor.

Despite the fact that Nicaragua is an area prone to seismicity, the mapping presented in this paper is only based on rainfall-triggered landslides. The possibility of earthquake-induced landsliding was not taken into account, which limits the validity of the resulting hazard assessment. In principle, there is a greater likelihood of seismic triggering of landslides during the wet season in the study area, when hydrologic conditions are more suitable. The preferred mass movement typologies triggered by earthquakes could differ considerably from those produced during rainfall events (Jibson, 1996). Some old (prior to Hurricane Mitch) and large landslides observed in the study area could have been triggered by seismic events rather than by rainfall. This could be the case of those mass movements not necessarily involving large amounts of water, such as earth flows and rockfalls. Nevertheless, according to Bommer and Rodríguez (2002), earthquakes in Nicaragua tend to trigger landslides over very small areas, suggesting that seismic triggering may be less relevant than in other areas of Central America.

It is commonly acknowledged that loss due to landslides can be considerably reduced by effective planning and management, which includes (1) restriction of development in susceptible areas, (2) development of warning systems, and (3) stabilisation of landslide areas by engineering works (Dai et al., 2002). The last line of action is not realistic in the study area given the large areas susceptible to landsliding, and the lack of funds. The approach and mapping presented in this paper could be implemented in management decisions and emergency planning in accordance with local needs. For example, new buildings and services could be restricted to areas where susceptibility has not been detected, while a local warning system and evacuation strategy could be developed for areas susceptible to landslides.

7. Conclusion

The most limiting aspect of the methodology suggested here is the low resolution of the DTM used to deduce the areas susceptible to debris flows. The same methodology could produce more reliable results if topographic maps at a resolution higher than 1:50,000 were available. A higher resolution DTM would permit further improvements by introducing into the analysis other morphological factors, such as the contributing areas to debris flow scars.

The most hazardous landslides in the study area are debris flows because they are the most widespread type of mass movement and because they are difficult to predict. The fact that landslide hazard is largely based on the occurrence of a single type of mass movement allows us to make a relatively simple approach to hazard assessment.

Landslide assessment is highly improved if an extreme event such as Hurricane Mitch can be used as a reference. Using extreme events has the advantage of providing a safety factor in hazard estimation. It is highly advisable to take full advantage of extreme events in order to produce consistent and complete landslide inventory maps. It is of paramount importance to undertake aerial photograph coverages immediately after any significant landslide-triggering event. If the effects of such extreme events are recorded and studied in detail immediately after their occurrence, a great deal of information and the opportunity of providing future hazard assessments with good quality data will not be lost.

The hazard map provided should reflect the hazard associated with landslides triggered only by rainfall. Although probably small, the seismic contribution to landslide hazard was not assessed.

On the basis of a pragmatic approach a qualitative hazard assessment is still possible in some cases even though the amount and type of data available is rather limited. Our approach has the advantage of being cost-effective and, although the resolution of the hazard map is low, the methodology is most helpful in highlighting the areas that are likely to be safe. This provides the local decision makers with guidelines on the areas to be settled, and on the most suitable land uses. Moreover, the information provided is useful for planning emergency strategies, and for raising the population's awareness of landslide hazard. We believe that a pragmatic and simplified approach similar to the one presented in this study could be helpful in reducing human and material loss in other rural areas of Nicaragua, Honduras and El Salvador.

Acknowledgements

Funding was provided by Fundació Solidaritat UB, the Departament de Geologia Dinàmica i Geofísica (Universitat de Barcelona), and Generalitat de Catalunya (research group SGR2001-0081). Field work would not have been possible without the logistic support given by the Centro de Investigaciones Geocientíficas, CIGEO (Universidad Nacional Autónoma de Nicaragua, Managua). We warmly thank the municipalities and people of Cinco Pinos and San Francisco del Norte for providing accommodation and support during the field work. The manuscript was significantly improved thanks to the reviews by F. Guzzetti and J. Bommer.

References

Alcántara-Ayala, I., 2002. Geomorphology, natural hazards, vulnerability and prevention of natural disasters in developing countries. Geomorphology 47, 107–124.

Alexander, D., 1995. A survey of the field of natural hazards and disaster studies. Geographical Information Systems in Assessing Natural Hazards. Kluwer Academic Publishing, Dordrecht, The Netherlands, pp. 1–19.

Baeza, C., Corominas, J., 1996. Assessment of shallow landslides susceptibility by means of statistical techniques. In: Senneset, K. (Ed.), Landslides/Glissements de terrain—Proceedings of the 7th International Symposium on Landslides, Trondheim, Norway, 17–21 June 1996, vol. 7. A.A. Balkema, Rotterdam. 196 pp.

Bommer, J.J., Rodríguez, C.E., 2002. Earthquake-induced landslides in Central America. Engineering Geology 63, 189–220.

Carrara, A., Guzzetti, F., Cardinali, M., Reichenbach, P., 1999. Use of GIS technology in the prediction and monitoring of landslide hazard. Natural Hazards 20, 117–135.

Consorcio BIT, 1999a. Plan de Desarrollo Municipal de San Francisco del Norte, Departamento de Chinandega. 47 pp. Unpublished report.

Consorcio BIT, 1999b. Plan de Desarrollo Municipal de San Juan de Cinco Pinos 200-2004. 71 pp. Unpublished report.

Dai, F.C., Lee, C.F., Wang-Sijing, 1999. Analysis of rainstorm-induced slide-debris flows on natural terrain of Lantau Island, Hong Kong. Engineering Geology 51, 279–290.

Dai, F.C., Lee, C.F., Ngai, Y.Y., 2002. Landslide risk assessment and management: an overview. Engineering Geology 64, 65–87.

Darce, M., Levi, B., Nyström, J.O., Troëng, B., 1989. Alteration patterns in volcanic rocks within an east–west traverse through central Nicaragua. Journal of South American Earth Sciences 2, 155–161.

Ehrenborg, J., 1996. A new stratigraphy for the Tertiary volcanic rocks of the Nicaraguan Highland. GSA Bulletin 108, 830–842.

Fenzl, N., 1988. Nicaragua: Geografia, Clima, Geologia y Hidrogeologia. UFPA/INETER/INAN, Belém. 62 pp.

Guzzetti, F., 2000. Landslide fatalities and the evaluation of landslide risk in Italy. Engineering Geology 58, 89–107.

Guzzetti, F., Cardinali, M., Reichenbach, P., 1994. The AVI project: a bibliographical and archive inventory of landslides and floods in Italy. Environmental Management 18, 623–633.

Guzzetti, F., Carrara, A., Cardinali, M., Reichenbach, P., 1999. Landslide hazard evaluation: a review of current techniques and their application in a multi-scale study, Central Italy. Geomorphology 31, 181–216.

Jibson, R.W., 1996. Use of landslides for paleoseismic analysis. Engineering Geology 43, 291–323.

Ibsen, M.-L., Brunsden, D., 1996. The nature, use and problems of historical archives for temporal occurrence of landslides, with specific reference to south coast of Britain, Ventnor, Isle of Wight. Geomorphology 15, 241–258.

INETER, 1990. Nicaragua, Regiones I y II, Departamentos de Madriz y Chinandega, Cinco Pinos 2855-IV, 1:50.000.

INETER, 1998. Las lluvias del Siglo en Nicaragua. Instituto Nicaragüense de Estudios Territoriales, Managua, Nicaragua. 159 pp.

Lorente, A., García-Ruiz, J.M., Beguería, S., Arnáez, J., 2002. Factors explaining the spatial distribution of hillslope debris flows. Mountain Research and Development 22, 32–39.

Mc Birney, A.R., Williams, H., 1965. Volcanic history of Nicaragua. University of California Publications in Geological Sciences 55, 1–65.

McGuire, B., Mason, I., Kilburn, C., 2002. Natural Hazards and Environmental Change, Key Issues in Environmental Change. Arnold, London, UK. 187 pp.

USGS, 1999. Digital Atlas of Central America: Prepared in Response to Hurricane Mitch, Version 2, Vols. 1–2. <http://130.11.52.118/mitch/views/eventimpact.html>.

Varnes, D.J., 1978. Slope movement types and processes. In: Schuster, R.L., Krizek, R.l.J. (Eds.), Landslides Analysis and Control. TRB Special Report, vol. 176, pp. 11–33.

Varnes, D.J., 1984. Landslide hazard zonation: a review of principles and practice. IAEG Commission on Landslides and Other Mass-Movements. UNESCO Press, Paris. 63 pp.

Weyl, R., 1980. Geology of Central America. Gebrüder, Borntraeger, Berlin. 371 pp.

Zhou, C.H., Lee, C.F., Li, J., Xu, Z.W., 2002. On the spatial relationship between landslides and causative factors on Lantau Island, Hong Kong. Geomorphology 43, 197–207.

Available online at www.sciencedirect.com
SCIENCE DIRECT®
ELSEVIER
Engineering Geology 80 (2005) 316–327
ENGINEERING GEOLOGY
www.elsevier.com/locate/enggeo

A feasible methodology for landslide susceptibility assessment in developing countries: A case-study of NW Nicaragua after Hurricane Mitch

Marta Guinau *, Raimon Pallàs, Joan Manuel Vilaplana

RISKNAT Research Group

Departament Geodinàmica i Geofísica, Facultat de Geologia, Universitat de Barcelona, Zona Universitària de Pedralbes, 08028, Barcelona, Spain

Received 1 July 2004; received in revised form 16 June 2005; accepted 1 July 2005
Available online 10 August 2005

Abstract

In October 1998, Hurricane Mitch triggered a large number of landslides (mainly debris flows) in Honduras and Nicaragua, resulting in a high death toll and in considerable damage to property. In recent years, a number of risk assessment methodologies have been devised to mitigate natural disasters. However, due to scarcity of funds and lack of specialised personnel few of these methodologies are accessible to developing countries. To explore the potential application of relatively simple and affordable landslide susceptibility methodologies in such countries, we focused on a region in NW Nicaragua which was among the most severely hit during the Mitch event. Our study included (1) detailed field work to produce a high-resolution inventory landslide map at 1 : 10,000 scale, and (2) a selection of the relevant instability factors from a Terrain Units Map which had previously been generated in a project for rural development. Based on the combination of these two datasets and using GIS tools we developed a comparative analysis of failure-zones and terrain factors in an attempt to classify the land into zones according to the propensity to landslides triggered by heavy rainfalls. The resulting susceptibility map was validated by using a training and a test zone, providing results comparable to those reached in studies based in more sophisticated methodologies. Thus, we provide an example of a methodology which is simple enough to be fully comprehended by non-specialised technicians and which could be of help in landslide risk mitigation through implementation of non-structural measures, such as land planning or emergency measures.

Keywords: Landslide susceptibility; Debris flows; Geographic information system; Developing countries; Nicaragua; Hurricane Mitch

* Corresponding author. Tel.: +34 93 402 13 78; fax: +34 93 402 13 40.
E-mail address: mguinau@ub.edu (M. Guinau).

0013-7952/$ - see front matter © 2005 Elsevier B.V. All rights reserved.
doi:10.1016/j.enggeo.2005.07.001

1. Introduction

Although natural hazards may occur in many parts of the world, their consequences depend on the relationship between the magnitude of natural phenomena and the vulnerability of human settlements to such an event (Alcántara-Ayala, 2002). Consequently, natural phenomena are more destructive in developing countries because of economic, political, social and cultural factors, which increase the vulnerability of these countries to natural hazards.

In recent years, a number of methodologies concerning natural hazard assessment and mapping have been devised in an attempt to determine suitable strategies to prevent and mitigate natural disasters (Brabb, 1984; Carrara et al., 1995; Soeters and van Westen, 1996). However, in developing countries insufficient funds, the absence of laws and the shortage of trained experts increase the difficulty in coping with natural disasters, which represents a considerable drawback to the socio-economic development. Moreover, many studies on the mitigation of natural hazards entail complex statistical techniques that provide results, which are often difficult to comprehend and, hence, implement by non-specialists in statistics such as planners or policy makers (Clerici et al., 2002). There is a pressing need to test simple and low cost methodologies, which can be adapted to and used by national organisations with a low level of specialisation.

In 1998 more than 9000 people lost their lives and about 11% (3.2 million people) of the total population in Central America was affected by Hurricane Mitch. Most damage due to this event in NW Nicaragua was caused by landslides, mainly fast-moving debris flows (Pallàs et al., 2004). These debris flows constituted the most destructive process, resulting in considerable human loss and damage to property in terms of both direct and indirect costs.

Following Hurricane Mitch, several national and international organisations carried out development projects in NW Nicaragua, the area most badly affected in this country (Solidaridad Internacional, 2001; Vilaplana et al., 2002; Pallàs et al., 2004; Guinau et al., in press). These projects involved the systematic collection of data considered to have some bearing on rural development and potential land use. Although these datasets were not directly developed for landslide hazard assessment we were interested in testing if they could be used to implement a methodology to assess and map landslide susceptibility.

The aims of the present study are (1) to explore the potential of combining new field data with a pre-existing non-specific dataset to develop a methodology for landslide susceptibility zoning, and (2) to show an example of a simple and low cost methodology adapted to the limitations found in most developing countries, which could be used to implement non-structural strategies to mitigate landslide risk.

1.1. Study area

Nicaragua, which occupies an area of 118.358 km^2, is located at the Isthmus of Central America, between 10°45′ and 15°05′ of north latitude and 83°15′ and 87°40′ of west longitude (Fig. 1). This location exposes Nicaragua to tropical rainfalls and cyclones that originate between the Caribbean Sea and the African Coast (INETER, 1998).

The study area (Fig. 1) extends over 473 km^2 and includes the municipalities of San Pedro del Norte, San Francisco del Norte, San Juan de Cinco Pinos, Santo Tomás del Norte and part of Somotillo, all of them in the Departamento de Chinandega, in NW Nicaragua. Located in the Interior Highland of Nicar-

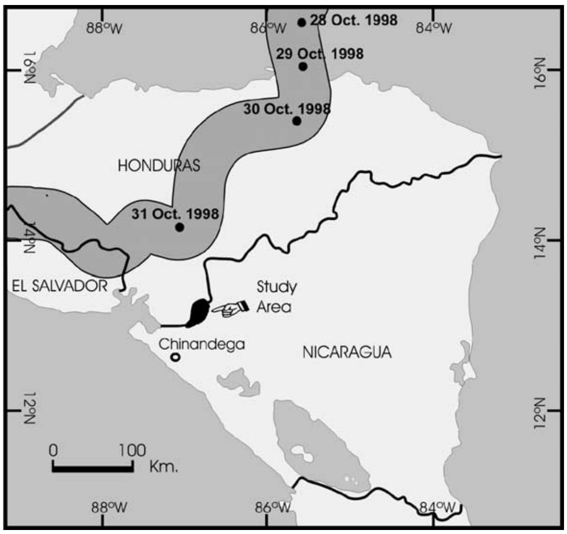

Fig. 1. Study area location (in black), and place names referred to in the text. The dark grey band shows Hurricane Mitch path, based on USGS (1999) data.

agua, this area has a hilly landscape and an altitude between 300 and 1200 m. The area is largely constituted by Tertiary volcanic rocks of the Coyol and Matagalpa groups and Tertiary plutonic intrusions (Weyl, 1980; Fenzl, 1988). The Oligocenic Matagalpa Group is composed of rhyolitic to dacitic pyroclastic rocks, whereas the Coyol Group emplaced during Miocene–Pliocene period is made up of basaltic rocks, rhyolitic lavas, breccias, lahars and pyroclastic flows (Darce et al., 1989; Ehrenborg, 1996). Most of these rocks are covered by an uneven layer of soil, which is composed of regolith and bedrock residual blocks.

The study area has a tropical climate with a marked dry season from November to April, during which only 10% of the annual rainfall is recorded, and a wet season from May to October with an average rainfall of 1200 mm (accounting for 90% of the annual rainfall). However, there is a marked decrease in rainfall from mid July to mid August. The temperature in the study area can fluctuate between 15 and 25 °C (INETER, 1998).

The Hurricane Mitch rainfalls affected Nicaragua from 21 to 31 October 1998. The total rainfall recorded in this period in Chinandega, about 100 km from the study area (Fig. 1), was 1597mm, more than the mean annual rainfall, which in this region is 1420 mm. Only on one day – 30 October – 485 mm were recorded in this zone (INETER, 1998). The effects of these torrential rains in the study area, i.e. mainly debris flows, affected 32% of the population, resulting in considerable damage to property and human life (Solidaridad Internacional, 2001).

2. Data available

Two types of information enabled us to develop and validate a methodology to produce a *landslide susceptibility map* in the study area: (1) a *landslide*

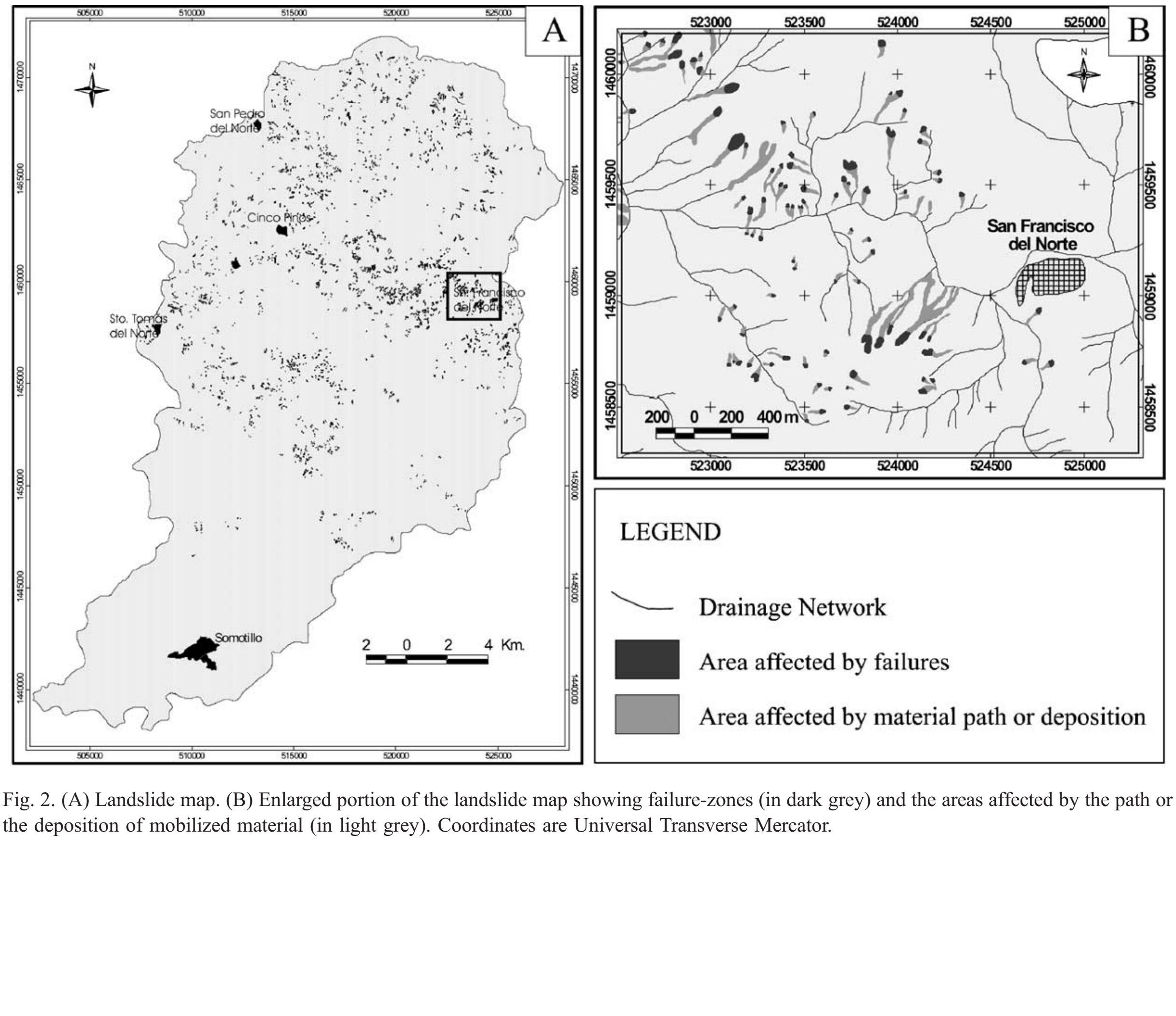

Fig. 2. (A) Landslide map. (B) Enlarged portion of the landslide map showing failure-zones (in dark grey) and the areas affected by the path or the deposition of mobilized material (in light grey). Coordinates are Universal Transverse Mercator.

A

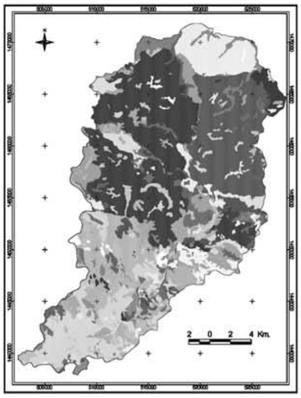

	T U Code	Lithology	Morphology	Slope (degree)	Soil type	Soil thick. (cm.)	Soil texture	...
1	Dcrc/G3S	Dacite	Ridge	> 30	A 3222/sc	< 40	Sand	
2	D/Gcrcc/G4F	Dacite	Ridge	> 30	A 3222/eecc	< 40	Sand	
3	Dvacc/C6M	Dacite	Valley	0 - 8	A 1452/ecc	> 90	Mud	
4	B/D/Glacc/F4F	Andecite	Slope	> 30	A 1442/eecc	> 90	Sand	
5	Dvac/C6M	Dacite	Valley	0 - 8	A 1342/ec	> 90	Sand	
6	D/Glacc/F4F	Dacite	Slope	> 30	A 1442/eecc	> 90	Sand	
7	Bvac/D6M	Basalt	Valley	8 - 15	A 1452/ec	> 90	Mud	
8	Dlac/F4S	Dacite	Slope	> 30	A 1452/9bsc	> 90	Mud	
9	Bcoc/E4M	Basalt	Hill	15 - 30	A 1452/ec	> 90	Mud	
10	Dcrc/G3S	Dacite	Ridge	> 30	A 3202/sc	< 40	Gravel	
11	Bvac/C5M	Basalt	Valley	0 - 8	A 1452/ec	> 90	Mud	
12	Blac/F4F	Basalt	Slope	> 30	A 1442/eec	> 90	Sand	
13	Btecc/C4M	Basalt	Terrace	0 - 8	A 1452/ecc	> 90	Mud	
14	Gcrcc/G4S	Granite	Ridge	> 30	A 1442/scc	> 90	Sand	
15	Bcoc/E4F	Basalt	Hill	15 - 30	A 1452/eec	> 90	Mud	
16	Bcrc/G3S	Basalt	Ridge	> 30	A 1452/sc	> 90	Mud	
17	Gtec/C5M	Granite	Terrace	0 - 8	A 1452/ec	> 90	Mud	
18	B/Dcrc/G4F	Basalt	Ridge	> 30	A 2452/9beec	40 - 90	Mud	
19	Bvacc/D6F	Basalt	Valley	15 - 30	A 1442/eecc	> 90	Sand	
20	Gcrcc/G4S	Granite	Ridge	> 30	A 1442/scc	> 90	Sand	
21	...							

B

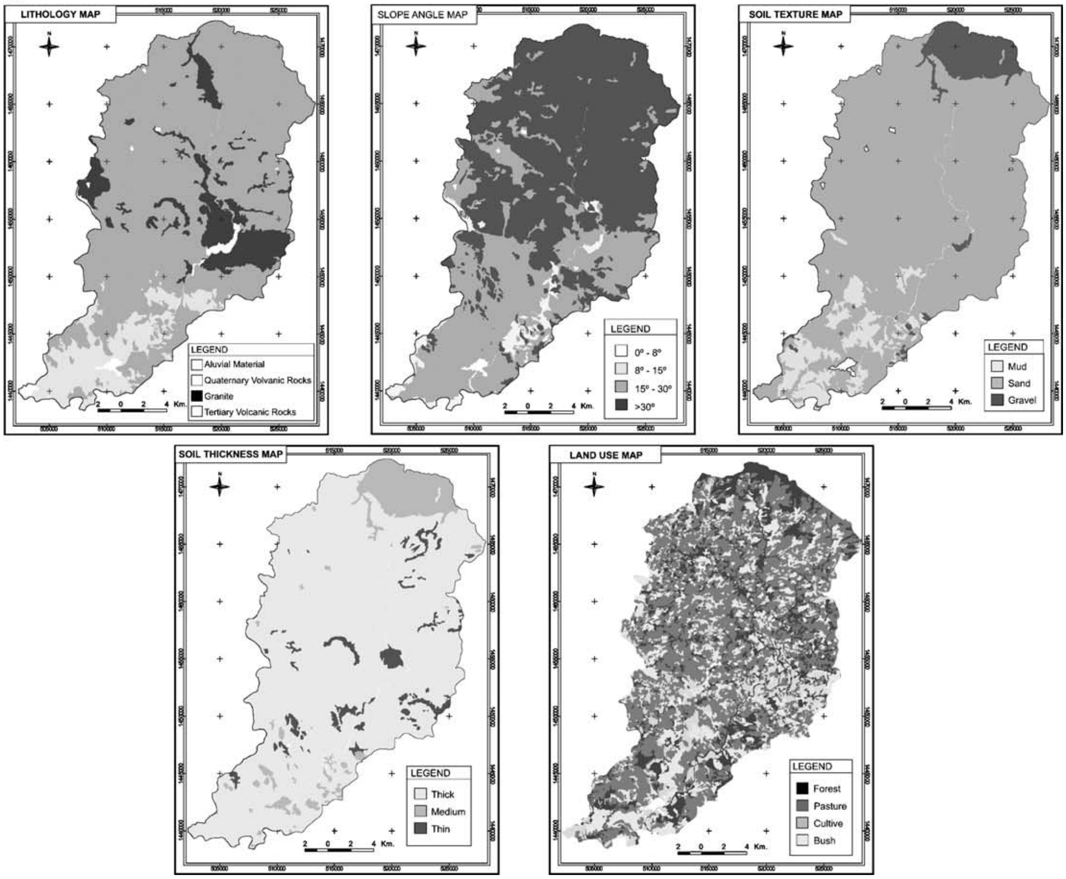

Fig. 3. (A) Terrain units map (grey levels corresponding to terrain units 1 to 491) and a portion of the associated data table showing the first twenty Terrain Units and six terrain factors. The values in the second column in the table correspond to terrain unit codes. Columns three to eight show an example of the classes of each terrain factor which characterize Terrain Units. (B) Example of thematic maps obtained from the terrain units map. Each one shows a terrain factor defined by a given number of classes.

inventory and map prepared by a member of RISKNAT and (2) a *terrain units map* obtained in the frame of a Solidaridad Internacional (Spanish non-governmental organisation) and UPOLI (Polytechnic University of Nicaragua) project (Solidaridad Internacional, 2001).

2.1. Landslide map

Landslide inventory and mapping is aimed at determining the processes concerning landslide development in the study area and the terrain instability factors involved.

To obtain the landslide inventory and map the procedure was as follows; (a) *aerial photographs interpretation*: the aerial photographs taken in 2000 at 1 : 40,000 scale, were enlarged at 1:20,000 scale yielding an acceptable resolution and allowing a more detailed interpretation. The landslides caused by Hurricane Mitch were mapped; (b) *compilation over orthophotos*: the compilation of these affected areas over orthophotos at 1 : 10,000 scale allowed us to

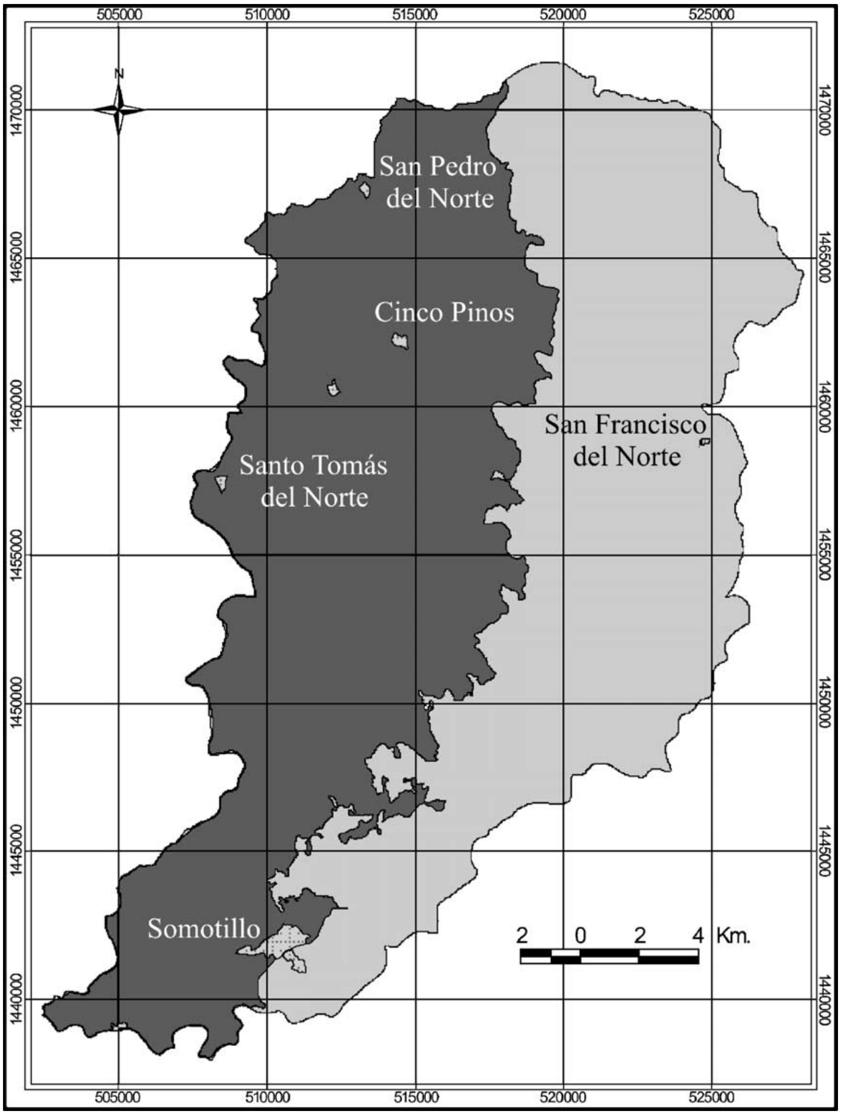

Fig. 4. Division of the study area into Training Zone (in dark grey) and Test Zone (in light grey).

obtain a preliminary *landslide map*; (c) *field work*: the landslide map was checked and corrected to obtain the definitive landslide map at 1 : 10,000 scale, and field observations were made in areas with the highest density of landslides to obtain information on the mechanisms and the instability factors involved in terrain-failures; (d) *digitising of the landslide map*: the resulting digital landslide map included the areas affected by landslides (Fig. 2A), making the distinction between the areas affected by terrain-failure, where landslides start, and the areas affected by the path and the accumulation of the mobilised material (Fig. 2B).

2.2. Terrain units map

With the aid of aerial photointerpretation and field observations, it is possible to obtain significant information on terrain characteristics such as lithology, slope, soil characteristics, land use, which is used to classify the terrain into Terrain Units (Fig. 3A) (Hansen et al., 1995; Guzzetti et al., 1999). This term refers to a portion of land surface, which contains uniform ground conditions that differ from the adjacent units across definable boundaries (Hansen, 1984; Guzzetti et al., 1999). Ground conditions are defined by a given combination of classes of each terrain factor (Fig. 3B).

The terrain units map used in the present study was developed in a GIS environment at 1 : 10,000 scale. Terrain Units were defined from fourteen different terrain factors. From this terrain units map it was possible to obtain *thematic maps*. Each map represents a terrain factor and the different classes that characterise it (Fig. 3A–B).

3. Methodology

According to the analysis of terrain conditions in areas affected by landslides in the past or present it is possible to determine zones with similar characteristics such as areas prone to landsliding, termed Landslide Susceptible Areas.

Although terrain instability is governed by a large number of geological and environmental factors, it is necessary to differentiate instability factors, which condition terrain-failure, from other factors, which influence the area affected by the reach of the mobilised material. In the present study only the areas affected by terrain-failures, i.e. the areas where landslides start, are taken into account when determining areas prone to failure (Irigaray et al., 1999; Baeza and Corominas, 2001; Dai et al., 2002; Chung and Fabbri, 2003). Thus, the susceptibility map resulting from this methodology represents the susceptibility to terrain-failure.

A given area is declared to be susceptible to terrain-failures when the terrain conditions at a given site are comparable to those in an area where the terrain-failure has occurred. Hence, a comparative analysis between terrain-failure zones affected by Hurricane Mitch and different instability factors allowed us to zone the study area according to its susceptibility to landslides.

Generally, a minimum of two rainfall events producing landslides are needed to validate a susceptibility map. In our study, lack of historical data or a rainfall event after Hurricane Mitch rules out the possibility of a validation of this kind. However, following the same approach as Baeza and Corominas (2001), Chung and Fabbri (2003) and Remondo et al.

Table 1
Example of the Terrain Units and the weights associated to their classes

Terrain unit code	Slope class weight	Lithology class weight	Soil thick. class weight	Soil texture class weight	Land use class weight	Cum. value
Gacc/G4F	<30° = 0.32	Granite = 0.45	Low = 0.00	Gravel = 0.31	Forest = 0.13	$\sum$W = 1.21
Dvacc/B3S	8–15° = 0.00	Tertiary V = 0.20	High = 0.33	Mud = 0.03	Cultivate = 0.10	$\sum$W = 0.66
Iva/B6L	0–4° = 0.00	Quat V = 0.00	Medium = 0.18	Sand = 0.20	Pasture = 0.22	$\sum$W = 0.60
Ava/F4M	10–30° = 0.30	Alluvial = 0.00	Low = 0.00	Gravel = 0.31	Bush = 0.21	$\sum$W = 0.82
Dplcc/D5L	0–4° = 0.00	Tertiary V = 0.20	High = 0.33	Gravel = 0.31	Pasture = 0.22	$\sum$W = 1.06
Dvacc/C6M	4–8° = 0.00	Tertiary V = 0.20	Medium = 0.18	Mud = 0.03	Cultivate = 0.10	$\sum$W = 0.51

Cumulative values are shown on the right column.
Tertiary V: tertiary volcanic rocks (andesite, dasite and basalt) and Quat V: quaternary volcanic rocks (ignimbrite and pyroclast)

(2003), the division of the study area into two zones (see Fig. 4) allowed us to develop the methodology in a Training Zone, and to validate it in a Test Zone. The main criteria for dividing the study area were the homogeneity of extension and terrain characteristics.

3.1. Selection of instability factors

Slope instability is governed by a complex set of interrelated terrain parameters but a simplified approach requires a selection of a limited number of key instability factors. The factors are selected in accordance with subjective expert opinion and depend on a prior knowledge of the external processes in the study area.

Field observations contribute to the understanding of terrain-failure mechanisms and their conditioning factors. In our study case, most terrain-failures involved the total thickness or a portion of soil formation mobilised over the bedrock (Vilaplana et al.,

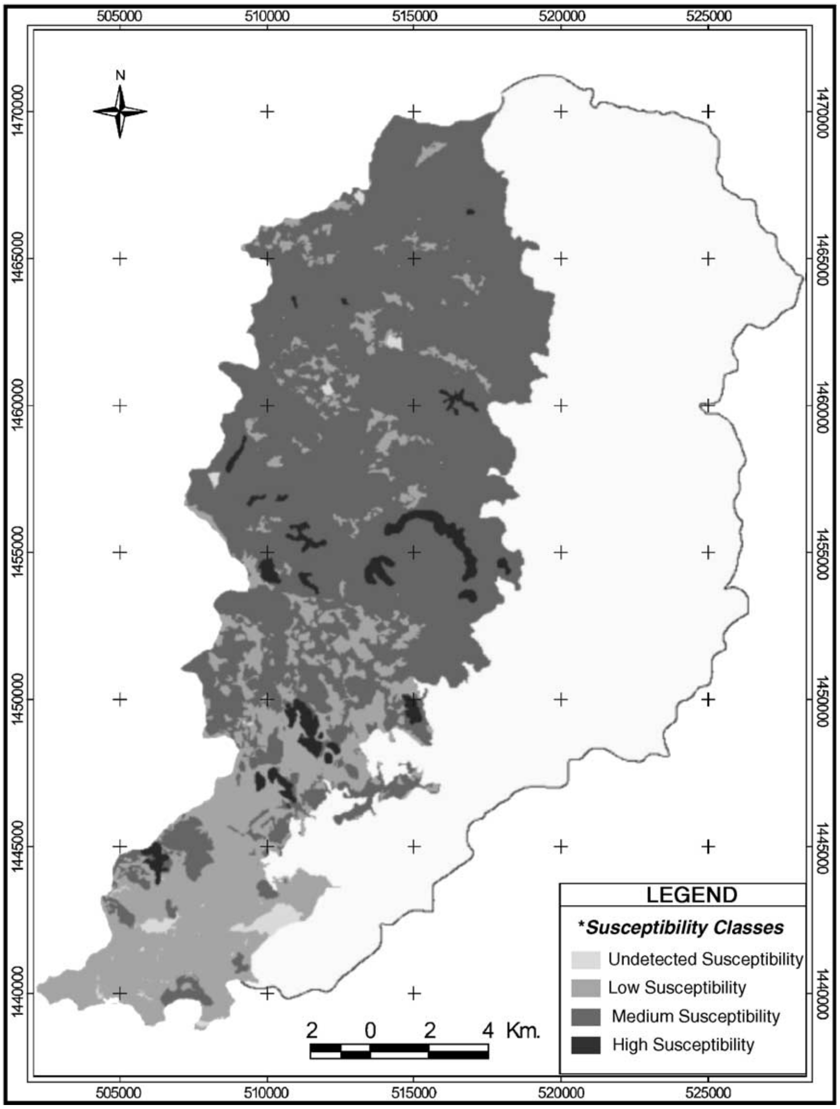

Fig. 5. Landslide susceptibility map obtained in Training Zone.

2002; Pallàs et al., 2004). Based on the field observations, the instability factors from the terrain units map that were selected in this study are: slope, lithology, soil thickness, soil texture and land use.

3.2. Weighting instability factors in the Training Zone

As pointed out by van Westen et al. (1997) and Carrara et al. (1999), the heuristic method used to choose the relevant instability factors involves a relatively high degree of subjectivity. To determine more objectively the weight of each class for the different instability factors influencing terrain-failure we made a comparative analysis between the terrain characteristics and the distribution of failure-zones by using a Geographic Information System (GIS).

The comparative analysis consisted in superimposing the *failure-zones map* on each thematic map. Given that each instability factor is divided into a number of classes, it is possible to calculate the

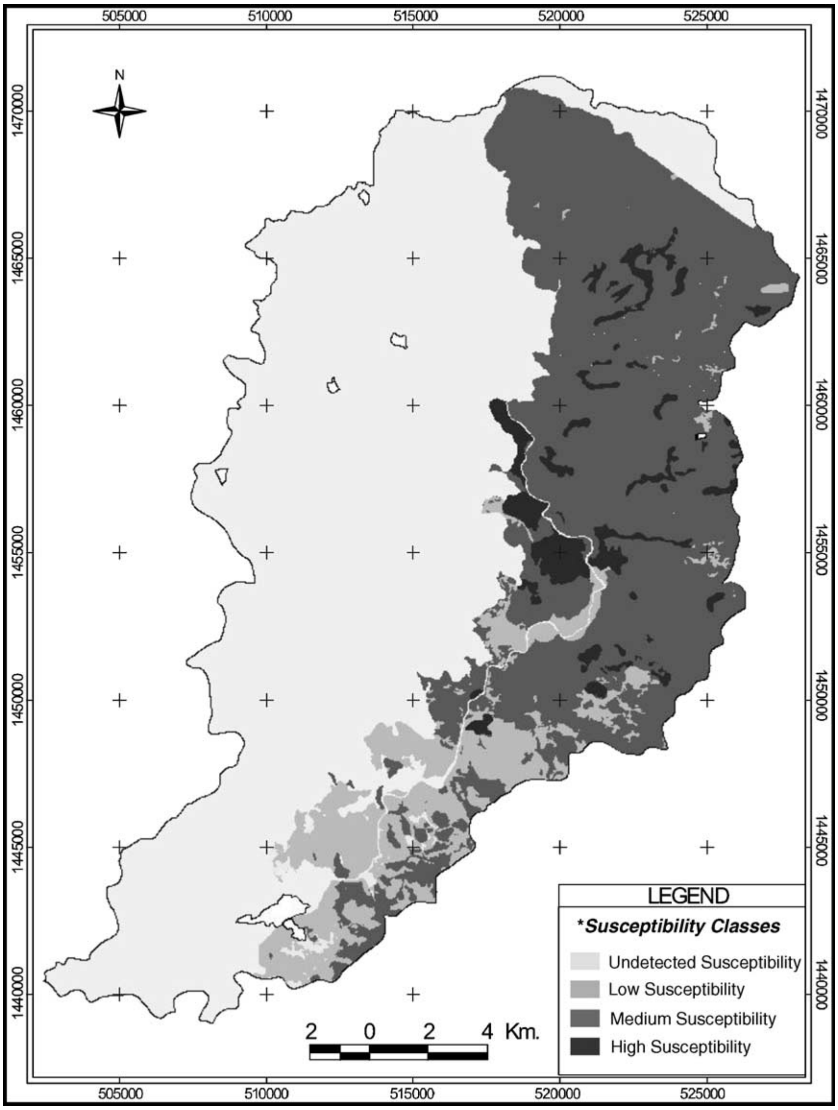

Fig. 6. Landslide susceptibility map obtained in Test Zone.

percentage of the area covered by failures in each class (W_i):

$$W_i = [A_{fi}/A_i] \times 100$$

where A_{fi} is the area covered by failures in a given class and A_i is the area of this class. This percentage W_i represents the weight or degree of influence of each class in terrain-failures (Campbell, 1973; Wright and Nilsen, 1974; Wright et al., 1974; DeGraff, 1985; Guzzetti et al., 1994; Clerici et al., 2002; Dai et al., 2002).

3.3. Landslide susceptibility calculation in the Training Zone

Given that each Terrain Unit is characterised by a combination of classes, each class corresponding to a terrain factor, it is possible to calculate a cumulative value, adding up the weights obtained previously (Table 1). This cumulative value represents the relative propensity of the terrain to failure in each Terrain Unit.

3.4. Landslide susceptibility classes and mapping in the Training Zone

Cumulative values obtained for each Terrain Unit can be classified into several intervals to define different susceptibility classes. These can be used to classify the land surface into different susceptibility degree domains. We divide the *maximum cumulative susceptibility value* (Cv_{max}) by the number of intervals (N), which we want to represent in the landslide susceptibility map, obtaining an interval size (X).

$$X = Cv_{max}/N$$

Once an interval size (X) has been chosen, GIS utilities allow the classification of the study area into N susceptibility classes. Fig. 5 shows an example of subdivision into four susceptibility classes.

3.5. Validation of the susceptibility map in the Test Zone

Given that the terrain characteristics in the Test Zone resemble those of the Training Zone, a landslide susceptibility map could be obtained by integrating the weights previously determined for each class. Using GIS tools, cumulative values of the weights previously attributed to each class in the Training Zone were calculated for each Terrain Unit in the Test Zone. These cumulative values were distributed in a number of intervals or susceptibility classes (N) in the Test Zone (Fig. 6), coinciding with the number chosen for the Training Zone.

The *susceptibility map* was then compared with the failure-zones for validation. GIS tools allowed us to obtain the percentage of the area of failure in each susceptibility class ($\%A_{fi}$) with respect to the total area of failure when considering the whole test zone. $\%A_{fi}$ was obtained using the following expression:

$$\%A_{fi} = 100(A_{fi}/A_{sci}) \Big/ \sum (A_{fi}/A_{sci})$$

were A_{fi} is the area affected by failures in a given susceptibility class, A_{sci} is the class area. $\%A_{fi}$ allows us evaluate whether failure-zones coincide with the areas regarded as being highly susceptible to failure.

Fig. 7 shows a gradual decrease in the percentage of failures between the areas of high susceptibility and the areas of low susceptibility. Equivalent distributions were found when applying this kind of validation to susceptibility maps corresponding to different number of susceptibility classes (N varying between 3 and 6). Such robust outputs suggest that our methodology is adequate to obtain landslide susceptibility maps in the study area.

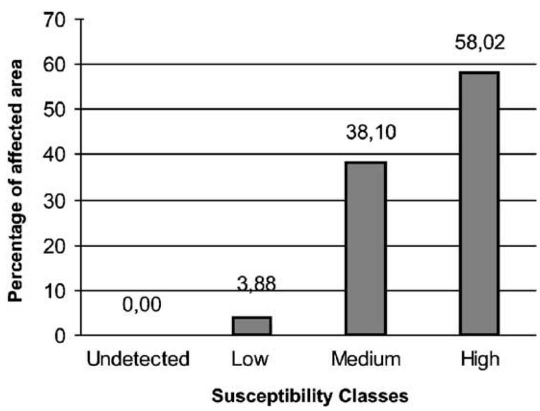

Fig. 7. Graph showing the percentage of area affected by failures on each Susceptibility Class.

4. Discussion

Hurricane Mitch constitutes the reference event in our study to develop a methodology to obtain landslide susceptibility maps. The dominant typology of landslides triggered by this event in the study area is debris flows. Therefore, the resulting landslide susceptibility map shows the propensity to debris flows resulting from heavy rainfalls.

The methodology developed in the present paper is based on a comparative analysis between the distribution of the observed failure-zones and the instability factors. Consequently, the landslide susceptibility map obtained shows the propensity of the terrain to failure but not the propensity to be affected by the path or the deposition area of the mobilised material. This is an important limitation of susceptibility maps, which could be improved by considering the fact that debris flows tend to merge with the drainage network. Thus, the methodology shown in the present paper could be complemented with the simplified method suggested by Pallàs et al. (2004) which, based on a Digital Terrain Model, permits the calculation of flow lines from potential source areas. The application of such a methodology is out of the scope of the present paper and is not shown here.

A limitation of the approach to susceptibility analysis presented here is that it implicitly considers that instability factors are mutually independent. Such an assumption may not be realistic and could produce a larger overestimation in the susceptibility values in high susceptibility classes. Thus, the susceptibility values assigned to each susceptibility class must be seen as relative, and need to be used as qualitative indexes. The resulting map is helpful in separating areas of increasing degrees of susceptibility, which is a reasonable first approach to hazard assessment considering the limited resources found in most developing countries.

The methodology suggested in the present paper enables to obtain landslide susceptibility maps with a variable number of susceptibility classes. It has to be pointed out that this number will depend on the requirements and possibilities of the study area. Thus, the technician in charge will need to base his choice on site specific criteria related to socio-economic factors and on the end use of the resulting susceptibility map. As an example, the best choice in the number of classes may vary if the map is to be used for management of emergencies or for land-use planning. Note that the landslide susceptibility map should only be used to establish non-structural strategies to mitigate landslide effects. To implement structural measures it would be necessary to estimate the magnitude of the landslides that can affect the area, which is beyond the scope of our general approach.

The main difficulty when trying to produce sound hazard assessments is the lack of reliable field and historical data. This is especially true in developing countries where data are scarce and where specific studies are rarely made. Our study relies on the combination of two main datasets: on the one hand we made a new collection of high resolution quality data in the field that enabled us (1) to construct a reliable landslide map at 1 : 10,000 scale and (2) to gain sufficient knowledge about the key factors involved in debris flow failure in the area. This was a key part of the study, and required the participation of personnel specialised in landslides and time-consuming work in the field. On the other hand we also used a pre-existing non-specific dataset from which the factors relevant to instability were chosen. Although the thematic maps and classes included in these datasets were far from ideal, we have shown that, complemented with good-quality high-resolution field data covering a large portion of the study area, they could be used as the basis for a consistent susceptibility analysis.

In recent years a number of methodologies to produce landslide susceptibility maps have been developed in an attempt to mitigate natural disasters. However, the complexity of these methodologies and the socio-economic situation of developing countries highlight the need for simple and low cost methodologies to obtain necessary information to mitigate natural risks. As recognised by Carrara et al. (1999) and Clerici et al. (2002), sophisticated statistic methods may provide relatively accurate results but may be too difficult to comprehend by non-specialists in statistics to be applied with success. A more simple methodology like the one presented in this paper may have the drawback of being less accurate but has the advantages of (1) being feasible when data is limited and (2) being easily learned, fully comprehended and handled by technicians trained in landslide assessment without a high level of specialisation in statistics.

The validation of our susceptibility assessment (Fig. 7) suggests that the application of relatively simple methodologies, even when using non-ideal datasets, can give results which are comparable with those based on sophisticated statistical methods and exhaustive, expensive selection of specific data (e.g. Neuland, 1976; Duque et al., 1990; Irigaray et al., 1999; Baeza and Corominas, 2001; Chung and Fabbri, 2003; Remondo et al., 2003). Obviously different areas and datasets may behave differently, and some kind of validation will always be required. Providing that division into two homogeneous areas is possible, the validation through a training and a test zone appears to be a good approach for those areas where only one reference event is available.

5. Conclusion

The methodology suggested in the present paper allows the detection of potential debris flows source areas under heavy rainfall conditions. This methodology, complemented with simple methods aimed at establishing preferential debris flows paths, could provide a useful document to help in the mitigation of debris flow risk through the implementation of non-structural measures.

Even in developing countries there are regions where datasets collected for purposes other than risk mitigation are available. When combined with good-quality high-resolution specific data and GIS technologies, the use of such datasets can help in reducing the costs of susceptibility analyses, making them available to areas where they could otherwise not be afforded.

Any susceptibility study using non-specific datasets needs to develop some kind of validation process. The division of the study area into training and test zones is a promising approach for validation in areas where, as in most developing countries, little historical information is available.

Simple methodologies for susceptibility assessment are more easily comprehended and handled than sophisticated ones. They may provide a good cost-effective compromise, making them accessible to developing countries where specialised personnel and funds are scarce.

Acknowledgements

This study could not have been possible without the agreement between the Spanish NGO, *Solidaridad Internacional*—SI, the *Instituto de Capacitación y Investigación para el Desarrollo Rural Integral*—ICIDRI of the Universidad Politécnica de Nicaragua—UPOLI and the *Departament de Geodinàmica i Geofísica* of the Universitat de Barcelona—UB. We are indebted to the municipalities and people of Cinco Pinos, San Francisco del Norte, San Pedro del Norte, Santo Tomás del Norte and Somotillo for providing accommodation and support during the fieldwork. This research received financial support from the Generalitat de Catalunya: project SGR 2001—00081.

References

Alcántara-Ayala, I., 2002. Geomorphology, natural hazards, vulnerability and prevention of natural disasters in developing countries. Geomorphology 47 (2–4), 107–124.

Baeza, C., Corominas, J., 2001. Assessment of shallow landslide susceptibility by means of multivariate statistical techniques. Earth Surface Processes and Landforms 26, 1251–1263.

Brabb, E.E., 1984. Innovative approaches to landslide hazard and risk mapping. Landslides—Glissements de Terrain, IV International Symposium on Landslides, vol. 1, pp. 307–323. Toronto, Canada.

Campbell, R., 1973. Dume Quadrangle, Los Angeles County, California; an experiment in generalising and quantifying areal distribution of landslides. US Geological Survey, Miscellaneous Field Studies. Map, MF-535 Scale 1:24,000.

Carrara, A., Cardinali, M., Guzzetti, F., Reichenbach, P., 1995. GIS-based techniques for mapping landslide hazard. http://deis158.deis.unibo.it.

Carrara, A., Guzzetti, F., Cardinali, M., Reichenbach, P., 1999. Use of GIS technology in the prediction and monitoring of landslide hazard. Natural Hazards 20, 117–135.

Chung, Ch.F., Fabbri, A.G., 2003. Validation of spatial prediction models for landslide hazard mapping. Natural Hazards 30 (3), 451–472.

Clerici, A., Perego, S., Tellini, C., Vescovi, P., 2002. A procedure for landslide susceptibility zonation by the conditional analysis method. Geomorphology 48 (4), 349–364.

Dai, F.C., Lee, C.F., Ngai, Y.Y., 2002. Landslide risk assessment and management: an overview. Engineering Geology 64 (1), 65–87.

Darce, M., Levi, B., Nyström, J.O., Troëng, B., 1989. Alteration patterns in volcanic rocks within an east–west traverse through central Nicaragua. Journal of South American Earth Sciences 2, 155–161.

DeGraff, J.V., 1985. Using isopleth maps of landslides deposits as a tool in timber sale planning. Bulletin American Association of Engineering Geologists 22, 445–453.

Duque, A., Echevarría, G., Fernández, E., Kerejeta, A., Cendrero, A., Tamés, P., 1990. Comprobación empírica de metodologías para la elaboración de mapas de amenaza de inestabilidad de laderas; aproximación de un modelo general de evaluación del riesgo. In: Hermelin, M. (Ed.) Environmental Geology and Natural Hazards in the Andean Region. AGID Report No. 13, Pereira, Colombia, pp. 189–206.

Ehrenborg, J., 1996. A new stratigraphy for the Tertiary volcanic rocks of the Nicaraguan Highland. GSA Bulletin 108, 830–842.

Fenzl, N., 1988. Nicaragua: Geografía, Clima, Geología y Hidrogeología. UFPA/INETER/INAN, Belém. 62 pp.

Guinau, M., Vilaplana, J.M., van der Zee, J., in press. Propuesta metodológica para la evaluación de la Susceptibilidad a los movimientos de ladera. In: Pobreza en el Trópico seco rural de Nicaragua, causas principales y perspectivas para su aliviación; Estudios aplicados en 9 municipios, con émfasis en el norte de Chinandega. Managua, Nicaragua.

Guzzetti, F., Cardinali, M., Reichenbach, P., 1994. The AVI project: a bibliographical and archive inventory of landslides and floods in Italy. Environmental Management 18, 623–633.

Guzzetti, F., Carrara, A., Cardinali, M., Reichenbach, P., 1999. Landslide hazard evaluation: a review of current techniques and their application in a multi-scale study, Central Italy. Geomorphology 31, 181–216.

Hansen, A., 1984. Landslide hazard analysis. In: Brunsden, D., Prior, D.B. (Eds.), Slope Instability. Chapter 13, pp. 523–602.

Hansen, A., Franks, C.A.M., Kirk, P.A., Brimicombe, A.J., Tung, F., 1995. Application of GIS to hazard assessment, with particular reference to landslides in Hong Kong. In: Carrara, A., Guzzetti, F. (Eds.), Geographical Information Systems in Assessing Natural Hazards. Kluwer Academic Publishers, Netherlands, pp. 273–298.

INETER, 1998. Las Lluvias del Siglo en Nicaragua. Instituto Nicaragüense de Estudios Territoriales, INETER. Managua, Nicaragua. 159 pp.

Irigaray, C., Fernández, T., El Hamdouni, R., Chacón, J., 1999. Verification of landslide susceptibility mapping: a case study. Earth Surface Processes and Landforms 24, 537–544.

Neuland, H., 1976. A prediction model of landslips. Catena 3, 215–230.

Pallàs, R., Vilaplana, J.M., Guinau, M., Falgàs, E., Alemany, X., Muñoz, A., 2004. A pragmatic approach to debris flow hazard mapping in areas affected by Hurricane Mitch: example from NW Nicaragua. Engineering Geology 72, 57–72.

Remondo, J., González, A., Díaz de Terán, J.R., Fabbri, A., Cheng, Ch.F., 2003. Validation of landslide susceptibility maps; examples and applications from a case study in Northern Spain. Natural Hazards 30 (3), 437–449.

Soeters, R., van Westen, C.J. 1996. Slope instability recognition, analysis, and zonation. In: Turner, A.K., Schuster, R.L. (Eds.), Landslides: Investigation and Mitigation. Transportation Research Board Special Report 247,129-177.

Solidaridad Internacional, 2001. Estrategias participativas para el desarrollo rural en seis municipios del norte del Departamento de Chinandega. Proyecto de Cooperación Internacional desarrollado conjuntamente con el Instituto de Capacitación e Investigación para el Desarrollo Rural Integral (ICIDRI) de la Universidad Politécnica de Nicaragua (UPOLI). Managua, Nicaragua. Unpublished Report.

USGS, 1999. Digital Atlas of Central America: Prepared in Response to Hurricane Mitch, version 2, vols. 1–2. http://130.11.52.118/mitch/views/eventimpact.html.

van Westen, C.J., Rengers, N., Terlien, M.T.J., 1997. Prediction of the occurrence of slope instability phenomena through GIS-based hazard zonation. Geologische Rundschao 86, 404–414.

Vilaplana, J.M., Pallàs, R., Guinau, M., Falgàs, E., Alemany, X., Muñoz, A., 2002. Peligrosidad Geológica Asociada a los Movimientos de Ladera en el Noroeste de Nicaragua. Serie Geográfica, vol. 10. Dpto. Geografía, Universidad Alcalá de Henares, Madrid, pp. 109–119.

Weyl, R., 1980. Geology of Central America. Gebrüder, Borntraeger, Berlin. 371 pp.

Wright, R.H., Nilsen, T.H., 1974. Isopleth map of landslide deposits, Southern San Francisco Bay Region, California. US Geological Survey Miscellaneous Field Studies Map, MF-550. scale 1:250,000.

Wright, R.H., Campbell, R.H., Nilsen, T.H., 1974. Preparation and use of isopleth maps of landslide deposits. Geological Society of America, Geology 2, 483–485.

Nat. Hazards Earth Syst. Sci.
www.nat-hazards-earth-syst-sci.net

GIS-based debris flow source and runout susceptibility assessment from DEM data. A case study in NW Nicaragua.

M. Guinau (1), I. Vilajosana (1) and J.M. Vilaplana (1)
(1) RISKNAT Research Group
Departament de Geodinàmica i Geofísica, Facultat de Geologia, Universitat de Barcelona, Zona Universitària de Pedralbes, 08028, Barcelona, Spain.

Article submitted: 7 June 2007

Abstract. In October 1998, Hurricane Mitch triggered numerous landslides (mainly debris flows) in Honduras and Nicaragua, resulting in a high death toll and in considerable damage to property. The potential application of relatively simple and affordable spatial prediction models for landslide hazard mapping in developing countries was studied. Our attention was focused on a region in NW Nicaragua, one of the most severely hit places during the Mitch event.
A landslide map was obtained at 1:10.000 scale in a Geographic Information System (GIS) environment from the interpretation of aerial photographs and detailed field work. In this map the terrain failure zones were distinguished from the areas within the reach of the mobilized materials. A Digital Elevation Model (DEM) with 20m x 20m of pixel size was also employed in the study area.
A comparative analysis of the terrain failures caused by Hurricane Mitch and a selection of 4 terrain factors extracted from the DEM which, contributed to the terrain instability, was carried out. Land propensity to failure was determined with the aid of a bivariate analysis and GIS tools in a terrain failure susceptibility map. In order to estimate the areas that could be affected by the path or deposition of the mobilized materials, we considered the fact that under intense rainfall events debris flows tend to travel long distances following the maximum slope and merging with the drainage network. Using the TauDEM extension for ArcGIS software we generated automatically flow lines following the maximum slope in the DEM starting from the areas prone to failure in the terrain failure susceptibility map. The areas crossed by the flow lines from each terrain failure susceptibility class correspond to the runout susceptibility classes represented in a runout susceptibility map.
The study of terrain failure and runout susceptibility enabled us to obtain a spatial prediction for landslides, which could contribute to landslide risk mitigation.

Correspondence to: M. Guinau
(mguinau@ub.edu)

1. Introduction

Landslide hazard is generally defined as the probability that a landslide may occur within a given area in a given period of time. This concept includes both spatial and time dimensions. Landslide hazard assessment is not always possible given that data on the temporal occurrence of past landslides are often not easy to obtain (Remondo et al. 2003a; Ayalew et al., 2005). Susceptibility assessment is sometimes used to overcome this problem. The term susceptibility is generally used to identify the location of potential landslides in a given region based on a set of terrain characteristics. Susceptibility analysis assumes that future landslides are likely to be produced by the same conditioning factors as landslides in the past and the present (Varnes, 1984; Carrara et al. 1995). Although these methods provide information on potentially unstable slopes, they do not supply direct information on landslide magnitude and frequency.
To develop an integrate landslide susceptibility analysis, some authors such as Mongomery & Dietrich (1994), Dai et al. (2002), Chung & Fabbri (2003), Corominas et al. (2003), Coe et al. (2004), Hürlimann et al. (2006) propose the following procedure: a) evaluation of terrain failure susceptibility and b) assessment of runout behaviour of the mobilized material. The probability of the spatial occurrence for future landslides is reflected in a terrain failure susceptibility map, which indicates the potential starting zones. This map can be elaborated by heuristic, statistic (bivariate or multivariate analysis) or deterministic approaches (van Westen, 1993; Carrara et al. 1995; van Westen,

et al., 1997; Remondo et al, 2003a, Dai et al. 2002; Hürlimann et al. 2006). After determining the potential landslide initiation zones, the runout behaviour is analysed in order to delimit zones that could be reached by the mobilized debris. Approaches to assessing the mobility of debris can be empirical, analytical and numerical (Mongomery & Dietrich, 1994; Dai et al. 2002; Corominas et al. 2003; Pallàs et al., 2004; Hürlimann et al. 2006).

In many parts of the world, especially in developing countries, the scarcity of good quality data, insufficient funds and lack of specialized personnel constitute a disadvantage for landslide susceptibility and hazard assessment. Thus, there is a pressing need for developing feasible and low cost methodologies of landslide hazard assessment, which can be readily tested and implemented under the conditions found in these countries (Pallàs et al. 2004; Coe et al., 2004; Guinau et al. 2005). A number of developing countries, especially in South and Central America and Asia, are currently implementing Geographic Information Systems (GIS) and acquiring digital data, which provide advantages in geoenvironmental analysis. GIS tools enable us to produce and to handle easily a large amount of data. Digital Elevation Models (DEM) also permits the extraction of geometrical variables which can be used in landslide susceptibility assessment. Thus, DEM data would obviate the need for costly and time consuming methods required to obtain geoenvironmental data from conventional processes such as aerial photointerpetation and field work.

The aims of the present study are 1) to develop a methodology for landslide susceptibility zoning considering landslide source and runout susceptibility, and 2) to provide a simple and low cost methodology that is suited to the conditions in most developing countries. This methodology could be implemented in large territories to devise policies for disaster prevention and mitigation.

1.1. Study area

The study area is located in the Interior Highlands of Nicaragua (Fig. 1), an extensive and heavily dissected volcanic plateau and corresponds to the upper part of the Sinecapa River basin. The area displays a hilly landscape with an average slope gradient of 20º and an altitude between 220 and 1265 m. This region is largely constituted by Tertiary volcanic rocks of the Coyol and Matagalpa groups (Fenzl, 1988). The Oligocenic Matagalpa group is composed of rhyolitic to dacitic pyroclastic rocks, whereas the Coyol group emplaced during Miocene-Pliocene period is made up of basaltic rocks, rhyolitic lavas, breccias, lahars and pyroclastic deposits (Darce et al., 1989; Ehrenborg, 1996). Most of these rocks are covered by a thick regolith and colluvial deposits.

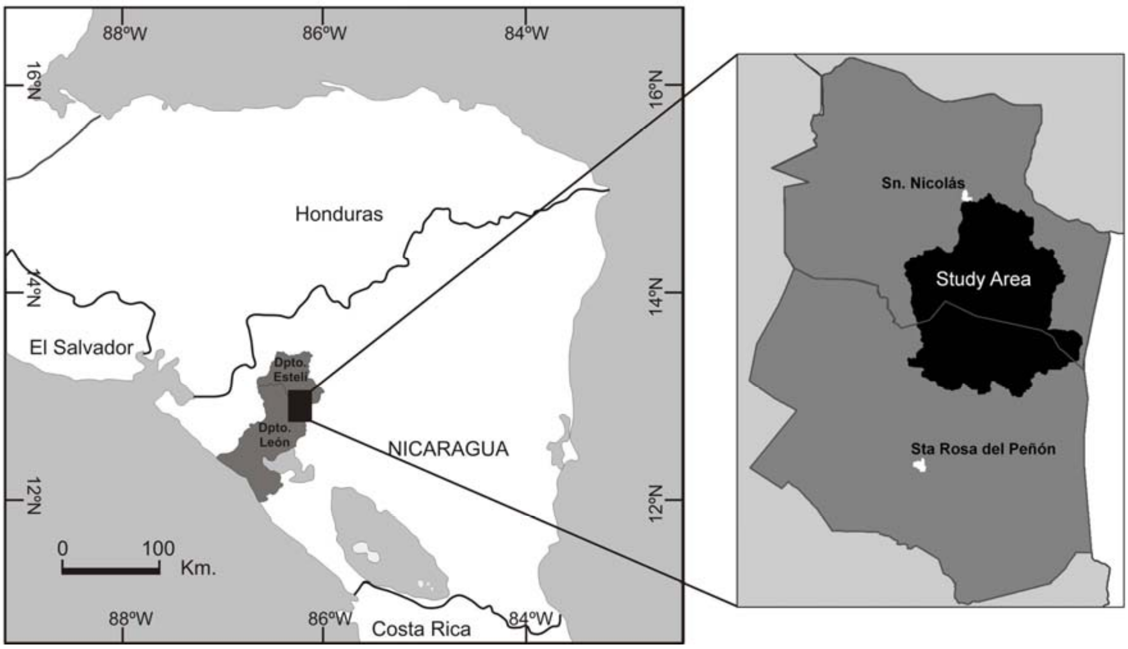

Fig. 1. Location of the Departamento de Estelí and Departamento de Leon in NW Nicaragua. In the enlarged zone, the study area (in black) and localities referred to in the text.

The study area covers about $68Km^2$ and forms part of the municipalities of San Nicolás and Santa Rosa del Peñón in the Estelí and Leon Departments, respectively (Fig. 1). The first settlements were established approximately one century ago, and since then around 90% of what used to be thickly forested land has been converted into bush land, degraded pastures and agricultural fields. The settlements are scattered, and construction materials consist of adobe and wood. The economy is based on subsistence corn, bean and cereal agriculture, and to a lesser extent, on cattle.

The region has a tropical climate characterized by hurricanes and tropical storms, especially in the wet months, from September to November. Although the study area has been affected historically by these phenomena, the most catastrophic event was Hurricane Mitch in 1998. This hurricane caused floods and thousands of landslides, mainly debris flows, resulting in a high death toll and in considerable damage to property.

2. Data acquisition

Two types of data enable us to develop and validate the landslide source and runout susceptibility assessment in the study area: 1) a Digital Elevation Model obtained recently for the Pacific region in Nicaragua and 2) a landslide inventory and map produced specifically for this analysis.

2.1. Digital Elevation Model

A 20m x 20m resolution DEM has been available in 15% of the Pacific Region of Nicaragua since August 2006. This model was generated from aerial photograph restitution and elevation control points in the frame of a project developed by INETER (Intituto Nicaragüense de Estudios Territoriales) in cooperation with JICA (Japan International Cooperation Agency).

2.2. Landslide inventory and map

The landslides triggered by Hurricane Mitch were catalogued and mapped to determine the mechanisms of landslides and the instability factors involved. A black and white aerial photograph set, taken in December 1998 (1 month after Hurricane Mitch), was available at 1:30.000 scale in the study area (special flight made by United States Geological Survey). These photographs yielded an acceptable resolution and allowed a detailed interpretation. The landslides caused by Hurricane Mitch were mapped and transferred over orthophotos at 1:10.000 scale, obtaining a preliminary landslide map. This map was checked and corrected in the field to obtain the definitive landslide map at 1:10.000 scale. Field observations were also made in the areas with most landslides to obtain information on the mechanisms and the instability factors involved in slope failure. 90% of the observed movements were shallow landslides controlled by groundwater flow convergence which quickly evolve to debris flow. The average rupture surface was 500 m^2 and the debris volume mean was 2500 m^3.

The resulting inventory and map were digitized in ArcInfoGIS software. In the landslide map the movements were systematically divided into the failure and the runout zones (Fig. 2). In order to carry out a joint analysis of landslides and DEM data, the failure zones were rasterized to the DEM resolution in ArcGIS. Each failure was assumed to be within a single 20m x 20m pixel (Dai & Lee, 2002; Coe et al, 2004).

3. Terrain failure susceptibility analysis

Bivariate statistical procedure is the most simple and the most quantitatively suitable method to assess terrain failure susceptibility. This analysis makes use of simple statistical calculations, which allows us to determine the contribution of each terrain parameter to the slope instability obviating the need for experts in statistics or specific statistical package. Thus, it can be developed using common GIS tools. The aim of the bivariate method is to combine landslide map and conditioning factors, which exert an influence on slope instability, in order to determine the weight of influence for each factor class. These weights are added up to obtain the terrain failure susceptibility index. Although scientifically a continuous variable is more informative than a stored categorical scale, most of the final users will find that a map with susceptibility classes (i.e. low, medium and high susceptibility) is easier to handle than a cryptic numerical value (Chung & Fabbri, 2003; Begueria, 2006). Thus, the terrain failure susceptibility indexes are generally classified in intervals in order better visualize the terrain failure susceptibility zonation in a map.

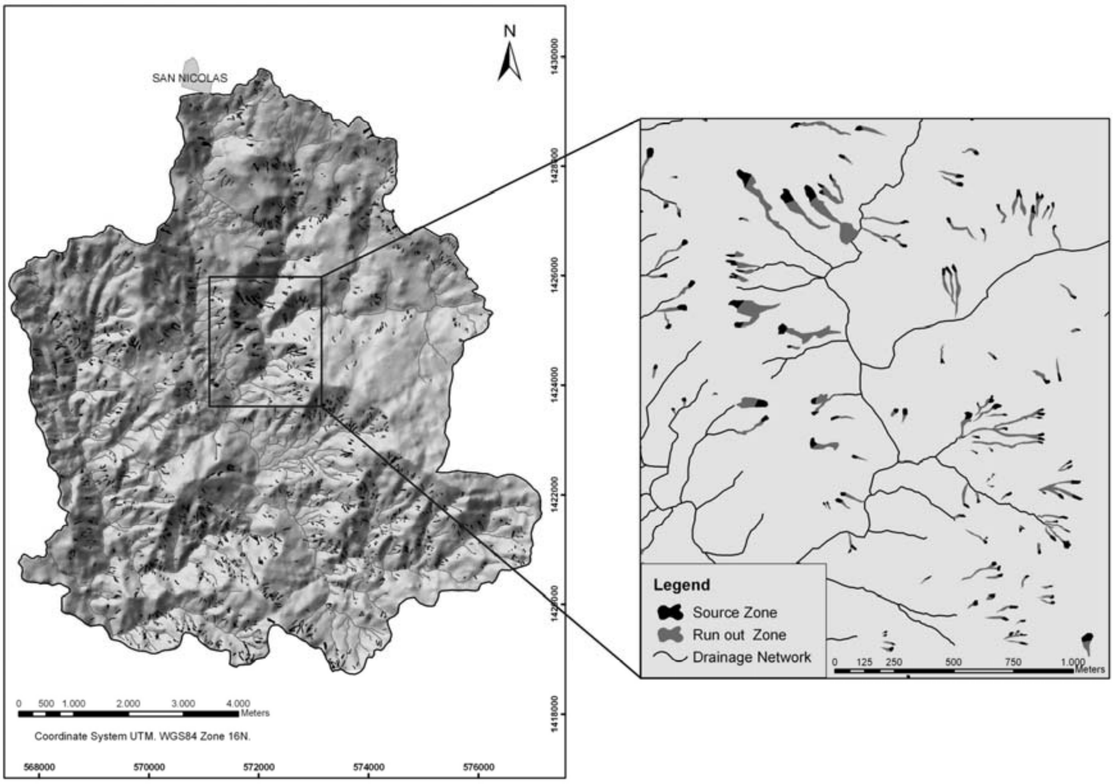

Fig. 2. Landslide map and an enlarged portion showing failure-zones (in dark grey) and the areas affected by the path or the deposition of mobilized material (in light grey).

Finally, it is of paramount importance to validate the model results. In this process the susceptibility map is compared with a failure population that is independent from the one used to obtain the map in order to determine the accuracy of the model. In the absence of historical data or of a landslide event after Hurricane Mitch, the same failure set should be used for validation. However, in order to obtain two independent failure samples the study area was divided into a training zone and a test zone (Fig. 3), following the approach of Baeza and Corominas (2001), Remondo et al. (2003b) Chung and Fabbri (2003, 2005) and Guinau et al. (2005).

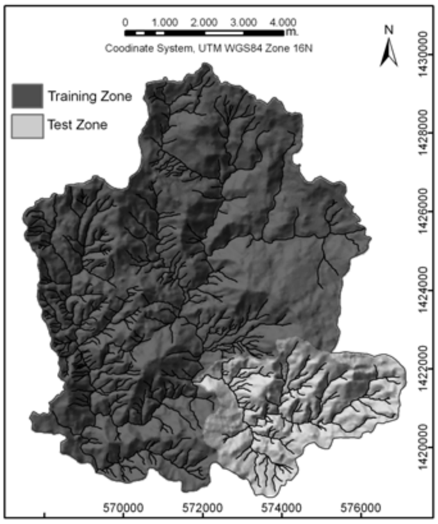

Fig. 3. Division of the study area into training zone (in dark grey) and test zone (in light grey).

3.1. Selection, extraction and discretisation of instability factors from DEM

In the absence of geoenvironmental maps and of accurate geological maps of the study area, we proposed a susceptibility model using geometrical parameters extracted from DEM. It has been demonstrated that reliable susceptibility maps can be produced by using conditional parameters exclusively derived from a DEM (Remondo et al., 2003b; Fabbri et al., 2003; Santacana et al. 2003; Pallàs et al. 2004,; Coe et al., 2004).

To determine the factors that contribute most to terrain instability, we considered field data and those parameters that could be directly extracted from DEM. Thus, *Aspect, Slope, Planar Curvature* (degree of concavity /convexity along a line perpendicular to slope profile) and *Profile Curvature* (degree of concavity/convexity of the slope profile) were obtained by using the 3D-

Spatial Analyst module of ArcInfoGIS software (Moore et al., 1991; Ayalev et al., 2004; Coe et al., 2004). These parameters, which were continuous variables, had to be converted into discrete ones in order to be incorporated at the bivariate analysis. Discretization was developed by using the Equal Interval process for aspect and slope and the Natural Breaks process for both planar and profile curvature (Dai & Lee, 2002). In Fig. 4 we can observe the thematic maps in which the discretized geometric parameters are represented. For Planar Curvature negative values show that the surface is upwardly concave and positive values indicate that the surface is upwardly convex. For profile curvature, negative values indicate that the surface is upwardly convex and positive values show that the surface is upwardly concave. A curvature value of zero indicates that the surface is flat for both planar and profile curvatures. Table 1 shows the percentage of the total study area covered by each class of the four parameters considered in the analysis.

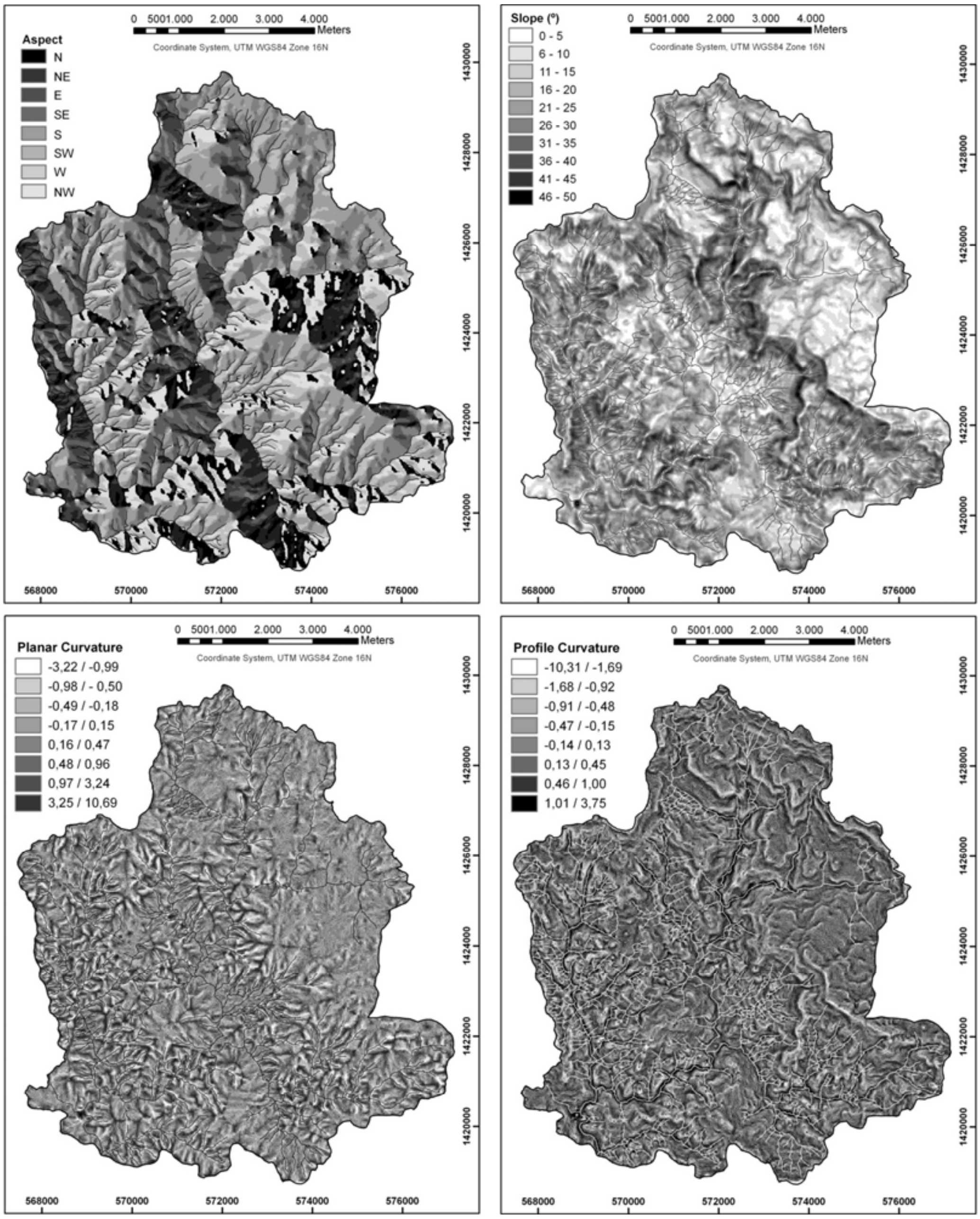

Fig. 4. Thematic maps obtained from the DEM. Each one shows a terrain factor defined by a given number of classes; (from left up to right down) Aspect, Slope, Planar Curvature and Profile Curvature.

Table 1; Percentage of the total study area covered by each parameter class

Aspect	% Area	Slope (º)	% Area	Planar Curvature	% Area	Profile Curvature	% Area
N	9	0-5	7	-3,22 / -0,99	3	-10,31 / -1,69	0
NE	10	6-10	14	-0,98 / -0,50	8	-1,68 / -0,92	3
E	10	11-15	17	-0,49 / -0,18	21	-0,91 / -0,48	9
SE	12	16-20	20	-0,17 / 0,15	31	-0,47 / -0,15	21
S	15	21-25	19	0,16 / 0,47	23	-0,14 / 0,13	28
SW	19	26-30	14	0,48 / 0,96	12	0,14 / 0,45	25
W	14	31-35	7	0,97 / 3,24	3	0,46 / 1,00	12
NW	11	36-40	2	3,25 / 10,69	0	1,01 / 3,75	3
		41-45	0				
		46-50	0				

3.2. Terrain failure susceptibility analysis in the Training Zone

Van Westen (1993) and Saha et al. (2005) propose the Information Value (InfoVal) method developed by Yin and Yan (1988) for terrain failure susceptibility assessment. In this procedure combining the failure map with each thematic map in the training zone allows us to determine the weight of influence on terrain instability for each parameter class with the following equation W_i (Eq. 1);

$$W_i = \log\left(\text{Densclass/Densmap}\right) = \log\left[\left(\text{Npix}(S_i) / \text{Npix}(N_i)\right) / \left(\sum_{i=1}^{n} \text{Npix}(S_i) / \sum_{i=1}^{n} \text{Npix}(N_i)\right)\right] \quad (1)$$

Where W_i is the weight for the *i*th class of a particular thematic map (i.e. 0º-10º or 20º-30º in the thematic map "*Slope*"), *Densclass* is the failure density in the factor class, *Densmap* is the failure density within the whole study area, *Npix(S$_i$)* is the number of failed pixels in the *i*th factor class, *Npix(N$_i$)* is the number of pixels in the *i*th factor class, and *n* is the number of classes in the thematic map. Once the Information Value for each variable class was calculated for all the input maps, the thematic maps were superimposed. The Information Values in each pixel were added in order to obtain a terrain failure susceptibility index (*TFSI*), which defines its landslide susceptibility level.

3.3. Terrain failure susceptibility discretization and validation in the test zone

In order to test this model, the weights determined for each factor class in the training zone were integrated into the thematic maps in the test zone. Terrain failure susceptibility indexes in this area were obtained by adding up the corresponding weights in each pixel.

The validation process allowed us to determine the degree of confidence of the method, which is important for transferring the results to the final users (Remondo et al., 2003a,b; Chung & Fabbri, 2003; Beguería, 2006; Guzzetti et al., 2006). The validation of the model also helps to define its suitability for the needs of the end users, which often involves terrain zonation in different susceptibility levels. Thus, the cumulative percentage of failures in the test zone in relation to the terrain failure susceptibility indexes (TFSI) (Fig. 5) was used to define susceptibility classes. Four susceptibility classes were defined as follows; very low susceptibility (-197<TFSI>-153, interval containing 0% of failures); low susceptibility (-152<TFSI>-31, interval containing 10% of failures); medium susceptibility (-30<TFSI>19, interval containing 30% of failures) and high susceptibility (20<TFSI>90, interval containing 60% of failures) (Süzen & Doyuran, 2004). These thresholds were used for the terrain failure susceptibility zonation in the whole study area.

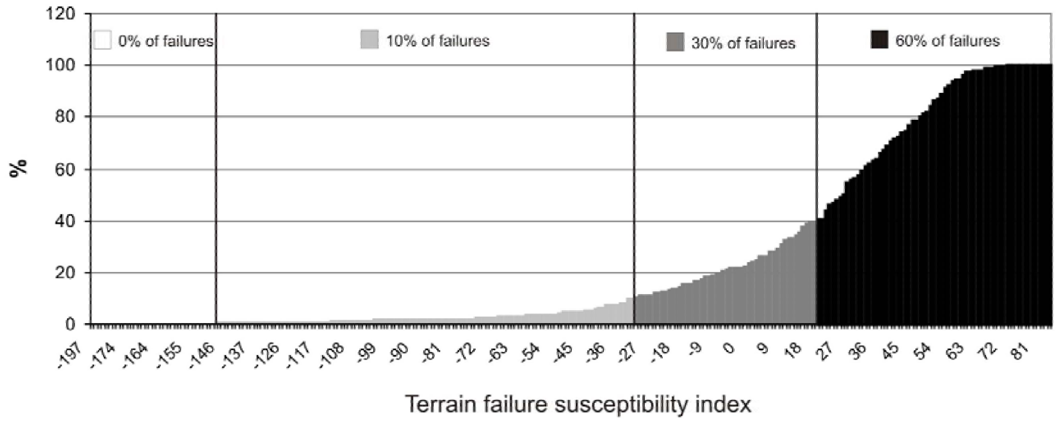

Fig. 5. Graphic showing the cumulative percentage of failures versus the terrain failure susceptibility index (TFSI). The intervals used to define the susceptibility classes are marked in different grey tones: In white the range containing 0% of failures, in light grey the range containing 10% of failures, in dark grey the range containing 30% of failures and in black the range containing 60% of failures.

In order to validate the accuracy of the model, the terrain failure susceptibility map was compared with the failure map in the test zone. A relative failure density (RFD) was used to quantify the accuracy of the method (Eq. 2) (Duque et al., 1990; Baeza and Corominas, 2001; Santacana et al., 2003; Fernández et al., 2003; Remondo et al., 2003b; Chung and Fabbri, 2003 & 2005; Guinau et al., 2005).

$$RFD_i = 100 \cdot \left(\text{Npix}(S_i)/\text{Npix}(N_i)\right) / \sum_{i=1}^{n} \left(\text{Npix}(S_i)/\text{Npix}(N_i)\right) \quad (2)$$

Where $Npix(S_i)$ is the number of pixels failed in the ith susceptibility class, $Npix(N_i)$ is the number of pixels in the ith susceptibility class and n is the number of susceptibility classes. Figure 6 shows the relative failure density in each susceptibility class resulting in a gradual decrease in the relative landslide density between the areas with high susceptibility and the areas with low susceptibility.

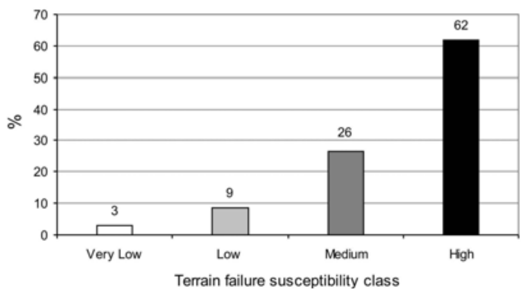

Fig. 6. Graphic showing the relative failure density (RFD) for each terrain failure susceptibility class.

Although this finding shows that the model is a good fit, it does not demonstrate its predictive capability. A set of failures triggered in a time period different from the one used in the analysis is necessary in order to determine this predictive capability.

Figure 7 shows the terrain failure susceptibility zonation in the whole study area, where; 8% has very low susceptibility, 34% has low susceptibility, 37% has medium susceptibility and 21% has high susceptibility.

4. Runout susceptibility analysis using TauDEM tools

Runout behaviour can be controlled by several parameters such as topography, soil type, land use, debris volume and the amount of interstitial fluids. Given the difficulty of characterizing these parameters for future debris flows, it is not easy to determine the runout path and the reach distance. However, this problem can be overcome by taking into account the fact that under intense rainfall debris flows tend to travel long distances following the steepest path and merging with the drainage network (Montgomery & Dietrich, 1994; Pallàs et al., 2004; Guinau et al., 2005). In order to determine the areas that are prone to debris flow, we propose a methodology based on the use of the open source TauDEM software developed by Tarboton (1997), which is available electronically on the Internet from the author (dtarb@cc.usu.edu, http://www.engineering.usu.edu/dtarb/taudem).

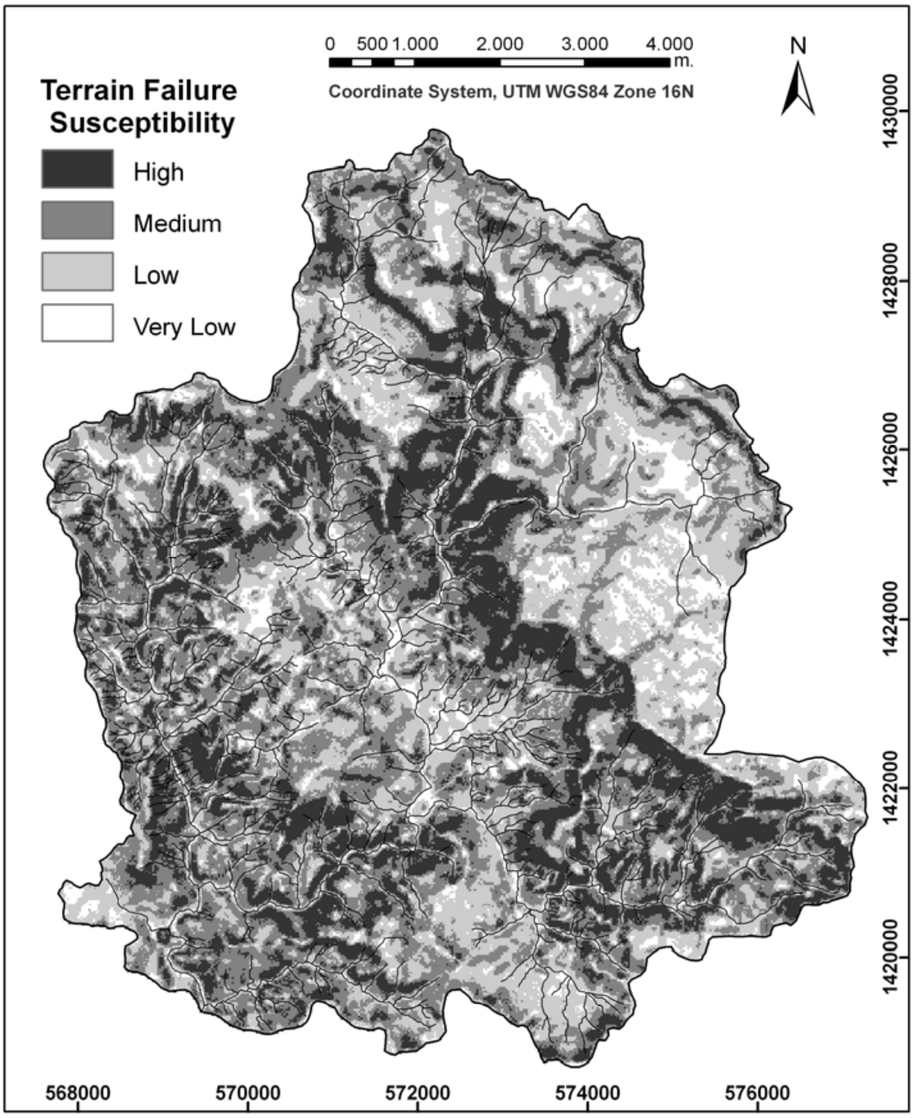

Fig. 7. Terrain failure susceptibility map obtained for the whole study area.

4.1. TauDEM tools description

TauDEM is software that can be executed as an ArcGIS extension. This software contains a set of tools which facilitate the assessment of hydrologic processes from DEM. In this study, two of these tools were used: the flow direction (D∞) and the downslope influence (DI).

The former is used to assign a multiple number of possible flow directions to each pixel based on the direction of the steepest downwards slope (Tarboton, 1997). The latter is employed to track the movement of sediment from a given source pixel, taking into account the flow direction in each downslope pixel (Tarboton, 1997).

4.2. Model calibration

The model was calibrated to determine its adjustment with the debris flow behaviour in the study area. This enabled us to compare the model results with a known event (in this case the landslides triggered by Hurricane Mitch resulting in debris flows corresponding to 90% of the total landslides mapped in the study area). The DI tool was used to determine the flow tracks from the pixels affected by terrain failure during Hurricane Mitch, taking into account the flow directions for each downslope pixel. In this way the model calculates the flow concentration for each pixel from the source point to the drainage network, where the flow concentration is the highest. Thus, the highest DI values coincide with the drainage network.

A comparison between the modelled flow paths and the Hurricane Mitch debris tracks shows that the model produced an overestimation (Fig. 8). The relative runout density was calculated to quantify this deviation (Eq. 3).

$$RRD_i = 100 \cdot \left(\mathrm{A(S_i)} / \mathrm{A(DI_i)}\right) / \sum_{i=1}^{n} \left(\mathrm{A(S_i)} / \mathrm{A(DI_i)}\right) \quad (3)$$

Where $A(S_i)$ is the area affected by debris flow track in the *i*th ID interval, $A(DI_i)$ is the area of the *i*th ID interval and *n* is the number of ID intervals.

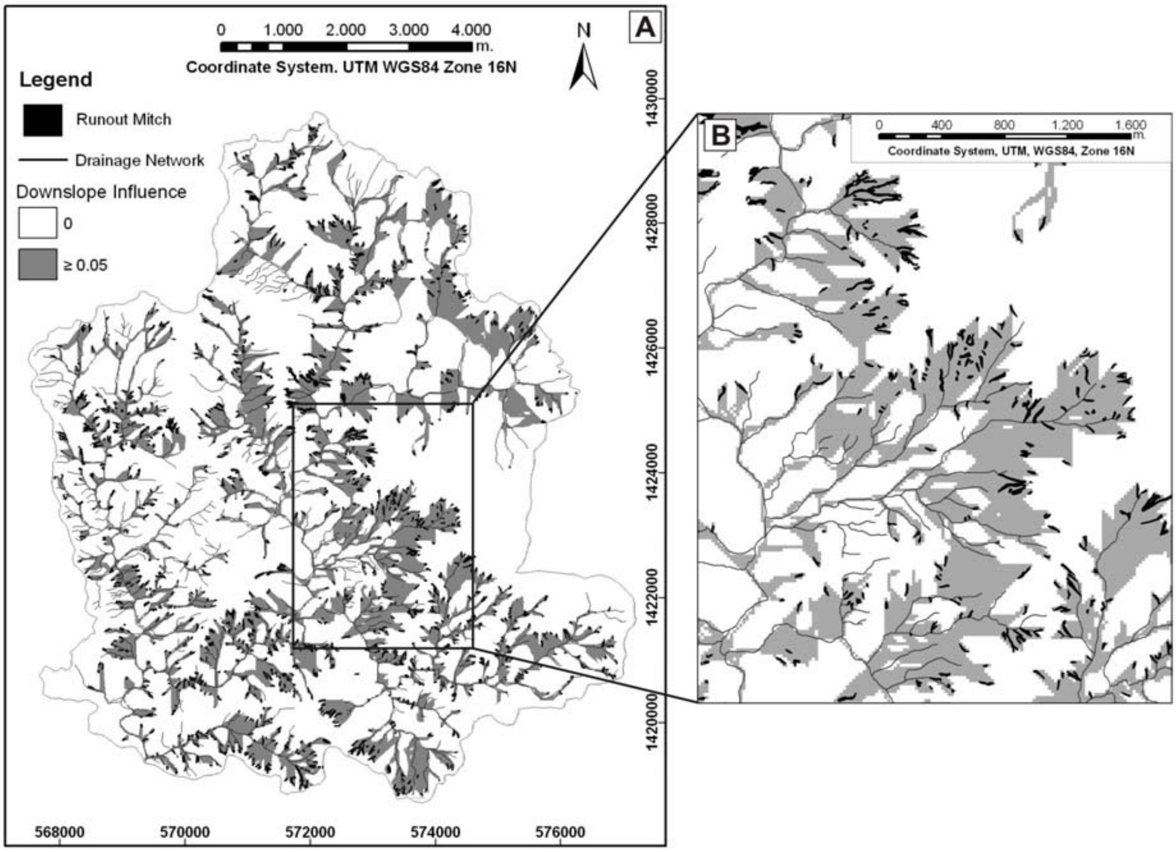

Fig. 8. A: Map showing the downslope influence obtained from the terrain failures triggered by Hurricane Mitch in grey tones and the Hurricane Mitch runout areas in black. B: An enlarged area of this map showing the overestimation of the model.

Figure 9 shows that when DI values are equal to or higher than 0.05 the relative runout density exceeds the value of 10%. This value was taken as the threshold to determine the areas susceptible to debris flows, where DI ≥ 0.05 and the non susceptible ones, where DI < 0.05. Figure 10 shows that the areas with 0 < DI < 0.05 recover a large area with less than 10% of the Hurricane Mitch affected area. Thus, if pixels with DI < 0.05 are considered non susceptible to debris tracks the overestimation of the model can be reduced.

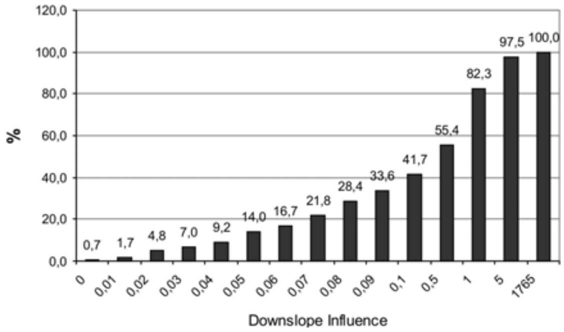

Fig. 9. Graphic showing the accumulated relative runout density (RRD) in % versus the Downslope Influence (DI) values.

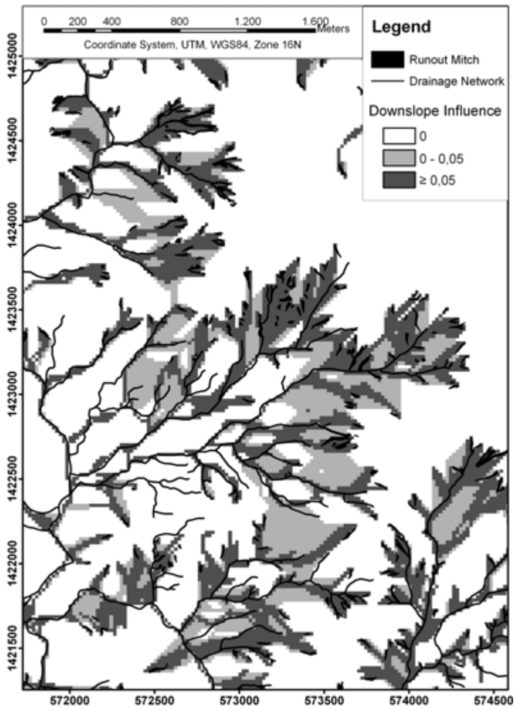

Figure 10. The same enlarged area of figure 8 where the DI values are showed in 3 classes; DI = 0 in white, 0 < DI < 0.05 in light grey and DI ≥ 0.05 in dark grey. Note that Hurricane Mitch affected areas (in black) are concentrated inside the area with DI ≥ 0.05.

4.3. Runout susceptibility assessment

Terrain failure susceptibility classes were used in this case as source zones to assess the runout susceptibility in the study area. Each terrain failure susceptibility class was divided into an independent raster file where the pixels susceptible to failure were identified by 1 and the others by 0. Each raster file was processed independently to determine the downslope influence for each susceptibility class. Given the results of the model calibration, the pixels were reclassified as runout susceptible if DI ≥ 0.05 or non susceptible if DI < 0.05. For each resulting file the runout susceptible pixels were identified by a number. The size of this number depended on whether the field was obtained from terrain failure susceptibility high (value assigned 4), medium (value assigned 3), low (value assigned 2) or very low (value assigned 1) (Fig. 11). Finally, the four resulting files were combined bearing in mind that the highest susceptibility value prevailed in each pixel. This resulted in a runout susceptibility map in which the pixels were classified into four susceptibility classes (Fig. 11).

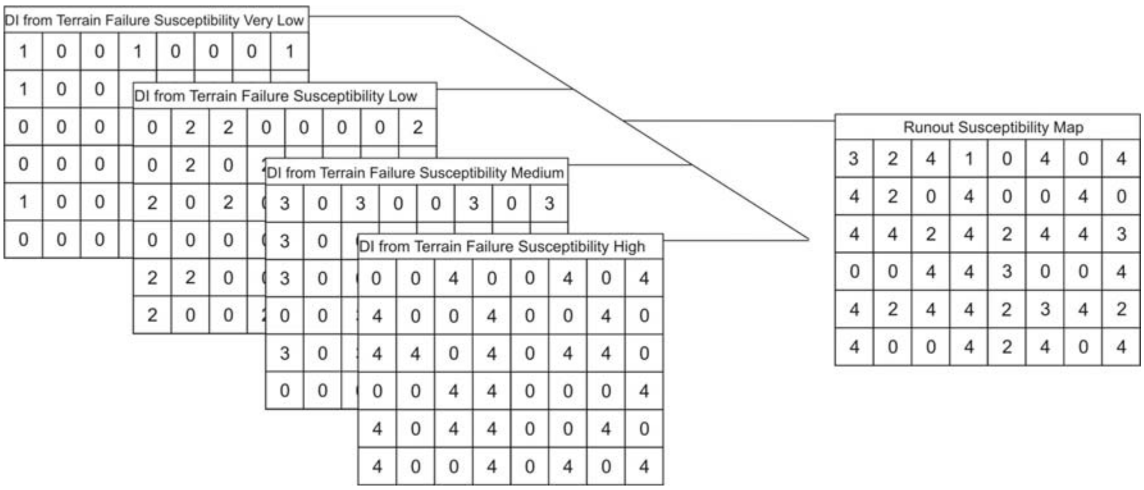

Fig. 11. A graphic example of the four raster files obtained after modelling the flow paths from each terrain failure susceptibility map. In each file the pixels that are non susceptible to debris flow were identified with zero and the pixels that are susceptible with a different value (1 to 4). The combination of these files enables to obtain the runout susceptibility map where the pixels were reclassified in four susceptibility classes.

4.4. Runout susceptibility map: description and validation.

Figure 12 shows the runout susceptibility zonation in the whole study area, where 3% has very low susceptibility, 13% has low susceptibility, 28% has medium susceptibility and 56% has high susceptibility. In order to validate the accuracy of the model, this zonation is compared with the Hurricane Mitch runout areas and the relative runout density (RRD) is calculated for each runout susceptibility class (Eq. 4).

$$RRD_i = 100 \cdot \left(A(S_i) / A(N_i) \right) / \sum_{i=1}^{n} \left(A(S_i) / A(N_i) \right) \quad (4)$$

Where $A(S_i)$ is the area affected by debris flow track in the ith susceptibility class, $A(N_i)$ is the area of the ith susceptibility class and n is the number of susceptibility classes.

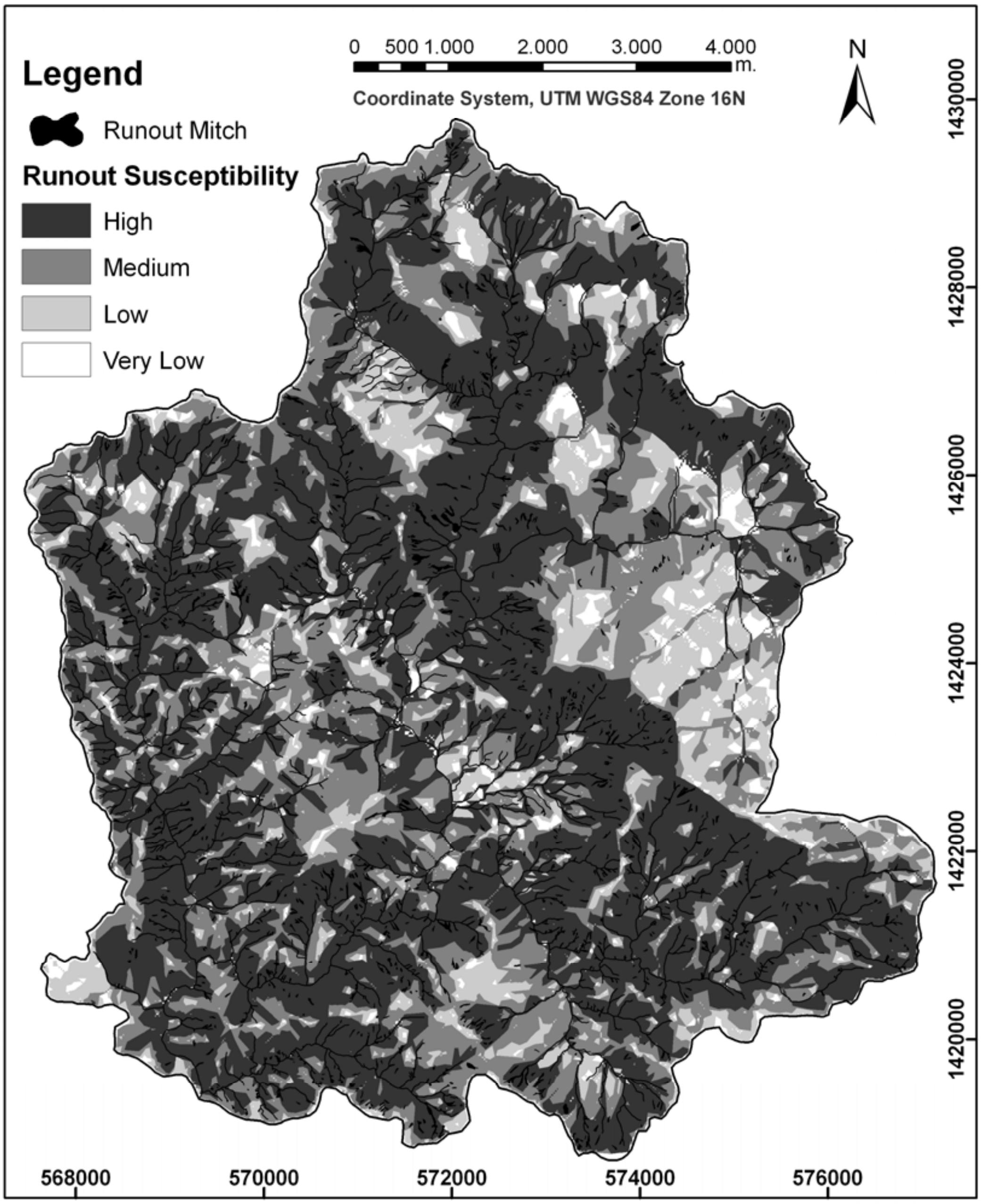

Fig. 12. Runout susceptibility map obtained in the whole study area.

Figure 13 shows a higher concentration of affected areas in zones with high susceptibility.

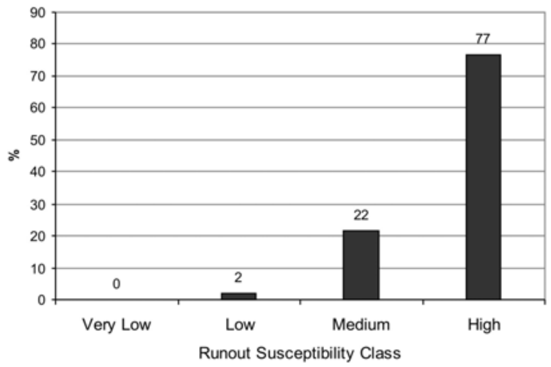

Fig. 13. Graphic showing the relative runout density (RRD) in % for each runout susceptibility class obtained from the combination of the Hurricane Mitch runout areas and the runout susceptibility map.

5. Source and runout susceptibility integration

Two concepts were used to assess landslide susceptibility: a) the terrain failure susceptibility and b) the runout susceptibility. The combination of these concepts yields an integrated susceptibility zonation which can be useful for land planning or for the implementation of non structural measures to mitigate debris flow risk.

Failure Susceptibility / Runout Susceptibility	High 40	Medium 30	Low 20	Very Low 10
High 4	44	34	24	14
Medium 3	43	33	23	13
Low 2	42	23	22	12
Very Low 1	41	31	21	11

Fig. 14. Matrix where the terrain failure susceptibility class on the columns and the runout susceptibility class on the rows were combined in order to define four susceptibility classes for the final susceptibility zonation.

To obtain an integrated evaluation of the susceptibility, we used a matrix to combine the terrain failure susceptibility values and the runout susceptibility values (Fig. 14). Values such as 40, 30, 20 and 10 were attributed to high, medium low and very low terrain failure susceptibility, respectively, whereas for runout susceptibility the values used were 4, 3, 2, and 1. We considered that the weight of failure susceptibility was higher than that of runout susceptibility given that the debris track depends on the slope failure occurrence. These values were added up and the results were grouped into four susceptibility classes. Thus, each pixel had a susceptibility class in relation to its terrain failure and runout susceptibility class. This result is shown in the debris flow susceptibility map in Fig. 15, where 41% of the study area has high susceptibility, 40% has medium susceptibility, 16% has low susceptibility and 3% has very low susceptibility. This map was compared with the debris flows triggered by Hurricane Mitch to determine the significance of each susceptibility class for land planning. Figure 16 shows the relative debris flow density measured for each susceptibility class. These results can help us to determine the best land use for debris flow risk mitigation.

6. Discussion and conclusions

Landslides triggered by Hurricane Mitch are used in the present study to develop a methodology to assess and map landslide source and runout susceptibility. Therefore, the resulting susceptibility maps show areas that may be affected by landslides under heavy rainfall conditions. Given that the return period for Hurricane Mitch rainfall is estimated at around 100 years (INETER, 1998), the resulting susceptibility zonation would be excessively pessimistic. However, adopting the worst-scenario approach has the advantage of providing a degree of safety.

The principal drawback of the method used to assess terrain failure susceptibility (bivariate analysis) is that it assumes the independence of the different terrain parameters with respect to slope instability. However, the most realistic approaches consider the dependence of the conditioning factors. Some authors overcome the problem by combining the dependent factors in a land unit map and by assessing the landslide susceptibility from this map (Carrara et al, 1995; van Westen et al., 1997). This approach assumes that the instability factors remain the same in the whole study area. In the absence of common factors in the study area, some land units could be present in one zone (i.e. the training area) but not in another (i.e. the test area), which makes the validation process difficult or even impossible (Guzzetti et al., 2006). Although multivariate statistical methods consider various parameters simultaneously, they demand complex and time-consuming analyses and a statistical background, which is not suitable for the conditions in some developing countries. Thus, the bivariate method is the most helpful in obtaining terrain failure susceptibility maps that differentiate areas of increasing degrees of susceptibility. This is a reasonable approach to hazard assessment given that the resources in developing countries are limited.

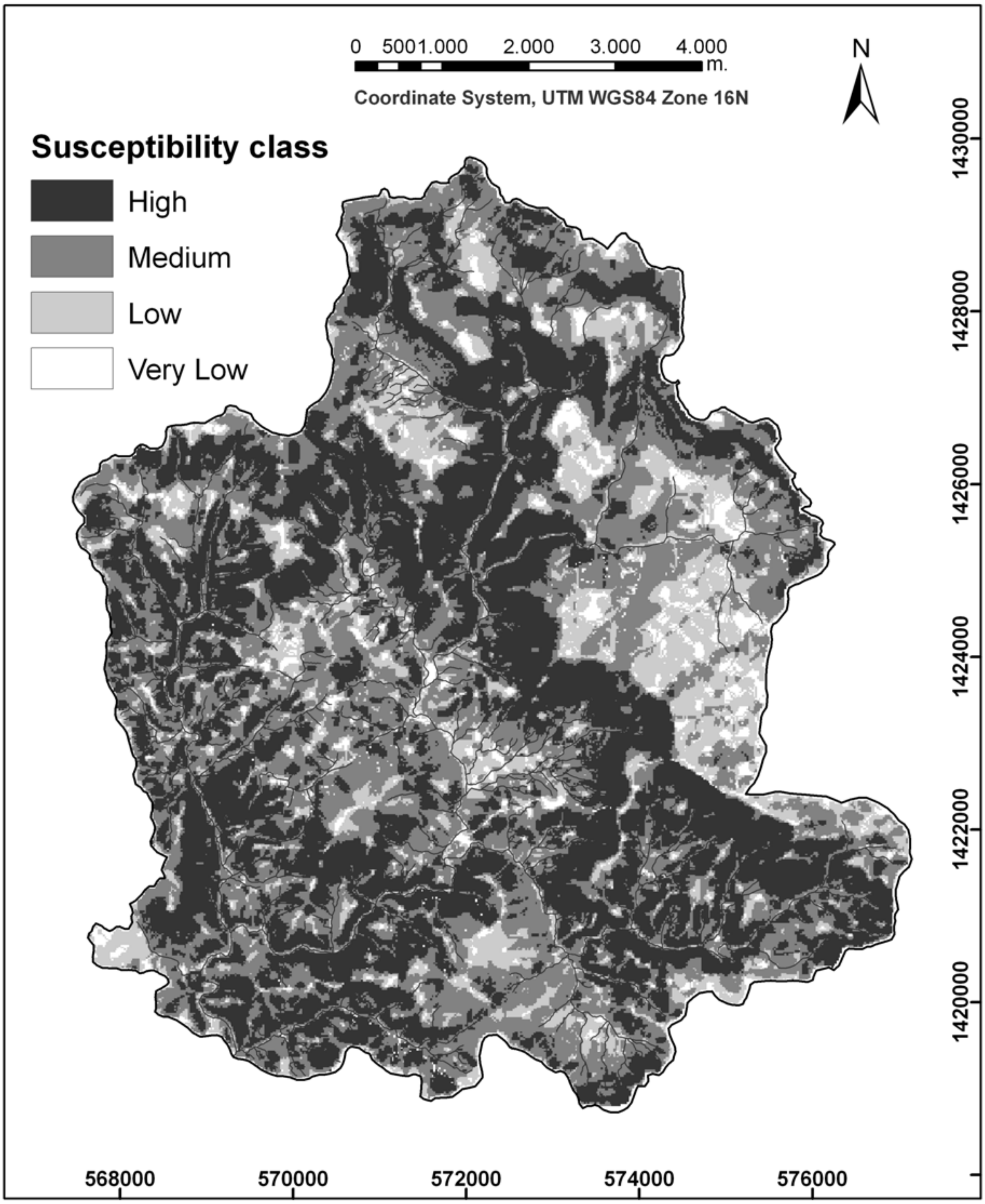

Fig. 15. Landslide susceptibility map obtained after terrain failure susceptibility and runout susceptibility integration.

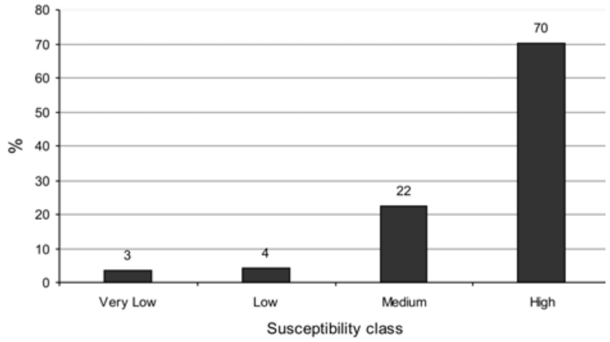

Fig. 16. Graphic showing the relative landslide density (in %) for each susceptibility class obtained from the combination of landslides triggered by Hurricane Mitch, and the final susceptibility map.

One problem encountered in the study area when assessing landslide susceptibility is the lack of detailed information about bedrock, soil and geomoprhologic characteristics. However, lithology and land cover are relatively uniform with slopes covered by a regolith cloak of volcanic rocks and thick vegetation which exert a homogeneous influence on terrain instability (Parise & Jibson 2000; Baeza & Corominas, 2001; Ayalew et al., 2005). Moreover, geoenvironmental variables are not independent from geometrical ones, i.e. slope is closely related to bedrock and land use could be conditioned by slope gradient. Thus, if both geoenvironmental and geometrical parameters are considered in the analysis, an overestimation of the susceptibility could result (Remondo et al., 2003a). Operations with the GIS enable us to readily obtain geometrical parameters from DEM. Four of these parameters (slope, aspect, planar and profile curvature) were selected to develop the terrain failure susceptibility analysis given that they are the ones that most affect water infiltration. Thus, they are considered the most important geometrical factors in rainfall triggered landslides in the study area.

DEM resolution exerts a considerable influence on the accuracy of the derived parameters. Although a coarse DEM resolution could be of poor quality in some cases, the gain in the quality of the results would not be worth the efforts (Remondo, et al., 2003b). Given the dimensions of the shallow landslide and debris flows in the study area, a 10m x 10m DEM could be optimal for analysing the landslide source and runout susceptibility (Tarolli and Tarboton, 2006). However, the results obtained with the 20m x 20m DEM available in the study area could constitute a good approach to failure and runout prone areas.

Debris flow is a complex phenomenon involving a highly unsteady motion of heterogeneous material ranging from water and slurries to boulders and timber remains. Debris flow mobility depends on parameters such as debris volume, the amount of interstitial fluids and terrain morphology. The assessment of flow velocities or impact energy to determine runout path and distance is not easy owing to the difficulty of determining these parameters for future debris flows. The methodology proposed to determine areas potentially affected by a debris flow path was based on DEM. The TauDEM extension allowed us to determine the flow paths following the steepest tracks from the potential source areas to the drainage network. However, the flow paths observed in the study area do not always merge with the drainage network with the result that the model overestimates the area that is potentially affected by debris flows.

The model calibration process allows us to determine a downslope influence threshold to adjust the model results to the debris flow behaviour. This process improves the model results. It should also be pointed out that the DEM resolution and the data available are not the best means to obtain a model adjusted to the debris flow behaviour. However, this model is a good way to determine areas prone to debris flows, and can be helpful in some developing countries to mitigate debris flow risk.

The validation of the model can provide useful information to build up the confidence of the end users. Despite the limitations of the validation process based on the division of the study area, it is a good approach in those areas where only one reference event is available. However, this process only provides information about how the model fits and not about the predictability power of the maps obtained. The validation results suggest that a careful selection of geometrical parameters from DEM and the application of feasible functions to calculate the parameter class contribution to terrain instability enable the detection of potential debris flow source areas. In the case of the runout susceptibility analysis, the validation results show a good model fit. However, the extension of high and medium susceptibilities occupy a considerable area (56% and 28% respectively), which could be disadvantageous for land planning or policy makers. These results are reflected in the susceptibility map obtained with the integration of terrain failure and runout susceptibility. In the debris flow susceptibility map (Fig. 13) 41% and 40% of the study area have high and medium susceptibilities, respectively. These results could be expected given the land characteristics of the study area (drainage network largely incised in altered bedrock and high slopes). Although the susceptibility zonation does not seem very precise, it is possible to propose land planning rules to mitigate landslide risk. Given that the economy is based on subsistence agriculture and that the settlements are scattered, a forested land use is proposed for areas with high susceptibility and agricultural activities for areas with medium susceptibility. The areas with low and very low susceptibility (16% and 3% respectively) are reserved for settlements, schools and churches. These last buildings are reserved for areas with very low susceptibility given their use as shelters in case of emergency.

*Acknowledgements.*This study was supported by the Generalitat de Catalunya (RISKNAT research group SGR2001-00081) and by the Consolider Igenio 2010 programme, under CSD 2006 "Topo-Iberia". Aerial photographs and DEM were provided by the Instituto Nicaragüense de Estudios Territoriales, INETER. Field work would not have been possible without the logistical support provided by the Centro de Investigaciones Geocientíficas, CIGEO (Universidad Nacional Autónoma de Nicaragua, Managua). We are indebted to the local emergency committees and to the people from San Nicolas and Santa Rosa del Peñón communities for providing accommodation and support during the fieldwork.

References

Ayalew, L., Yamagishi, H., Ugawa, N.: Landslide susceptibility mapping using GIS-based weighted linear combination, the case in Tsugawa area of Agano River, Niigata Prefecture, Japa. Landslides, 1, 73 – 81, 2004.

Ayalew, L., Yamagishi, H., Marui, H., Kanno, T.: Landslides in Sado Island of Japan: Part II. GIS-based susceptibility mapping with comparison of results from two methods and verifications. Engineering Geology, 81, 432 – 445, 2005.

Baeza, C. and Corominas, J.: Assessment of shallow landslide susceptibility by means of multivariate statistical techniques. Earth Surface Processes and Landforms, 26, 1251 – 1263, 2001.

Begueria, S.: Validation and evaluation of predictive models in hazard assessment and risk management. Natural Hazards, 37, 315 – 329, 2006.

Carrara, A., Cardinali, M., Guzzetti, F., Reichenbach, P.: GIS Technology in Mapping Landslide Hazard. In: Geographical Information Systems in Assessing Natural Hazards. Carrara, A. Guzzetti, F. (Eds.) Academic Pub., Dordrecht, the Netherlands, 360p.1995.

Chung, C.F., Fabbri, A.G.: Validation of spatial prediction Models for Landslide Hazard Mapping. Natural Hazards, 30, 451-472, 2003.

Chung, C.F., Fabbri, A.G.: Systematic procedures of landslide hazard mapping for risk assessment using spatial prediction models. In: Landslide Risk Assessment, Glade, T., Anderson, M.G., Crozier, M.J. (Eds.),. John Wiley, 139-174, 2005.

Coe, J.A., Godt, J.W., Baum, R.L., Bucknam, R.C., Michael, J.A.: Landslide susceptibility from topography in Guatemala. In: Landslides: Evaluation and stabilization. Lacerda, W.A.; Ehrlich, M.; Fontura, S.A.B.; Sayao (eds.). Taylor & Francis Group, London, 1, 69 – 78, 2004.

Corominas, J., Copons, R., Vilaplana, J.M., Altimir, J., Amigó, J.: Integrated landslide susceptibility analysis and hazard assessment in the Principality of Andorra. Natural Hazards, 30, 421 – 435, 2003.

Dai, F.C. and Lee, C.F.: Landslide characteristics and slope instability modelling using GIS, Lantau Island, Hong Kong. Geomorphology, 42, 213 – 228, 2002.

Dai, F.C., Lee, C.F., Ngai, Y.Y.: Landslide risk assessment and management: an overview. Engineering Geology, 64, 65 – 87, 2002.

Darce, M., Levi, B., Nyström, J.O., Troëng, B.: Alteration patterns in volcanic rocks within an east-west transverse through central Nicaragua. Journal of South American Earth Sciences, 2, 155 – 161, 1989.

Duque, A., Echevarría, G., Kerejeta, A., Cendrero, A., Tamés, P.: Comprobación empírica de metodologías para la elaboración de mapas de amenaza de inestabilidad de laderas; aproximación a un modelo general de evaluación del riesgo. In: Environmental geology and natural hazards in the Andean region. Hermelin, M. (Ed). AGID Report nº 13, Pereira, Colombia, 189 – 206, 1990.

Ehrenborg, J.: A new estratigraphy for the Tertiary volcanic rocks of the Nicaraguan Highland. GSA Bulletin, 108, 830 – 842, 1996.

Fabbri, A., Chung, C.F., Cendrero, A., Remondo, J.: Is prediction of future landslides possible with a GIS? Natural Hazards, 30, 487 – 499, 2003.

Fenzl, N.: Nicaragua, Geografía, Clima, Geología y Hidrogeología. UFPA/INETER/INAN, Belem (Eds). 62p., 1988.

Fernández, T., Irigaray, C., El Hamdouni, R., Chacón, J.: Methodology for landslide susceptibility mapping by means of a GIS. Application to the Contraviesa Area (Granada, Spain). Natural Hazards, 30, 297 – 308, 2003.

Guinau, M., Pallàs, R., Vilaplana, J.M.: A feasible methodology for landslide susceptibility assessment in developing countries: A case-study of NW Nicaragua after Hurricane Match. Engineering Geology, 80, 316 – 327, 2005.

Guzzetti, F., Reichenbach, P., Ardizone, F., Cardinali, M., Galli, M.: Estimating the quality of landslide susceptibility models. Geomorphology, 81, 166 – 184, 2006.

Hürlimann, M., Copons, R., Altimir, J.: Detailed debris flow hazard assessment in Andorra: A multidisciplinary approach. Geomorphology, 78, 359-372, 2006.

INETER: Las lluvias del siglo en Nicaragua. Instituto Nicaragüense de Estudios Territoriales, INETER. Managua, Nicaragua, 159 pp, 1998.

Montgomery, D.R. and Dietrich, W.E.: A physically based model for the topographic control on shallow landsliding. Water Resources Research, 30, 1153 – 1171, 1994.

Moore, I.D., Grayson, R.B., Ladson, A.R.: Digital terrain modelling: a review of hydrological, geomorphological and biological applications. Hydrolog. Process., 5, 3 – 30, 1991.

Pallàs, R., Vilaplana, J.M., Guinau, M., Falgàs, E., Alemany, X., Muñoz, A.: A pragmatic approach to debris flow hazard mapping in areas affected by Hurricane Match: example from NW Nicaragua. Engineering Geology, 72, 57 – 72, 2004.

Parise, M. and Jibson, R.W.: A seismic landslide susceptibility rating of geologic units based on analysis of characteristics of landslides triggered by the 17 January, 1994 Northridge, California earthquake. Engineering Geology, 58, 251 – 270, 2000.

Remondo, J., González-Díez, A., Díaz de Terán, J.R., Cendrero, A.: Landslide susceptibility models using spatial data analysis techniques. A case study from the Lower Deba Valley, Guipúzcoa (Spain). Natural Hazards, 30, 267 – 279, 2003a.

Remondo, J., González-Díez, A., Díaz de Terán, J.R., Cendrero, A., Fabbri, A., Chung, C.F.: Validation of landslide susceptibility maps; examples and applications from a case study in Northern Spain. Natural Hazards, 30, 437 – 449, 2003b.

Saha, A.K., Gupta, R.P., Sarkar, I., Arora, M.K., Csaplovics, E.: An approach for GIS-based statistical landslide susceptibility zonation – with a case study in the Himalayas. Landslides, 2, 61 – 69, 2005.

Santacana, N., Baeza, C., Corominas, J., de Paz, A., Marturià, J.: A GIS-based multivariate statistical analysis for shallow landslide mapping in La Pobla de Lillet Area (Eastern Pyrenees, Spain). Natural Hazards, 30, 281 – 295, 2003.

Süzen, M. and Doyuran, V.: A comparison of the GIS based landslide susceptibility assessment methods: multivariate versus bivariate. Environmental Geology, 45, 665 – 679, 2004.

Tarboton, D.G.: A new method for the determination of flow directions and upslope areas in grid digital elevation models, Water Resources Research, 33, 309 – 319, 1997.

Tarolli, P. and Tarboton, D.G.: A new method for determination of most likely landslide initiation points and the evaluation of digital terrain model scale in terrain stability mapping. Hydrol. Earth Syst. Sci., 10, 663 – 677, 2006.

van Westen, C.J.: Application of Geographical Information Systems to Landslide Hazard Zonation. ITC Publication Number 15, Enschede, The Netherlands. 1993.

van Westen, C.J., Rengers, N., Terlien, M.T.J., Soeters, R.: Prediction of the occurrence of slope instability phenomena through GIS-based hazard zonation. Geol Rundsh, 86, 404 – 414, 1997.

Varnes, D.J.: Landslide Hazard Zonation: a review of principles and practice. IAEG Commission on Landslides and Other Mass-Movements. UNESCO Press, Paris. 63 pp. 1984.

Yin, K.L. and Yan, T.Z.: Statistical prediction model for slope instability of metamorphosed rocks. In: Landslides-Glissements de Terrain. Proceedings V International Symposium on Landslides, vol. 2, Lausanne, Switzerland, 1269–1272, 1988.

III- MAPAS TEMÁTICOS DEL BLOQUE II

Mapa de Pendientes – Chinandega Norte

Mapa de Litologías – Chinandega Norte

Mapa de Textura del Suelo – Chinandega Norte

Mapa de Espesor del Suelo – Chinandega Norte

Mapa de Uso del Suelo – Chinandega Norte

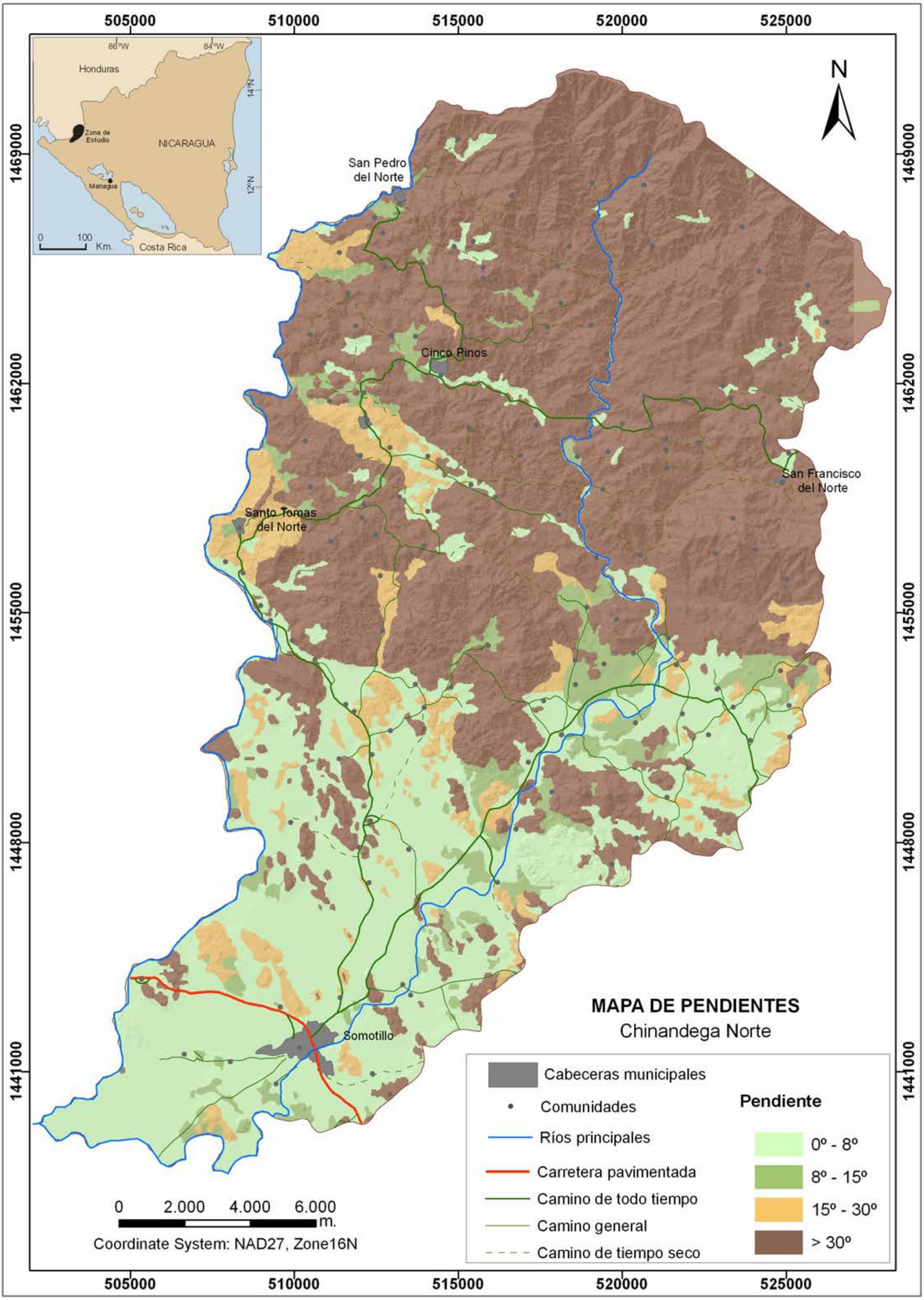
505000
510000
515000
520000
525000
1469000
1462000
1455000
1448000
1441000
86°W
84°W
14°N
12°N
Honduras
Zona de Estudio
NICARAGUA
Managua
Costa Rica
0
100
Km.
N
San Pedro del Norte
Cinco Pinos
San Francisco del Norte
Santo Tomas del Norte
Somotillo
MAPA DE PENDIENTES
Chinandega Norte
Cabeceras municipales
Comunidades
Ríos principales
Carretera pavimentada
Camino de todo tiempo
Camino general
Camino de tiempo seco
Pendiente
0º - 8º
8º - 15º
15º - 30º
> 30º
0
2.000
4.000
6.000
m.
Coordinate System: NAD27, Zone16N

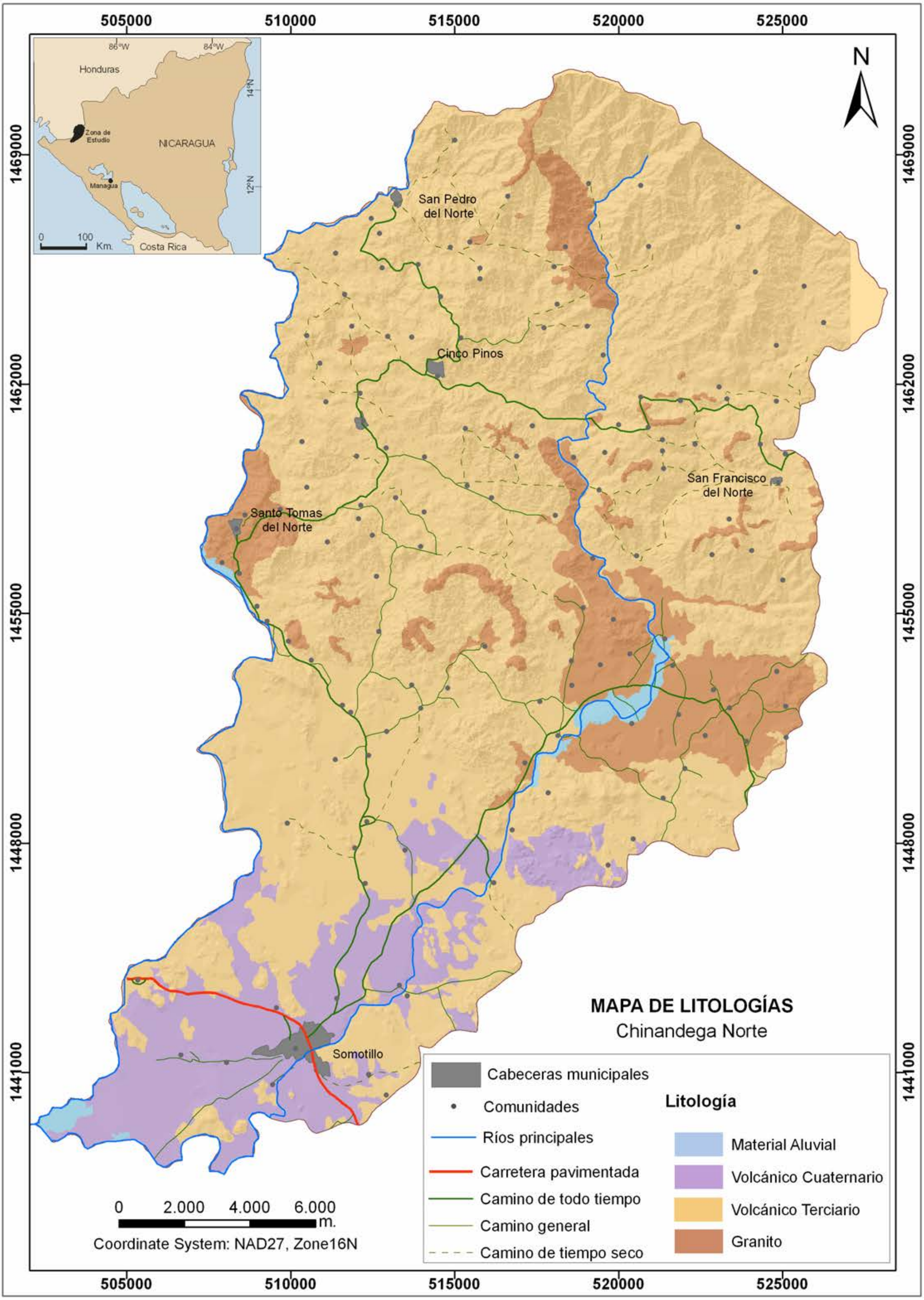
MAPA DE LITOLOGÍAS
Chinandega Norte
505000
510000
515000
520000
525000
1469000
1462000
1455000
1448000
1441000
N
Honduras
NICARAGUA
Zona de Estudio
Managua
Costa Rica
86°W
84°W
14°N
12°N
0
100
Km.
San Pedro del Norte
Cinco Pinos
San Francisco del Norte
Santo Tomas del Norte
Somotillo
Cabeceras municipales
Comunidades
Ríos principales
Carretera pavimentada
Camino de todo tiempo
Camino general
Camino de tiempo seco
Litología
Material Aluvial
Volcánico Cuaternario
Volcánico Terciario
Granito
0
2.000
4.000
6.000
m.
Coordinate System: NAD27, Zone16N

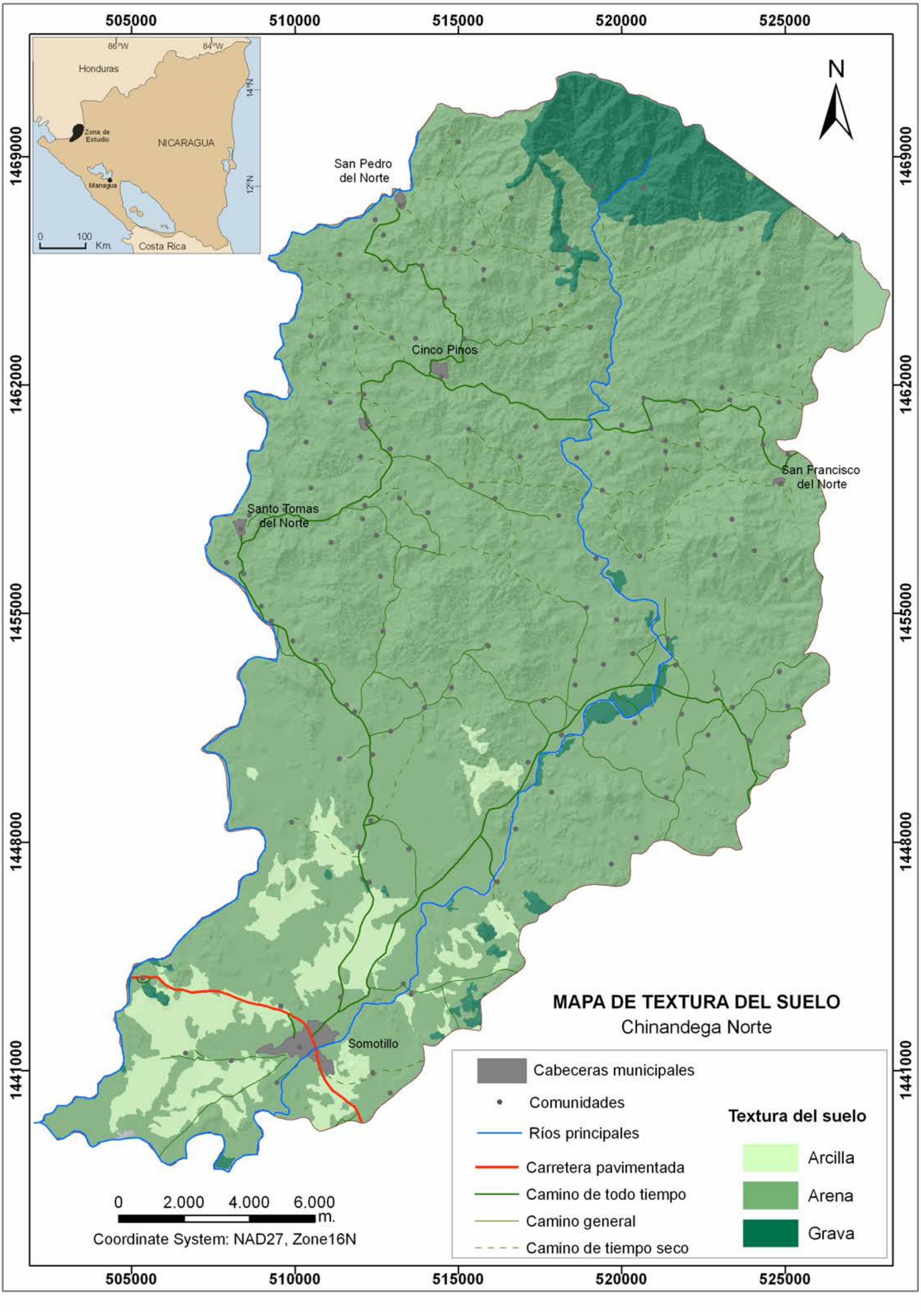
505000
510000
515000
520000
525000
1469000
1462000
1455000
1448000
1441000
86°W
84°W
Honduras
14°N
Zona de Estudio
NICARAGUA
Managua
12°N
0
100
Km.
Costa Rica
N
San Pedro del Norte
Cinco Pinos
San Francisco del Norte
Santo Tomas del Norte
Somotillo
MAPA DE TEXTURA DEL SUELO
Chinandega Norte
Cabeceras municipales
Comunidades
Ríos principales
Carretera pavimentada
Camino de todo tiempo
Camino general
Camino de tiempo seco
Textura del suelo
Arcilla
Arena
Grava
0
2.000
4.000
6.000
m.
Coordinate System: NAD27, Zone16N

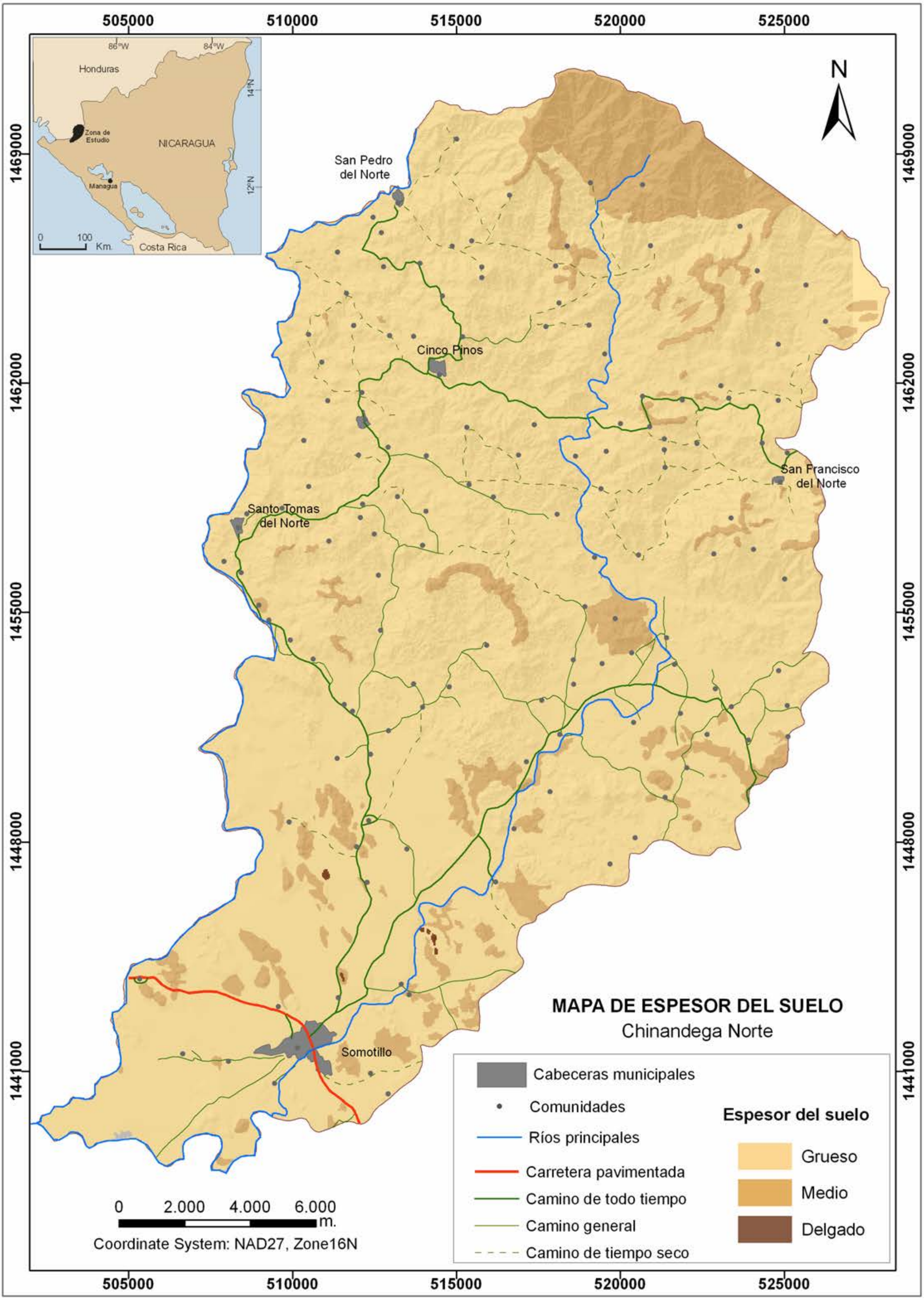
505000
510000
515000
520000
525000
1469000
1462000
1455000
1448000
1441000
86°W
84°W
14°N
12°N
Honduras
Zona de Estudio
NICARAGUA
Managua
Costa Rica
0
100
Km.
N
San Pedro del Norte
Cinco Pinos
San Francisco del Norte
Santo Tomas del Norte
Somotillo
MAPA DE ESPESOR DEL SUELO
Chinandega Norte
Cabeceras municipales
Comunidades
Ríos principales
Carretera pavimentada
Camino de todo tiempo
Camino general
Camino de tiempo seco
Espesor del suelo
Grueso
Medio
Delgado
0
2.000
4.000
6.000
m.
Coordinate System: NAD27, Zone16N

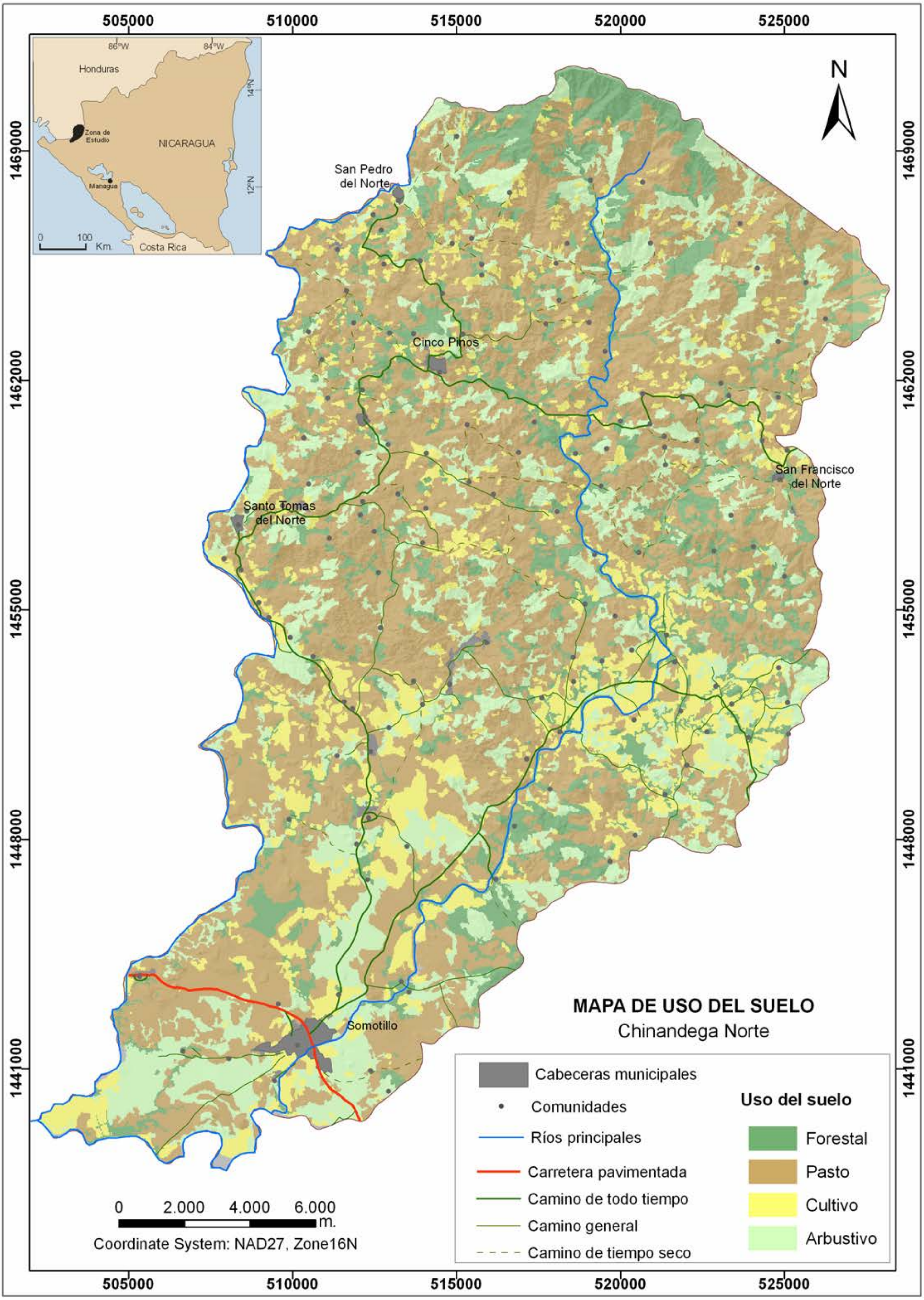
MAPA DE USO DEL SUELO
Chinandega Norte
505000
510000
515000
520000
525000
1469000
1462000
1455000
1448000
1441000
N
Honduras
NICARAGUA
Zona de Estudio
Managua
Costa Rica
86°W
84°W
14°N
12°N
0
100
Km.
San Pedro del Norte
Cinco Pinos
San Francisco del Norte
Santo Tomas del Norte
Somotillo
Cabeceras municipales
Comunidades
Ríos principales
Carretera pavimentada
Camino de todo tiempo
Camino general
Camino de tiempo seco
Uso del suelo
Forestal
Pasto
Cultivo
Arbustivo
0
2.000
4.000
6.000
m.
Coordinate System: NAD27, Zone16N

VI- MAPAS TEMÁTICOS DEL BLOQUE III

Mapa de Orientación – Cuenca alta del río Sinecapa

Mapa de Pendientes – Cuenca alta del río Sinecapa

Mapa de Curvatura Planar – Cuenca alta del río Sinecapa

Mapa de Curvatura en Perfil – Cuenca alta del río Sinecapa

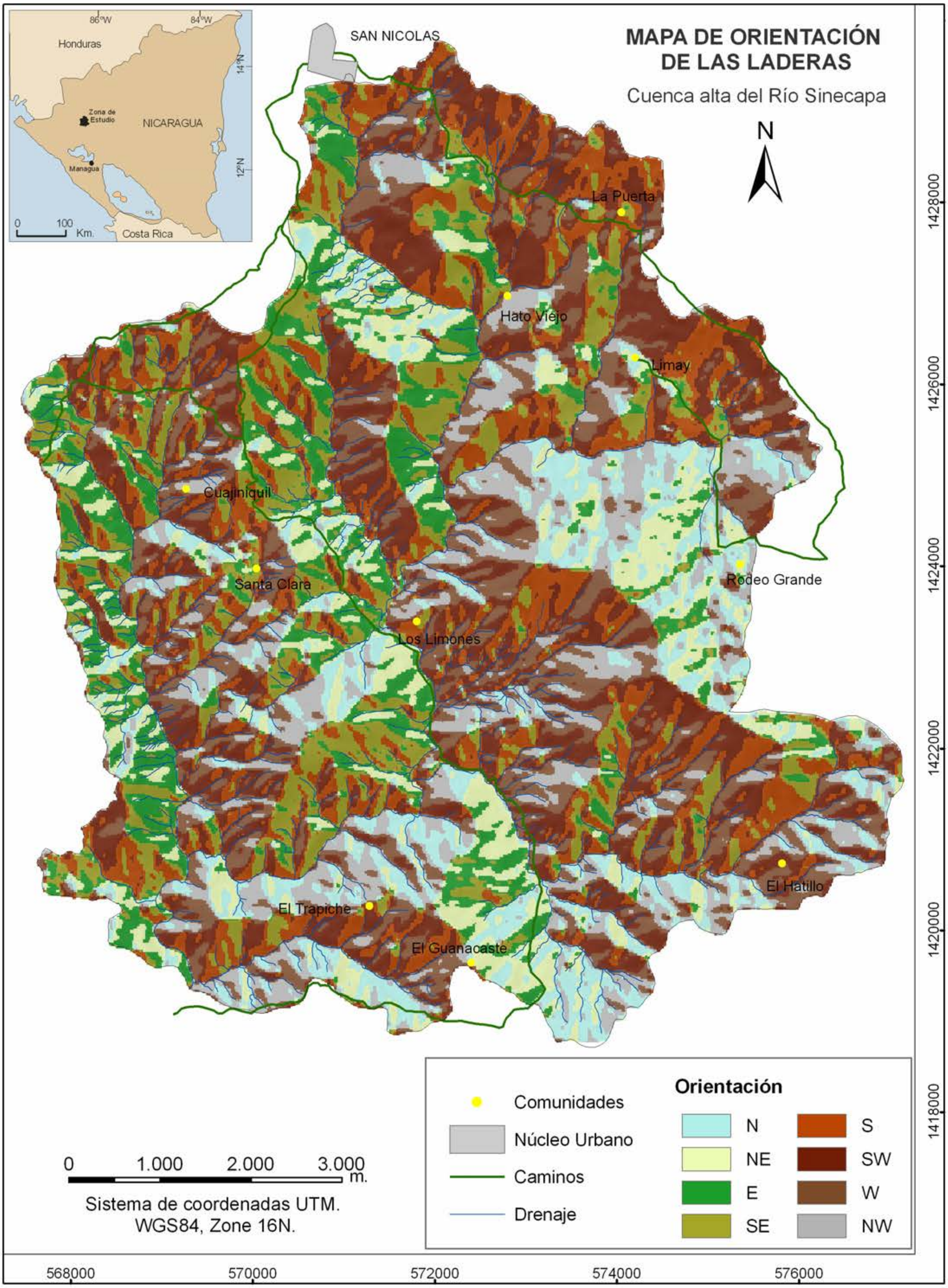
MAPA DE ORIENTACIÓN DE LAS LADERAS
Cuenca alta del Río Sinecapa
N
86°W
84°W
Honduras
14°N
12°N
Zona de Estudio
NICARAGUA
Managua
0 100 Km.
Costa Rica
SAN NICOLAS
La Puerta
Hato Viejo
Limay
Cuajiniquil
Santa Clara
Rodeo Grande
Los Limones
El Hatillo
El Trapiche
El Guanacaste
Comunidades
Núcleo Urbano
Caminos
Drenaje
Orientación
N
NE
E
SE
S
SW
W
NW
0 1.000 2.000 3.000 m.
Sistema de coordenadas UTM.
WGS84, Zone 16N.
568000
570000
572000
574000
576000
1418000
1420000
1422000
1424000
1426000
1428000

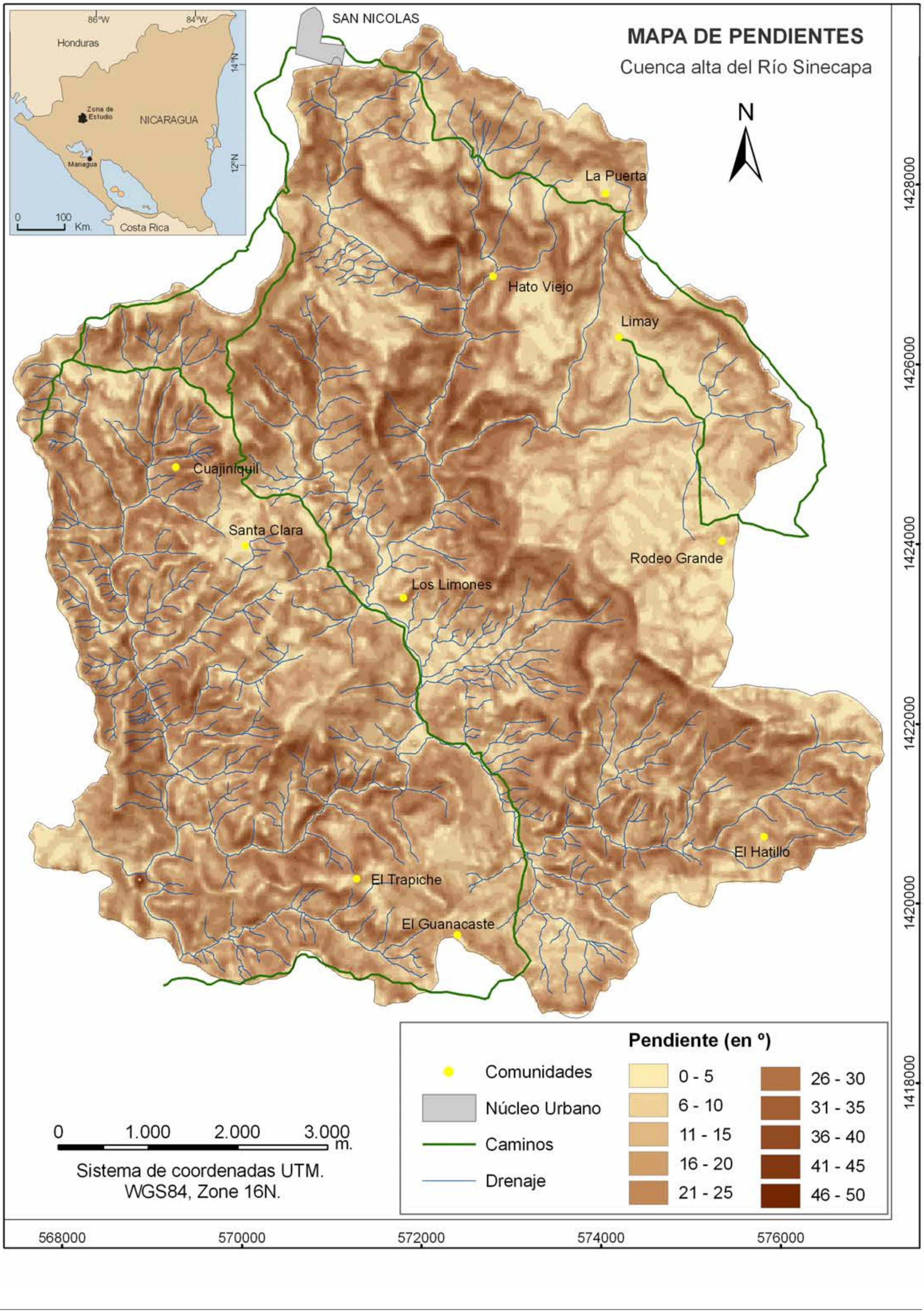
MAPA DE PENDIENTES
Cuenca alta del Río Sinecapa
N
SAN NICOLAS
86°W
84°W
Honduras
Zona de Estudio
NICARAGUA
Managua
Costa Rica
14°N
12°N
0
100
Km.
La Puerta
Hato Viejo
Limay
Cuajiniquil
Santa Clara
Rodeo Grande
Los Limones
El Hatillo
El Trapiche
El Guanacaste
Pendiente (en º)
Comunidades
Núcleo Urbano
Caminos
Drenaje
0 - 5
6 - 10
11 - 15
16 - 20
21 - 25
26 - 30
31 - 35
36 - 40
41 - 45
46 - 50
0
1.000
2.000
3.000
m.
Sistema de coordenadas UTM.
WGS84, Zone 16N.
568000
570000
572000
574000
576000
1428000
1426000
1424000
1422000
1420000
1418000

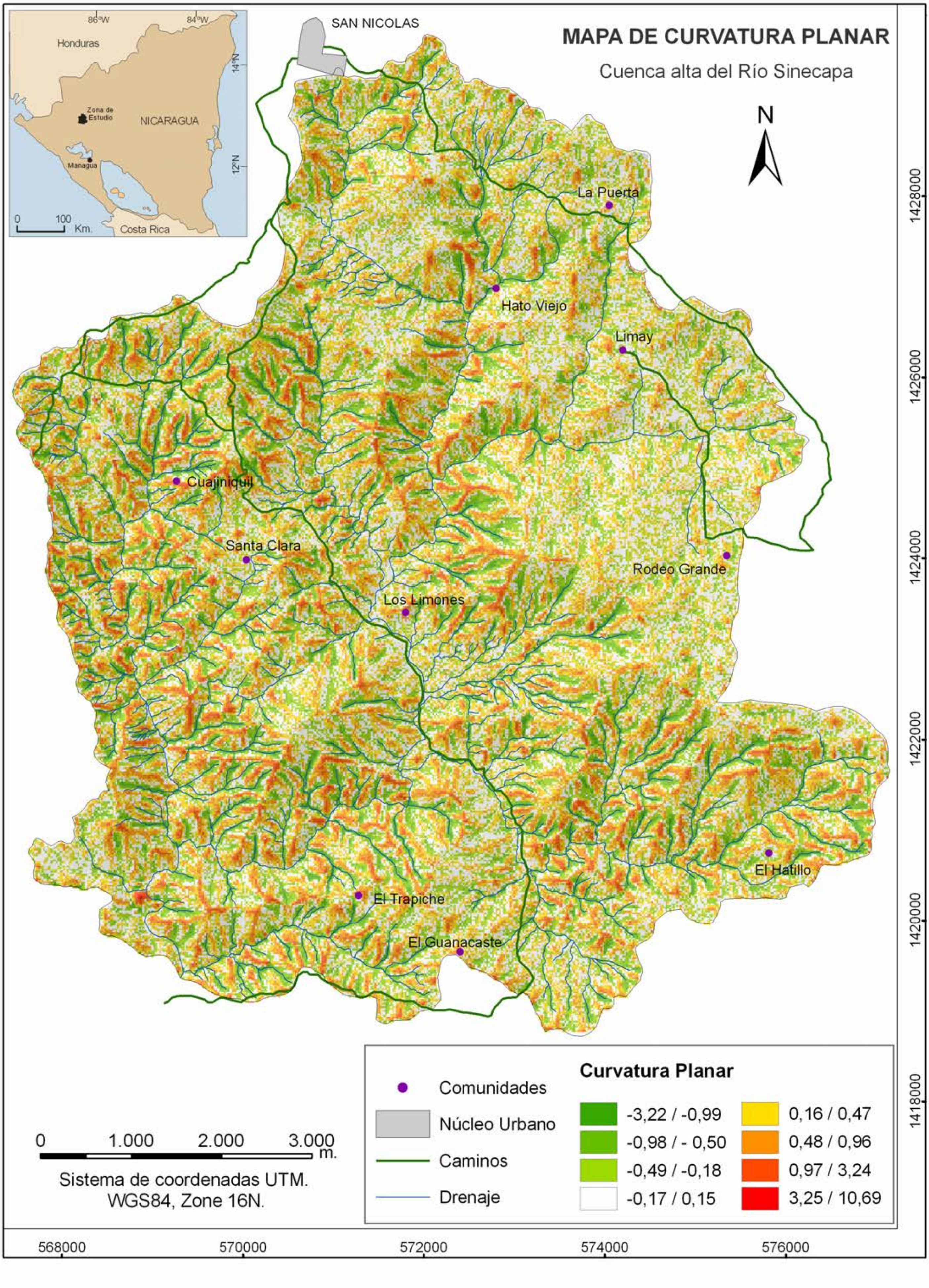

MAPA DE CURVATURA PLANAR
Cuenca alta del Río Sinecapa
N
86°W
84°W
Honduras
14°N
Zona de Estudio
NICARAGUA
Managua
12°N
0
100
Km.
Costa Rica
SAN NICOLAS
La Puerta
Hato Viejo
Limay
Cuajiniquil
Santa Clara
Rodeo Grande
Los Limones
El Hatillo
El Trapiche
El Guanacaste
Comunidades
Núcleo Urbano
Caminos
Drenaje
Curvatura Planar
-3,22 / -0,99
-0,98 / - 0,50
-0,49 / -0,18
-0,17 / 0,15
0,16 / 0,47
0,48 / 0,96
0,97 / 3,24
3,25 / 10,69
0
1.000
2.000
3.000
m.
Sistema de coordenadas UTM.
WGS84, Zone 16N.
568000
570000
572000
574000
576000
1418000
1420000
1422000
1424000
1426000
1428000

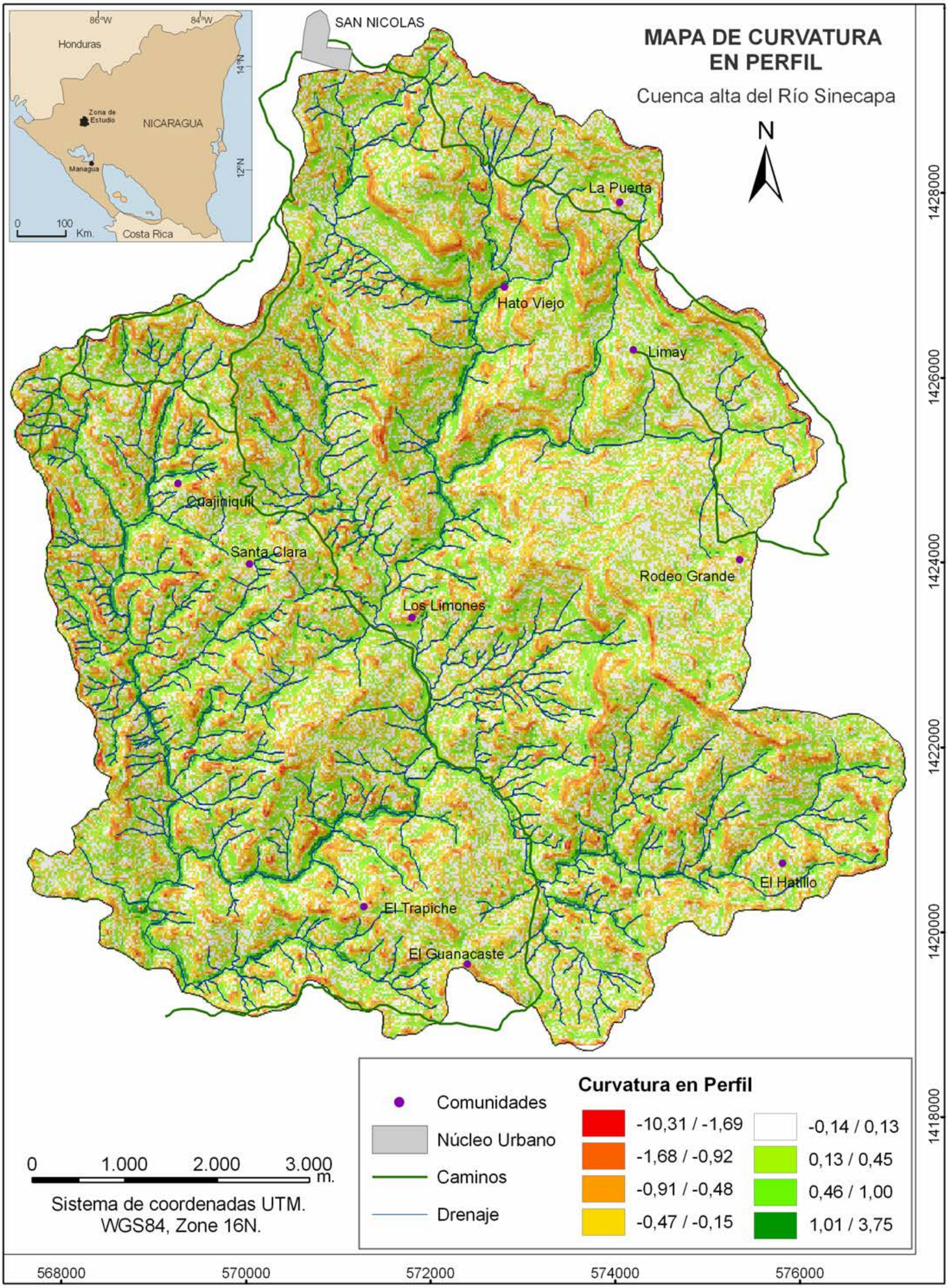
MAPA DE CURVATURA
EN PERFIL
Cuenca alta del Río Sinecapa
N
SAN NICOLAS
86°W
84°W
Honduras
14°N
Zona de Estudio
NICARAGUA
Managua
12°N
0
100
Km.
Costa Rica
La Puerta
Hato Viejo
Limay
Guajiniquil
Santa Clara
Rodeo Grande
Los Limones
El Hatillo
El Trapiche
El Guanacaste
1428000
1426000
1424000
1422000
1420000
1418000
568000
570000
572000
574000
576000
0
1.000
2.000
3.000
m.
Sistema de coordenadas UTM.
WGS84, Zone 16N.
Comunidades
Núcleo Urbano
Caminos
Drenaje
Curvatura en Perfil
-10,31 / -1,69
-1,68 / -0,92
-0,91 / -0,48
-0,47 / -0,15
-0,14 / 0,13
0,13 / 0,45
0,46 / 1,00
1,01 / 3,75